Theses and dissertations

1-1-2011

A novel configuration and control of CSI wind energy system with diode rectifier and buck converter

Xiatian Tan
Ryerson University

Follow this and additional works at: http://digitalcommons.ryerson.ca/dissertations

Part of the Electrical and Computer Engineering Commons

A Novel Configuration and Control of CSI Wind Energy System with Diode Rectifier and Buck Converter

by

Xiaotian Tan

Bachelor of Engineering, Changsha University of Science & Technology,

Changsha, China, 1994

A thesis

presented to Ryerson University

in partial fulfillment of the

requirements for the degree of

Master of Applied Science

in the Program of

Electrical and Computer Engineering

Toronto, Ontario, Canada, 2011

AUTHOR'S DECLARATION

I hereby declare that I am the sole author of this thesis.

I authorize Ryerson University to lend this thesis to other institutions or individuals for the purpose of scholarly research.

I further authorize Ryerson University to reproduce this thesis by photocopying or by other means, in total or in part, at the request of other institutions or individuals for the purpose of scholarly research.

BORROWER'S PAGE

Ryerson University requires the signatures of all persons using or photocopying this thesis.

Please sign below, and give address and date

Name	Address	Signature	Date

A Novel Configuration and Control of CSI Wind Energy System with Diode rectifier and Buck Converter

Xiaotian Tan

Electrical and Computer Engineering

Ryerson University, Toronto, Canada, 2011

Abstract

This thesis is dedicated to the research of a new converter configuration and control scheme development for direct drive permanent magnet synchronous generator (PMSG) based high power wind energy conversion system (WECS). The proposed converter consists of a diode rectifier, a buck converter and a pulse-width modulated (PWM) current source inverter (CSI).

Detailed feasibility study of the proposed configuration is conducted based on the theoretical analysis. A suitable control scheme is designed to optimize the system performance. The maximum power point tracking (MPPT) is achieved through duty cycle adjustment of the buck converter, while the reactive power delivery and the DC current regulation are realized by the CSI controller through manipulating modulation index and delay angle. More importantly, the DC current is evaluated and controlled to the minimum value at various operating conditions.

Simulation of a 2 MW WECS is carried out in Matlab/Simulink to verify the control objectives of MPPT, power factor adjustment and DC current minimization. The simulation results prove the feasibility of the proposed system that serves as an attracting alternative for high power WECS.

Acknowledgement

I would like to thank my supervisor, Professor Bin Wu, for his consistent help, financial support and great patience during my graduate studies at Ryerson University. His profound scholarship and precise advice has largely enhanced my academic knowledge, professional skill and scientific methodology.

I want to give my thanks to Professors Dewei (David) Xu and Richard Cheung for teaching me different courses and solving questions on my studies.

I am grateful to Dr. Jingya (Moya) Dai for providing me invaluable suggestions in preparation of the thesis and sharing technical experience in the research. My appreciation also goes to Jiacheng Wang, Yaramasu Venkata, Popat Mitesh, to name a few, and all other fellow students with Professor Bin Wu for the useful discussions.

The financial support and the study opportunity provided by Ryerson University are highly acknowledged.

The encouragement and support from my family and parents are much appreciated.

Table of Contents

List of Figures and Tables

Figures

Tables

List of Publications

[1]   X. Tan, J. Dai, and B. Wu, "A Novel Converter Configuration for Wind Applications Using PWM CSI with Diode Rectifier and Buck Converter," presented at the *International Electric Machines and Drives Conference (IEMDC 2011)*, Niagara Falls, Canada, May 15-18, 2011.

(Accepted, paper no. #1569382461)

Glossary of Acronyms and Symbols

AC	Alternating Current
DC	Direct Current
CSC	Current Source Converter
CSI	Current Source Inverter
CSR	Current Source Rectifier
DFIG	Doubly-Fed Induction Generator
DPC	Direct Power Control
DTC	Direct Torque Control
EESG	Electrically Excited Synchronous Generator
FOC	Field Oriented Control
FRT	Fault Ride Through
GW	Giga Watt
IGBT	Insulated Gate Bipolar Transistor
LV	Low Voltage
MPPT	Maximum Power Point Tracking
MV	Medium Voltage
MW	Mega Watt
NPC	Neutral Point Clamped
PF	Power Factor
PLL	Phase Locked Loop
PMSG	Permanent Magnet Synchronous Generator
PWM	Pulse Width Modulation
SCIG	Squirrel Cage Induction Generator
SGCT	Symmetrical Gate Commutated Thyristor
SVM	Space Vector Modulation

TSO	Transmission System Operator
UPF	Unity Power Factor
VOC	Voltage Oriented Control
VSC	Voltage Source Converter
VSI	Voltage Source Inverter
VSR	Voltage Source Rectifier
WECS	Wind Energy Conversion System
WRIG	Wound Rotor Induction Generator

The general considerations for defining the variables are as follows.

- The small letters normally refer to instantaneous quantities and the capital letters refer to constant, average or root-mean-square (RMS) values.

- The superscript '*' denotes the reference value, and superscript '^{o}' represents the value corresponding to the reference.

- The subscript '$_g$' or '$_s$' represents the generator side or the grid (power system) side, respectively.

- The subscript '$_d$' or '$_q$' stands for the corresponding direct-axis (d-axis) or quadrature-axis (q-axis) components in the defined synchronous reference frame, respectively.

- The subscript '$_i$' or '$_r$' denotes the inverter or the rectifier, respectively.

The following provides explanations to the variables that are commonly used in the thesis. Other variables which only appear in specific sections are explained in the context.

Voltages

E_g, v_g	generator induced electromotive force and terminal voltage
v_{dg}, v_{qg}	d-axis, q-axis generator terminal voltages
V_{dcr}	output DC voltage of the diode rectifier
V_{dci}	input DC voltage for the PWM CSI
v_s	grid voltage
v_{ds}, v_{qs}	d-axis, q-axis grid voltages
v_c	grid voltage across the capacitor
v_{cd}, v_{cq}	d-axis, q-axis voltages across grid side capacitor

Current

I_g	generator stator winding current
i_{dg}, i_{qg}	d-axis, q-axis generator stator winding currents
I_{dcr}	output DC current of the diode rectifier
I_{dci}	input DC current for the PWM CSI
i_s	grid current
i_{sd}	active component of the grid current
i_c	grid side capacitor current
i_{wi}	output current of the PWM CSI
i_{cdi}, i_{cqi}	d-axis, q-axis grid side capacitor currents

Power

S	apparent power
P_w	power contained in the wind
P_T	output power of the wind turbine
P_g	output active power of the generator
P_{dc}	power stored in the DC link choke
P_s	active power delivered to the grid
Q_s	reactive power delivered to the grid
Q_c	reactive power produced by the grid side capacitor
Q_i	reactive power produced by the CSI

LC components and generator parameters

L_g	generator stator winding synchronous inductance
L_d	generator d-axis synchronous inductance
L_q	generator q-axis synchronous inductance
L_{dc}	DC link inductance
C_i	capacitance of the grid side AC capacitor

Converter control related

D	duty cycle of the buck converter
m_i	modulation index of the PWM CSI
α_i	delay angle of the PWM CSI

Frequencies and flux linkage

ω_T mechanical angular frequency of the wind turbine (generator)

ω_g electrical angular frequency of the generator

ω_s grid voltage frequency

ψ magnetic flux linkage of the generator rotor

Wind turbine related

v_w wind speed

C_p power coefficient

λ tip speed ratio

β blade pitch angle

R turbine radius

Chapter 1   Introduction

Wind power is one of the cheap and endless alternative energy sources, and is now increasingly utilized in electric power system for the sustainable development. The worldwide installed wind turbine capacity reaches 196.6 gigawatts (GW) by the end of 2010, whose energy production equals to 2.5% of the global electricity consumption. With the advancement of wind energy related technologies and increasing support from government policies, it is predicted that the global installed capacity will be more than 1,500 GW by the year 2020 [1].

This chapter first reviews the status of wind energy development for electric power generation in the world as well as in Canada. A brief introduction to the basic configurations and technology development of the wind energy conversion system (WECS) is then put forth, based on which the research objectives and organization of the thesis are described.

1.1 Wind Energy Utilization

The history of wind energy utilization can be traced back as early as at least 5000 years ago, while windmills have been used for at least 3000 years. Wind energy has been employed to sail ships, grind grain and pump water [2]. It was not until the late nineteenth century that wind turbines were developed to generate electricity. However, for much of the twentieth century, there was little interest in applying wind energy for electrical power generation, largely due to the uneconomical and unreliable vulnerabilities resulting from early small size wind turbine in comparison with conventional electrical generators, e.g. hydro or coal burnt steam turbines.

The 1973 oil crisis changed the situation. The sharp increase of the oil price and concerns over limited fossil-fuel resources substantially stimulated the research and development of wind power generation. Another main driving force is environmental benefit of wind energy such that it can help reduce green house gas emission caused by the fossil-fuel generation and realize sustainable development in energy sector. The improvements in the wind turbine design and corresponding electrical power generation systems have brought down the cost of wind power

and made it competitive in electric power generation industry.

1.1.1 Global wind power development status

Wind energy now plays an increasing role in the energy sector as the tremendous growing forth continues. Lots of wind turbines are erected to capture the power and converter it into electricity. The booming wind power benefits from the technological advancement in related mechanical manufacturing and electrical engineering. The government stimulus package provides further fresh impetus to the investment.

Year	1996	1997	1998	1999	2000	2001	2002	2003	2004	2005	2006	2007	2008	2009	2010
Cap.	6.1	7.6	10.2	13.6	17.4	23.9	31.1	39.4	47.6	59.1	74.1	93.8	120.9	159.2	196.6
%	27	24.6	34.2	33.3	27.9	37.3	30.1	26.7	20.8	24.1	25.4	26.7	28.9	31.7	23.5
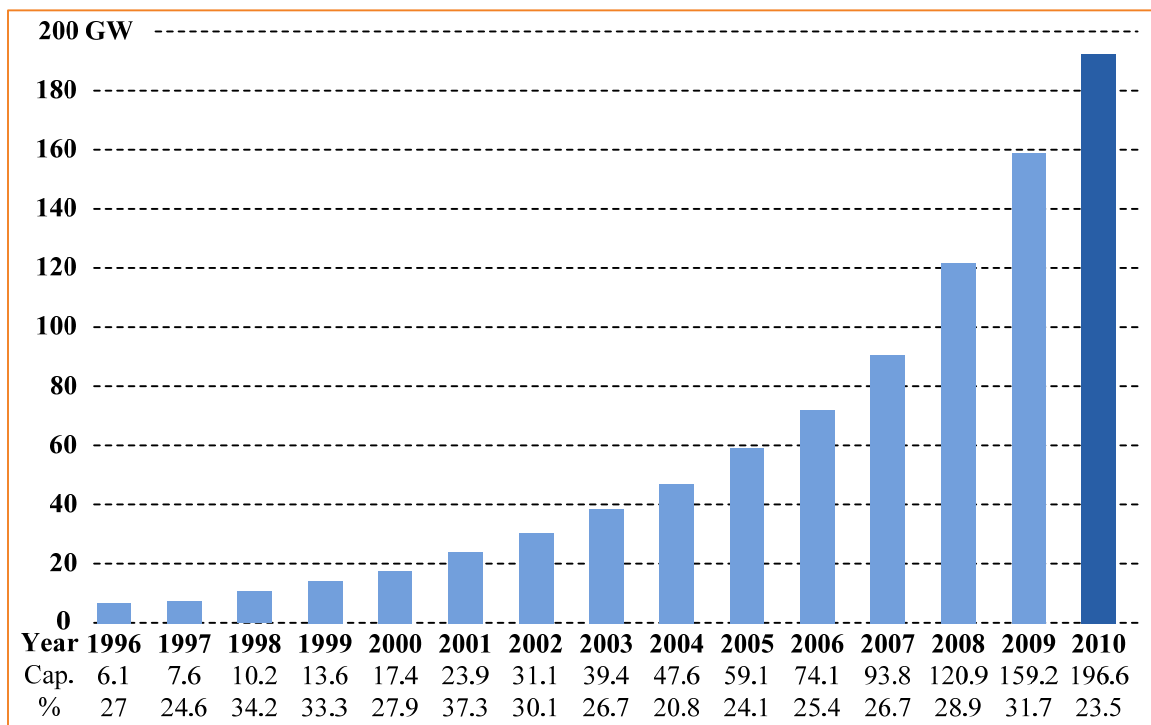
Fig. 1.1-1 Global cumulative installed wind power capacity

The global cumulative installed wind power capacity from 1996 to 2010 [1] [3] is summarized in Fig. 1.1-1. It can be observed that the global wind energy market has experienced vigorous growth during these fifteen years, with the installed capacity increasing at an average annual growth rate of more than 28%. Even when the financial crisis in 2009 badly affected the worldwide economy, the annual market grew 41.5% compared to 2008 [3]. The effective utilization of wind energy for electrical power generation will remain as a major research and

development interests in both developing and developed countries for the coming ages.

The wind resources are almost unlimited and can be harvested without the restriction of national boundaries. After decades of development, the wind power technology proves to be reliable and quick to apply in practice. With the increasing penetration of wind power in the electric power system, wind power generation is now regarded as not only the possible solution to the sustainable development in energy sector, but also the booster or the core of the economic recovery. The global wind energy council forecasts the global market from 2010 to 2014 in the global wind 2009 report [3], as shown in Fig. 1.1-2. Although the growth rate of the cumulative capacity tends to decrease due to the increasing base over the years, continuous and steady development in wind energy is expected for the next five years.

	2009	2010	2011	2012	2013	2014
Annual installed cap. (GW)	38.3	40.8	44.0	48.1	54.5	62.5
Cumulative cap. (GW)	158.5	199.9	243.9	292.0	346.5	409.0
Cumulative cap. growth rate (%)	31.7	25.8	22.0	19.7	18.7	18.0
Annual installed cap. growth rate (%)	41.3	6.6	7.8	9.3	13.3	14.7
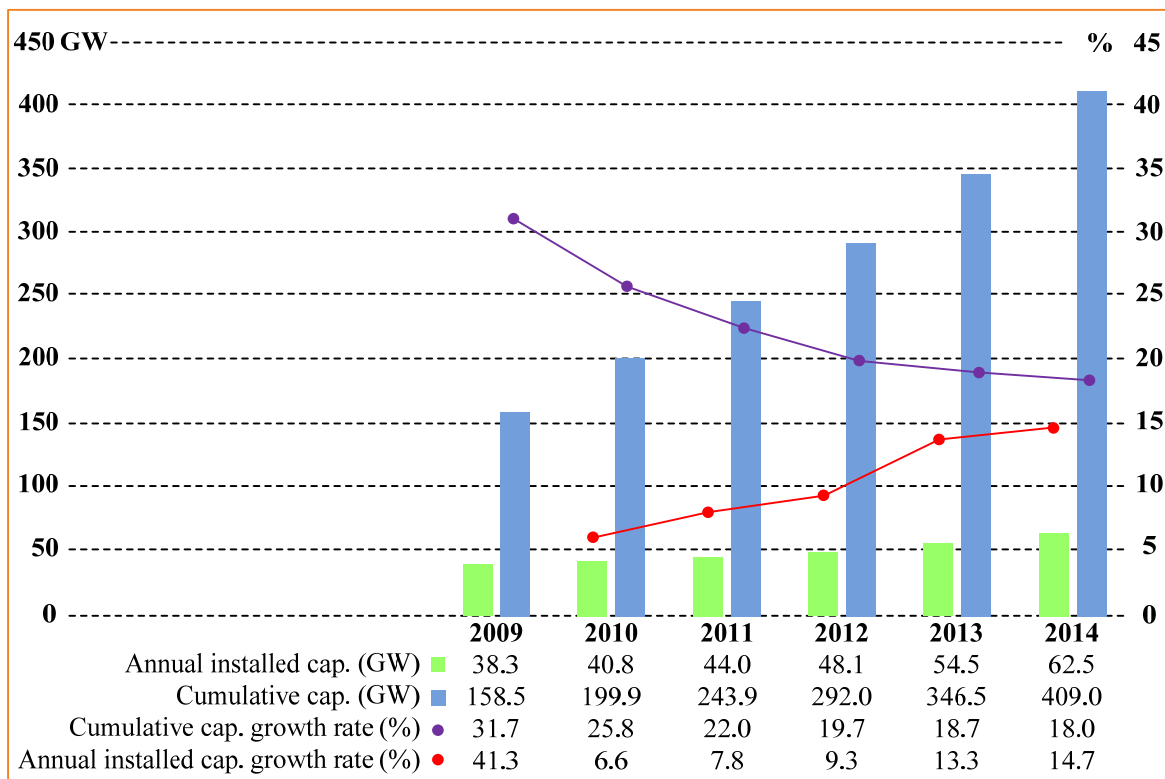
Fig. 1.1-2 Global wind power market forecast year 2010 – 2014

1.1.2 Wind power development in Canada

Canada has been exploiting wind power for more than 100 years [4], and its wind power generation nowadays is keeping in pace with the global development. The cumulative installed capacity in Canada increased steadily since 2000, as demonstrated in Table 1.1-1 [1] [3] [5].

Table 1.1-1 Development of total installed wind power capacity in Canada

Year	2000	2001	2002	2003	2004	2005	2006	2007	2008	2009	2010
Cap. (MW)	137	198	236	322	444	684	1,460	1,846	2,369	3,319	4008

The quality of Canada's wind resource is as good as or even better than any of the world's leading wind energy nations such as Germany, Spain and the United States [6]. However, the development of wind power in Canada is not satisfactory and trails most of the countries in the developed world. Although every province now has at least one operating wind farm, the electricity produced account for only about 1.1% of Canada's total power generation [6]. By the end of 2010, Canada ranks the 9th in the world in terms of installed capacity [1].

One of the reasons is that the control and protection of wind power generation systems to be integrated to the electric grid remains a major obstacle to the increased deployment of wind energy in Canada [6]; besides, even though the wind energy conversion systems consisting power electronic devices for wind turbines are evolving rapidly, they also face technical challenges in determining wind turbine performance both in normal and abnormal grid operations, including maintaining the optimal efficiency, withstanding severe weather conditions, and so forth. Another possible excuse for neglecting wind power development is the big share of existing renewable energy in Canada's electric power system, which mainly comes from the hydroelectric power and accounts for about 60 percent of the total electricity generation. This results in reliable service and the lowest price in the world for the good aspect, while the lack of pursuing new type of technology for the negative one.

Fortunately, the worldwide rapid progress and the domestic demand for the industry upgrade promote the application and development of wind power. As a practice of emphasizing the wind

power utilization, the first feed-in law in North America was adopted in Ontario on May 14, 2009 [7], which encourages the development of wind energy in Ontario. Wind power facilities of 2,004.5 MW capacity will be built under the tender call from Hydro-Québec for the purchase of wind energy produced in Québec and the electricity production will begin at various dates between December 2011 and year-end of 2015 [8] [9]. The WindVision 2025 prepared by Canadian Wind Energy Association (CanWEA) in October 2008 set a goal of producing 20 percent or more of the country's electricity production from wind energy by 2025.

1.2 Wind Energy Conversion System

1.2.1 Basic configuration

The development of a WECS involves technologies in various aspects. Up-to-date technologies have been consistently applied to WECS and results in miscellaneous designs available on the market or in the literature. However, the modern grid connected high power WECS utilizes power converters without exception and shares a common configuration, as shown in Fig. 1.2-1. A variable-speed WECS typically consists of a wind turbine, an optional drive train (gear or gearless), a generator (synchronous or induction), a power converter and a step-up transformer.
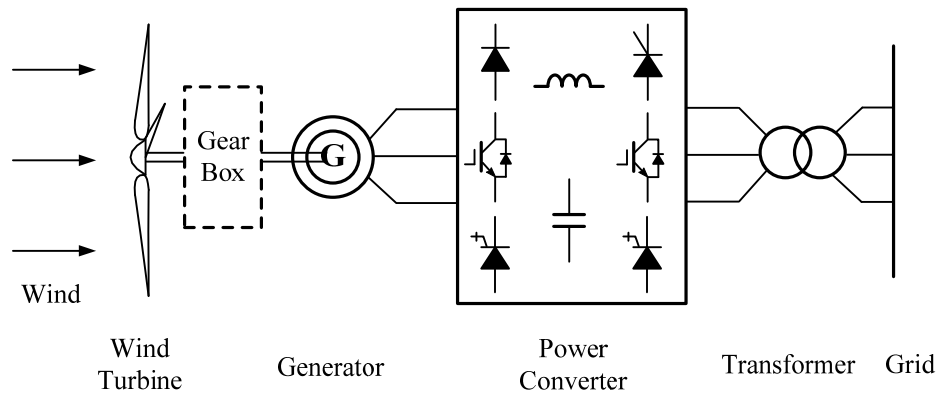
Fig. 1.2-1 Basic configuration of the contemporary WECS

The wind blows and pushes wind turbine blades to rotate. In this process, the kinetic energy from the wind is converted into the rotational mechanical energy in the wind turbine. The

generator rotor is mechanically coupled with the wind turbine through the drive train, which can be either directly connected or through a gearbox. The gearbox works as a speed multiplier to step up the rotational speed of wind turbine to match that of the generator. The mechanical energy is then transformed into electric energy by the generator, whose output fluctuates with the wind. A power converter is therefore necessary for grid integration to convert the variable voltage variable frequency generator output to a fixed voltage fixed frequency power. Finally, the WECS is connected to the grid through a voltage step-up transformer.

The power converter for WECS can be categorized into two main groups: voltage source converter (VSC) and current source converter (CSC). Both types of converters include two-stage power conversions, AC to DC and DC to AC. As the name indicates, VSC has a large DC capacitor to maintain desired DC voltage level in the DC link, while CSC uses a DC inductor to smooth the DC-link current. Although the commercially available WECS today all employs voltage source converter, current source converter also exhibits particular advantages and potential options for this application.

1.2.2 Wind turbine characteristics

The mechanical power extracted by the wind turbine depends on a few factors. (1.2-1) indicates the power contained in the flowing air passing the defined area of the wind turbine blades, where ρ is the mass density of air, A is the swept area of turbine blade and v_w is the wind speed. Furthermore, with consideration of the power coefficient C_p, the mechanical power obtained in the wind turbine can be expressed in (1.2-2) [10]:

$$P_w = \frac{1}{2}\rho A v_w^3 \tag{1.2-1}$$

$$P_T = \frac{1}{2}\rho A C_p(\lambda, \beta) v_w^3 \tag{1.2-2}$$

The power coefficient C_p is determined by the aerodynamic design of the turbine and varies with the turbine blade pitch angle β and tip speed ratio λ. λ is the ratio of turbine blade tip linear velocity to the wind speed defined by (1.2-3) [10], where ω_T and R are turbine rotational speed and radius respectively.

$$\lambda = \frac{\omega_T R}{v_w} \tag{1.2-3}$$

The power coefficient C_p can be modeled by following equation [11],

$$C_p(\lambda, \beta) = c_1 \left(\frac{c_2}{\lambda_i} - c_3 \beta - c_4 \right) e^{\frac{-c_5}{\lambda_i}} + c_6 \lambda \tag{1.2-4}$$

in which

$$\frac{1}{\lambda_i} = \frac{1}{\lambda + 0.08\beta} - \frac{0.035}{\beta^3 + 1} \tag{1.2-5}$$

Table 1.2-1 lists the values for the coefficients of c_1 to c_6, from which the sample curves of C_p can be plotted and are shown in Fig. 1.2-2. It can be viewed that there is a maximum power coefficient for a defined pitch angle β. For example, the correspondent maximum C_p is about 0.48 when the optimal tip speed ratio λ_{opt} equals 8.1 in the case of zero degree pitch angle. Further, the output mechanical power of the wind turbine can then be calculated and the related curves are plotted in Fig. 1.2-3, in which the pitch angle is set as zero degree.

Table 1.2-1 Values of c_1 to c_6

c_1	c_2	c_3	c_4	c_5	c_6
0.5176	116	0.4	5	21	0.0068

Similarly, it can be found from Fig. 1.2-3 that for each wind speed, the power coefficient C_p peaks at a certain rotational speed, which means the maximum power can be drawn from the wind at this operating point. It is a natural expectation that the WECS should be controlled to operate at the optimal rotational speed to maximize the generated power at different wind speeds, that is the so-called maximum power point tracking (MPPT).
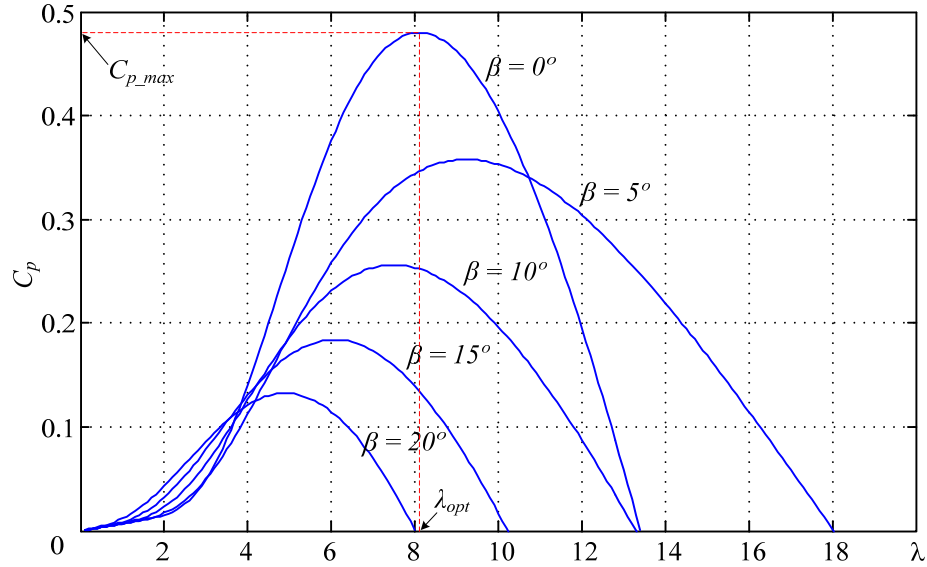
Fig. 1.2-2 Power coefficients over tip speed ratio at various pitch angles
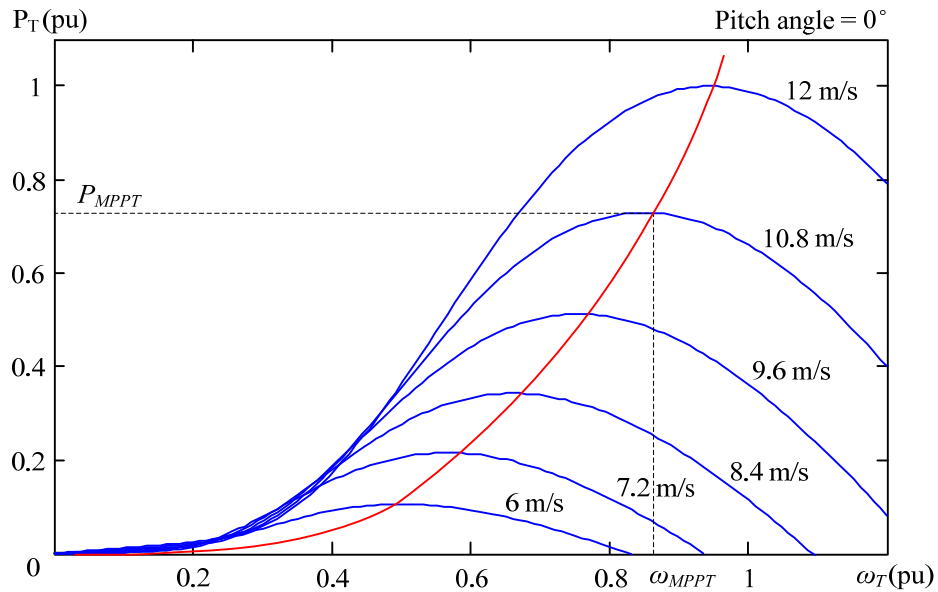
Fig. 1.2-3 Wind turbine power characteristics at zero degree pitch angle

In practical operation, the power control of the wind turbine can be divided into four different zones based on the variation of the wind speed, shown in Fig. 1.2-4 [12]. In Zone 1, the wind speed varies between zero and the cut-in velocity V_{in}, which is the minimum wind speed to drive the wind turbine, the power extracted from the wind is not sufficient to overcome the inertia of the rotor and the frictions, the wind turbine stays in standstill and is disconnected from

the grid; in Zone 2, the wind speed is between V_{in} and the designed rated velocity V_{rated}, there is enough power drawn from the wind, the wind turbine is driven and connected to the grid, it is in this stage that MPPT is applied; in Zone 3, the wind speed is greater than V_{rated}. To fully exploit the wind energy and make the best use of the turbine capacity, the wind turbine is controlled to produce the rated power; in Zone 4, the wind speed is greater than the cut-out velocity V_{out}, under which the available power in the wind is too much, therefore the turbine is forced to stop operation and disconnected from the grid to prevent it from damage.
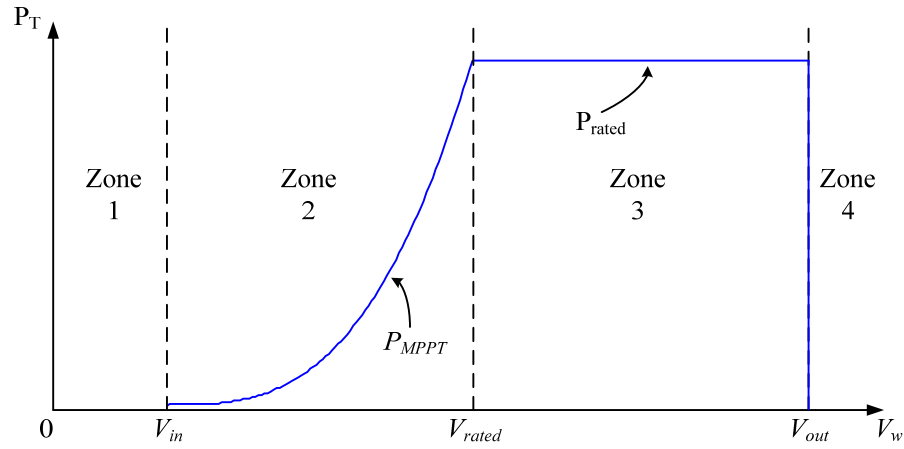
Fig. 1.2-4 Wind turbine output power control strategy

When the MPPT is maintained, the turbine speed is controlled in such a way that the maximum value of C_p is achieved, based on which the corresponding optimum tip speed ratio λ_{opt} can be determined by Fig. 1.2-2, resulting in the calculation of the wind turbine speed reference from (1.2-3),

$$\omega_{opt} = \frac{\lambda_{opt} v_w}{R} \tag{1.2-6}$$

in which ω_{opt} is the speed reference at which the maximum active power is maintained.

Under the MPPT condition, which is also regarded as the optimal operation, (1.2-2) and (1.2-6) can be further simplified as follows by introducing constants K_ω and K_p, which are determined by the aerodynamic characteristic of the wind turbine, namely, rotational speed is proportional to wind speed and mechanical power is proportional to the cube of the wind speed.

$$\omega_{opt} = K_{\omega} v_w \tag{1.2-7}$$

$$P_{opt} = K_p v_w^3 \tag{1.2-8}$$

1.2.3 Grid code requirements

Historically, after the wind turbine was introduced into the grid, there is no specific code requirements issued for a relatively long time. Nowadays the increasing wind power penetration to the grid has led to the elaboration of specific technical requirements for the connection of large WECS, usually as a part of the grid codes issued by the transmission system operators (TSOs). The grid code defines the behavior of the WECS under the normal operation as well as grid fault conditions. Typical grid connection code requirements for WECS include active power control, reactive power control and grid fault ride through.

Although different countries or TSOs issue their own specific requirements, they share some common objectives. They are to improve and stabilize wind turbine behavior, decrease the amounts or rule the ramps of wind power to be lost following system disturbances, ensure the power quality, system reliability and grid security, and anticipate the wind farms having operational characteristics similar to those of the conventional power plants.

(1) Active power control

The active power control is related to the frequency regulation in the power system. The grid normally operates under fixed frequency (50 or 60 Hz) within an acceptable small variation. In the early stage of the WECS development, the contribution of wind power to the frequency adjustment can be neglected or easily offset by the system reserves due to the relatively small amount; besides, the small wind turbines are generally regarded as negative load [13] because they usually connected to the distribution network. With the expanding of the wind power penetration and the increasing size of individual wind turbines, wind turbines or the wind farms are now required to be connected to the medium voltage or even high voltage transmission networks. Large WECSs are now considered as the real power source similar to the conventional power plants and should obey the same grid code regulation. Further, as the power electronic

devices applied in modern WECS may be affected largely by the grid operating state, e.g., the dip of the grid voltage, the variation of active power of the different types of wind turbines need to be classified and normalized.

In addition to frequency regulation, the acceptable changing rate of the generated power is normally defined in the codes by ramp-rate limitations to avoid large power transients under normal operation and to ensure in-time reestablishment of generated power after a fault,

(2) Reactive power control

The reactive power control is related to the voltage regulation. This is important not only under normal grid operations, but also during the grid disturbances or faults.

The control for reactive power (or the power factor) is a little complicated and varies according to the countries or TSOs, as it is directly related to characteristics of the power system, such as the grid topology, voltage variation and load level, as well as the capacity of wind turbine or wind farm. Fig. 1.2-5 shows the reactive power requirements in relation to active power according to Danish, British and German grid codes in principle. The Danish code limits the reactive power of the wind farm within the red parallelogram, under which the reactive power is 0.1 pu and the related power factor is 0.995 (leading or lagging). According to the German code, the wind farms with nominal power of less than 100 MW may have reactive power variation of 0.313 pu, which is the equivalence of 0.95 power factor (leading or lagging); for the rated capacity of wind farms no less than 100 MW, the reactive power is 0.313 pu (capacitive) and 0.38 pu (inductive), the related power factor is 0.95 leading and 0.925 lagging. The reactive power variation based on British code is more complex. Besides the limit of 0.313 pu reactive power, three more points, that is, 0.5 pu, -0.5 pu and -0.12pu are defined in extra.
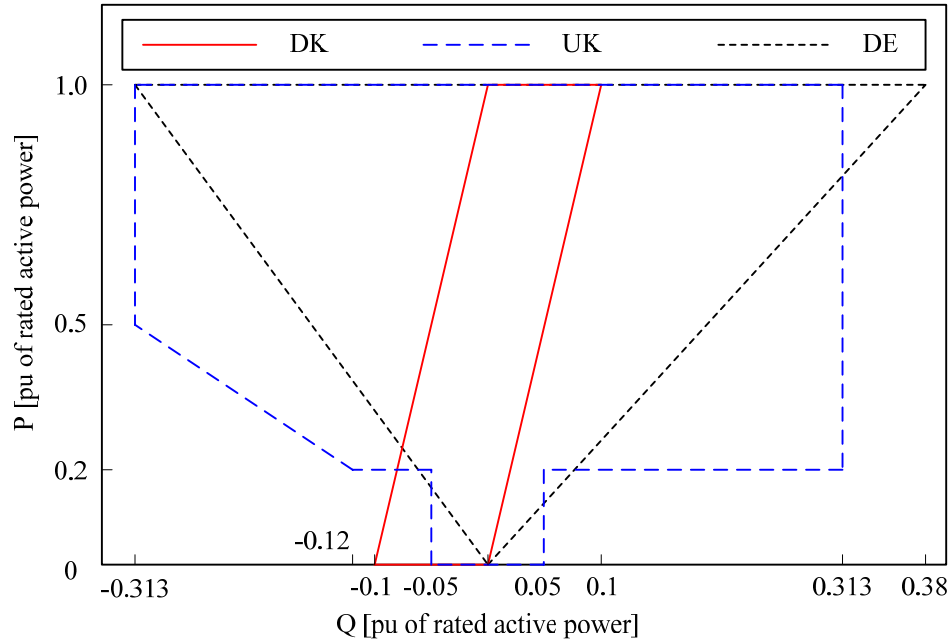
Fig. 1.2-5 Reactive power requirements related to active power - Danish, British and German codes

(3) Grid fault ride through

The behavior of WECS under grid disturbances or fault conditions is also defined in most of the grid codes in order to maintain the continuity and reliability of the power system operation. The fault types include a variety of symmetrical or unsymmetrical cases with different voltage levels and different time durations. A typical low voltage ride through requirement enforced by the German E. ON code is to request the wind turbines to remain in operation as long as the grid voltage envelop is above the defined curve, in which the grid voltage drops to zero for 150 ms and then recovers gradually back to its lower voltage band. Other grid codes have similar requirements but with different load and voltage profiles.

The research and development on the fault ride through (FRT) capability of wind turbine unit are attracting more and more interest lately. A common method is to employ external circuits with dynamic braking resistors or energy storage components to help dissipate the excessive power from the generator while the grid loses its capability to properly control the output power. These methods can be applied to various WECS configurations although detailed implementation may vary.

1.3 System Configurations of WECS

Prior wind power technology is reviewed in this section. A variety of system configurations have been developed for WECS. Each of the configurations has its own application areas and advantages/disadvantages.

1.3.1 Fixed speed WECS

When the wind energy conversion system began its application in power system in early 1990s, the standard installed wind turbines operated at fixed speed, which is usually equipped with squirrel cage induction generator (SCIG) directly connected to the power grid (The so-called "Danish concept"). This kind of WECS may have a power rating up to 2.3 MW [14].
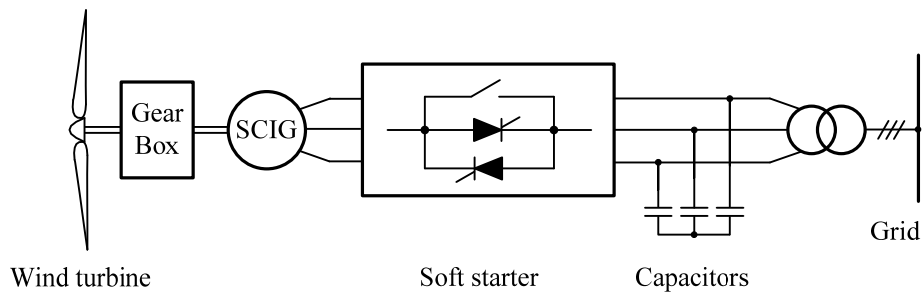
Fig. 1.3-1 Fixed speed type WECS

The structure of this concept is shown in Fig. 1.3-1. The extra capacitor bank at the grid side is used for reactive power compensation. A soft starter containing two thyristors connected anti-parallel in each phase may be inserted between the generator and the capacitor bank to provide smooth grid connection. This system is attractive because it is simple, robust, reliable and well-proven. However, the tower and the drive chain may suffer intense mechanical stress under sharp change of the wind speed. Moreover, the generator speed is locked within the small vicinity centering around the corresponding synchronous speed, and hence MPPT cannot be achieved in most of the operating points.

1.3.2 Limited variable speed WECS with dynamic slip control

As the wind is highly variable resulting in the variation of the wind power contained, the fixed speed WECS cannot satisfy the increasing demand of efficient power transferring under different operating conditions. The concept of variable speed wind turbine stands out in order to obtain higher energy yield and reduce the mechanical stress of the wind turbine. The limited variable speed WECS with dynamic slip control made a useful attempt towards increasing power transferring efficiency at different wind speed level. A typical example is the OptiSlip® concept applied by Danish manufacturer Vestas [15], shown in Fig. 1.3-2.
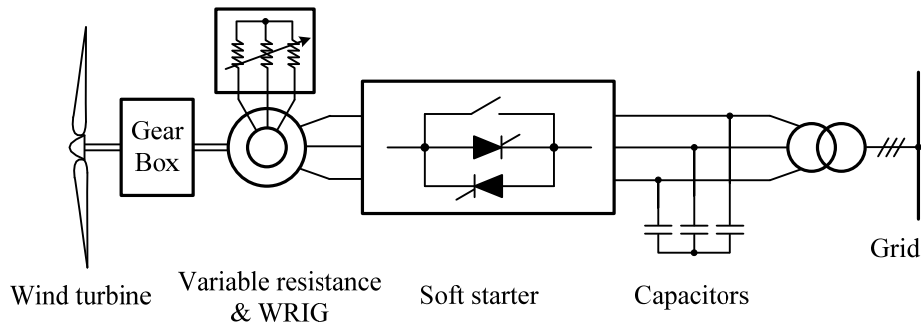
Fig. 1.3-2 Limited variable speed WECS - OptiSlip® concept

The main structure of this concept is similar to the fixed speed WECS, but the generator uses wound rotor induction generator (WRIG). This makes it possible to control the total rotor resistance through power electronic converter and external resistance mounted on the rotor shaft. The generator slip can be adjusted over a 0~10% range. Another major benefit of this arrangement is the elimination of costly slip ring and the brushes.

The main drawback of this WECS lies in the high power loss in the rotor windings. The high slip indicates high power consumption in the rotor and low generator efficiency. Taking a 2 MW wind turbine for example, a slip of 6% will result in a rotor power loss of 113 kW which brings the concern of heat dissipation.

1.3.3 Variable speed WECS with partial-scale power converter

New concepts for the WECS aiming at even wider variable speed operating range are further developed to increase the power transferring efficiency under various wind speeds. The mostly used variable speed configuration in the existing market is known as the doubly fed induction generator (DFIG) concept [16]. The configuration of a DFIG system is shown in Fig. 1.3-3.
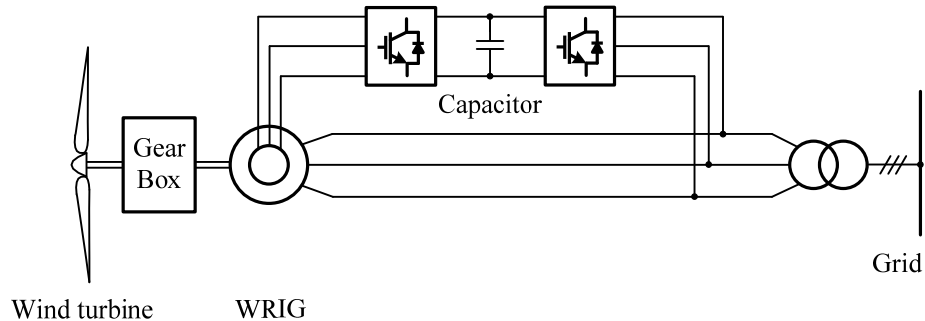
Fig. 1.3-3 Variable speed WECS with DFIG

The WRIG is also used in this WECS. The stator winding is connected directly to the grid, while approximately 30% of nominal power is delivered to the grid via a partial-scale power converter connecting the rotor winding and the grid.

In DFIG system, the capacitor bank and the soft starter used in previous system structures can be eliminated since the partial-scale power converter can provide the functions of reactive power compensation and smooth grid connection. The speed variation range is further increased to ±30% around the synchronous speed.

The costly gear box and the slip rings are the possible vulnerabilities which may contribute significantly to the initial investment, operation maintenance and downtime. The capability to control grid active/reactive power as well as to ride through grid faults is limited because of the reduced capacity of the power converter. External devices, such as crowbar, may be needed to further aid the grid fault ride through. These drawbacks shadow the future development of this type of WECS.

1.3.4 Variable speed WECS with full power converters

Nowadays the variable speed WECS connected to the grid via full power converters attracts more and more interests. This type of WECS can be controlled flexibly to track the maximum power at any operating wind speeds, reduce mechanical stress on the wind turbine, and provide better performance under grid fault conditions compared with other types of WECS. Fig. 1.3-4 shows the basic structure of WECS with full power converters [17].
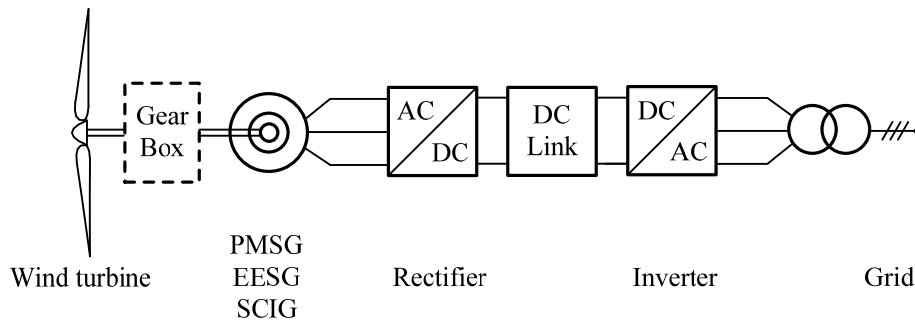
Fig. 1.3-4 Block diagram of WECS with full power converters

The generator in Fig. 1.3-4 can be electrically excited synchronous generator (EESG), permanent magnet synchronous generators (PMSG), or squirrel cage induction generator (SCIG). The converter in this configuration is relatively expensive and low in efficiency since it's designed to handle the full power. However, the very converter fully decouples the generator and the grid sides, and offers full controllability over the entire operating range. In addition, this configuration is possible to work with the direct drive or semi-direct-drive technology to eliminate or reduce the complexity of the costly gearbox, thus offsets the disadvantage of increased converter cost.

Table 1.3-1 summarizes the characteristics of the full power converter WECS configurations with different generators, and related main manufacturers are also listed. All of the above mentioned three types of generators have been applied in the commercial products. The squirrel cage induction generator is simple and robust but cannot be operated under the stand-alone state and is not suitable for the direct drive design. A multiple-stage gear box is often necessary. The EESG involves extra field winding and converter to produce field current, and is therefore

bulkier and produces more rotor loss than PMSG.

Lately, with the development of the permanent magnet material and the advancement of the mechanical manufacturing, the direct drive PMSG WECS becomes more and more preferable. The generator is designed with multi-pole for low speed operation and thus has a relatively large diameter [18]. The advantages include high overall system efficiency, compact structure, reduced rotor loss because of the permanent magnet, and low maintenance due to the elimination of the gear box.

Table 1.3-1 Characteristic of the configurations with different generators

Type	Asynchronous Generator	PMSG		Direct drive	
				EESG	PMSG
Gearbox	Multiple	Single stage	Multiple stage	No	No
Weight	Moderate	Moderate	Heavier	Heaviest	Half of EESG
Efficiency	High	High	High	Higher	Highest
Cost	Moderate	Moderate	Higher	Highest	High
Manufacturer	Siemens Vestas	Multibrid WinWind	GE Vestas	Enercon	GE Siemens Goldwind

1.3.5 Technology trend

The above introduction and review of prior art imply the future development of WECS and its rising role in contemporary electricity production. A few major technology trends are summarized as follows.

The power level of the WECS continues to increase. The main driving force is the associated cost saving in initial foundation and the increase of energy harvest capability at higher altitudes with higher wind speeds. The unit capacity of early installed commercial wind turbines in 1970s was 10 to 15 kW [19], and then the mainstream wind turbine amounted to 0.6 MW in 1990s [20], which is regarded as utility scale level. In the middle age of 2000s, megawatt wind turbine with a rated power of 1.5 to 3 MW became an onshore standard [21]. For the offshore WECS

application, the unit capacity was once 0.45 MW [22], and 5 MW wind turbine is now put into commission [23]. An even larger unit capacity WECS of 10 MW is currently under design and development [24].

Another important propulsion towards the higher turbine ratings is the emerging offshore wind farm technology. A few challenges present for the offshore applications, such as high initial construction cost, severe working condition and relative long distance cable to onshore power grid. Nevertheless, offshore wind characterizes higher speed and more stable conditions than that on land [25], which boost the energy harvest efficiency of offshore wind turbines. Besides, the impact on the environment and human life of offshore wind turbines is less than that of onshore ones. All these render the offshore WECS attractive and increasing investments was found in the most recent years. In 2010, the investments on offshore wind energy sector grew by 30% as compared to that of 2009 [1].

Large wind turbines or wind farms have to be connected to the power system to effectively utilize the generated electrical energy [26]. With high penetration of wind power, the power quality and system stability caused by WECS become significant and raise concerns. It is therefore widely recognized that the turbines should be designed to be compliant with the grid connection codes to enable large scale wind penetration without compromising system stability.

Variable speed operation becomes the dominant technology in large WECSs due to its higher energy efficiency and lower mechanical stress. Among all the available variable speed configurations, permanent magnet synchronous generator (PMSG) with full power converter is more and more favored [27] although doubly-fed induction generator (DFIG) still dominant the market. Detailed advantages and disadvantages of these two configurations can be found in subsection 1.3.3 and 1.3.4.

In terms of the full power converter for the configuration of the PMSG WECS, low voltage (LV) voltage source converter (VSC) is widely applied in commercial WECS. In order to adapt to the high power wind turbine system, several LV converters has to be paralleled in order to produce the desired power, which is inefficient and unreliable as compared to the medium voltage (MV) converter solutions. By far, there are limited MV converters running in the field

for large WECS. However a movement towards the application of MV converters in WECS can be noticed nowadays. It is therefore worthwhile to exam existing converter technologies and develop suitable solutions for the application.

1.4 Research Objectives

This thesis aims at presenting a suitable power converter for high power medium voltage WECS. The configuration of PMSG with full power converters appears to be promising in the future and is therefore adopted in the thesis. The main objectives lie in the novel configuration design, control scheme development and system optimization.

(1) Converter topology evaluation and selection

The main objective and mission of this thesis is to find a simple, low cost and practical converter configuration for WECS. The selection of converter topology requires detailed analysis and evaluation so as to achieve a proper balance between the premium performance and the simplicity of the system.

(2) Appropriate design of power components

Once the converter topology is determined, the design of the power components in the system becomes crucial for overall performance. The work includes design of system voltage and current ratings, filter structure and size, and etc.

(3) Control system development and optimization

The main control objectives in the proposed WECS need to be identified for the control system development, such as MPPT or grid power factor control or both. In addition, the applicable control scheme is also dependent on the generator configuration, converter topology and system specifications. Therefore, the objective involves intensive work on steady-state operating condition calculation, control loop design and analysis, and system optimization.

(4) Simulation model development and verification

An appropriate and comprehensive simulation model for the proposed system should be developed to facilitate the theoretic analysis and the design. Reasonable predefined conditions and assumptions need to be made to ensure the accurate reflection of the practical system.

1.5 Thesis Organization

There are five chapters in this thesis. Chapter one serves as the background study and general introduction of the research work. The status of world-wide wind power utilization is introduced first, followed by the basics of wind energy conversion systems. Various system configurations used in practice are reviewed, based on which the developing trend of WECS can be summarized. The main research objectives are then explained with related challenges and difficulties identified and discussed.

Chapter 2 gives extensive and comprehensive literature review on the various topologies of power converters, which are applied in different types of WECSs. The role and function of the power converters are discussed, and related control schemes are evaluated. The review helps in the choice of a suitable converter solution for high-power WECS.

Chapter 3 presents the proposed system configuration and converter topology. The steady-state operating values are calculated and employed for the analysis of system operating range. The control scheme for the proposed system is then developed to achieve the control objectives and optimize the system performance.

Chapter 4 illustrates the simulation results for the proposed system. The simulation model is constructed in Matlab Simulink and explained in detail. Simulation results are provided in various operating conditions to help verify the feasibility of the proposed system and the control system performance.

In conclusion, Chapter 5 summarizes the main contributions and conclusions of the work. Possible future work is discussed briefly in the end.

Chapter 2   Power Converters for WECS

Variable speed technology is widely applied in modern WECS for maximum energy harvest, minimum mechanical stress and other optimum control objectives. To accommodate the wide-range variable speed operation, a power electronic converter is indispensable, which converts the variable wind power to the form that can be integrated to the grid. The power converter performs AC-AC power conversion, where the input voltage varies in both frequency and magnitude greatly, and the output voltage is fixed both in frequency and magnitude. A wide selection of converter topologies can be employed to achieve the goal.

This chapter reviews the converter topologies commercially operated or proposed in the literature for high power WECS. The advantages and disadvantages of each converter topology are discussed, based on which a new converter topology to be used for the thesis is initiated. In the end, the most commonly used control schemes are introduced to facilitate the control system development for the proposed system.

2.1 Voltage Source Converters

Among the commercially available WECSs, voltage source converters dominate the market for wind power conversion. As the name indicates, this category of converter generally employs large capacitor in the DC link to maintain the desired voltage level. A few mainstream VSC topologies applied in practical or under research are discussed in this section.

2.1.1 Two-level back-to-back voltage source converter

A WECS using two-level back-to-back voltage source converter is shown in Fig. 2.1-1 [17]. The converter is composed of two PWM voltage source converters, namely voltage source rectifier (VSR) and voltage source inverter (VSI) connected back to back. The DC link capacitor functions as the energy storage component and the filter for the DC voltage. The switching devices used are generally IGBTs, which can be actively turned on and off by providing proper gating signals and has an anti-paralleled diode embedded.

The topology is a mature technology and is widely used in various variable speed WECS configurations, such as DFIG or direct drive PMSG configuration. In a direct drive PMSG WECS as shown in Fig. 2.1-1 [28], the converter enables fully decoupling of the wind turbine unit from the grid, and offers flexible control for turbine speed regulation, power delivery and even the grid fault ride through. Besides, this topology features the ability to operate completely in a stand-by situation, which can be applied to form the islanding network [29].
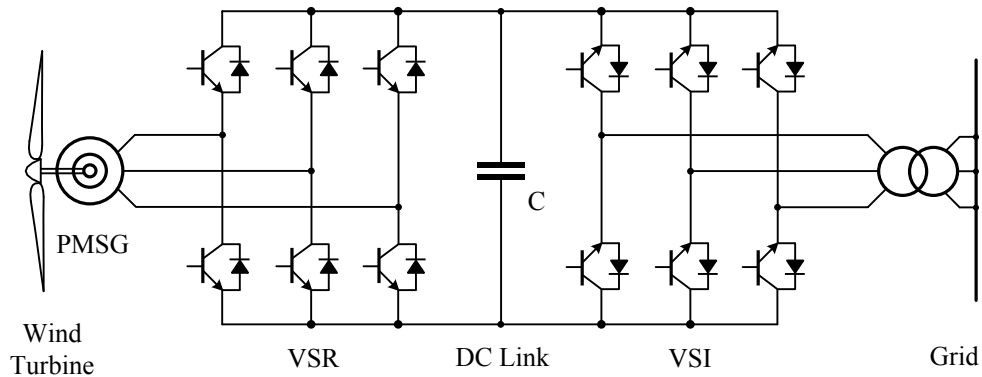

Fig. 2.1-1 Direct drive PMSG with back-to-back voltage source converter

In order to obtain higher power level, it is necessary to connect several low voltage modules in parallel to provide the required current and power. Fig. 2.1-2 shows the block diagram of the converter topology used by Enercon E series wind energy converters.
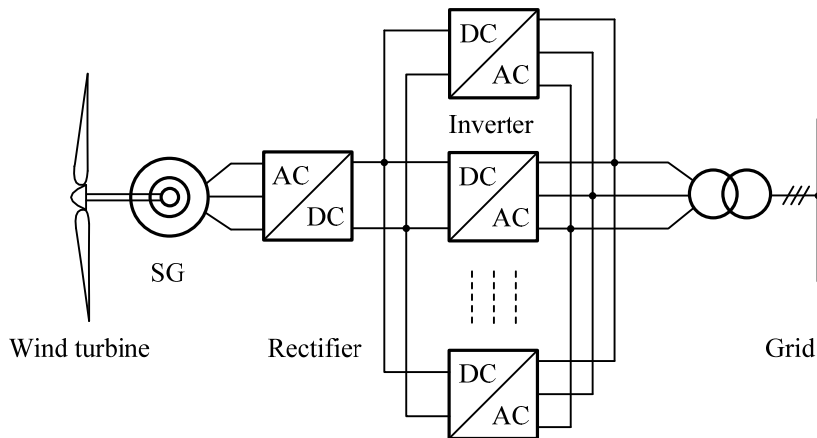
Fig. 2.1-2 Enercon E series wind energy converter topology

To date, the wind energy system normally supports low voltage (690V) converter technology, where the converters are typically rated at 0.3MW to 0.75MW each using standard IGBT modules. However, this design presents a number of technical concerns: reduced reliability due to possible circulating currents, high component count, low efficiency and increased cost.

2.1.2 Reduced cost VSC using diode rectifier and boost converter

The power flow for the WECS is usually unidirectional from the generator to the grid. Diode rectifier is therefore possible to be applied to save the cost and simplify the control scheme. Fig. 2.1-3 shows the configuration of diode rectifier and VSI assisted by boost converter in the DC link. Vensys has applied this topology for its products as early as in 2000 [30].

Diode rectifier provides simplified low-cost AC-DC conversion without using actively switching devices. In this sense, the converter switching signal generation and consequential switching loss of the VSR in Fig. 2.1-1 are eliminated. On the other side, the harmonics in the generator stator winding will increase due to the lack of PWM switching.

The boost converter is essential for the full-range variable speed operation of this WECS. As the diode rectifier cannot be controlled, its output voltage varies in a large range with the wind speed. Specifically, the output DC voltage is relatively low under low wind speeds, which may not be able to satisfy the voltage requirement for the normal operation of the VSI. By controlling the boost converter properly, the DC voltage for the VSI can be elevated to support proper control of the grid side converter.
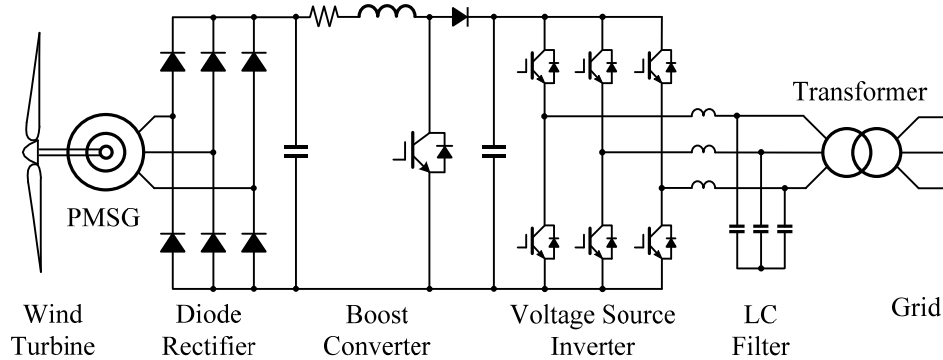
Fig. 2.1-3 Direct drive PMSG using PWM VSI with diode rectifier and boost converter

The above converter topology can be evolved to be applied for high power medium voltage applications through the series connection of the power electronic devices and parallel connection of the converters. A topology proposed in the literature [31] is shown in Fig. 2.1-4, where the component count is substantially increased.
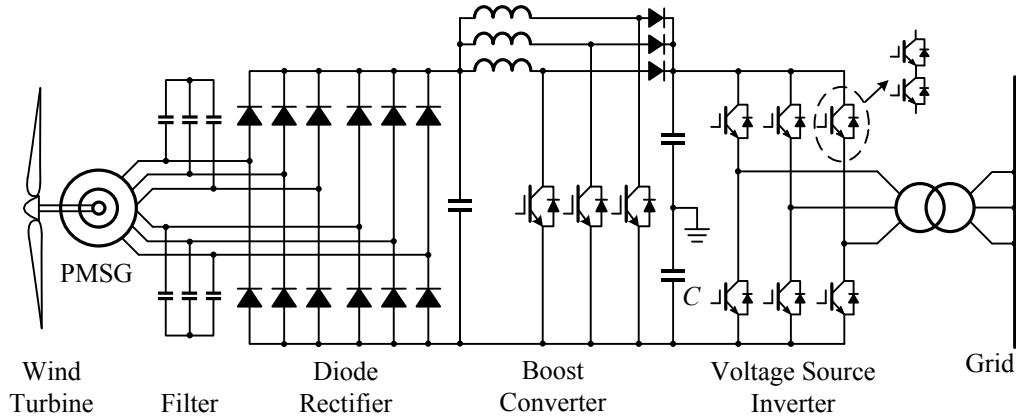
Fig. 2.1-4 Direct drive PMSG using PWM VSI with diode rectifiers and boost converters for high power application

On the grid side, the converter is still two-level PWM VSI, but each of the leg has more than one IGBT devices connected in series to withstand the voltage level. On the generator side, parallel connection of diode rectifier is not practical due to lack of control and possible large circulating current. The PMSG is designed to have two or more sets of three-phase windings, each of which fed a diode rectifier bridge. Generally, the phase angle of the two sets of windings can be 30 degree apart so that the machine works as a phase-shifted multi-pulse transformer to cancel out some certain orders of harmonics in the generator and in the mean time reduces the DC voltage ripple at the rectifier output. The three-phase capacitor bank at the generator terminals assists the current commutation in the generator and diode rectifier. The boost converters are parallel connected at both inputs and outputs. The switching device control signals of each boost converter are interleaved to reduce the output DC voltage ripple. As a result, the current rating and inductor size of each boost converter are reduced for high power applications.

2.1.3 Multi-level voltage source converters

The above two sections demonstrates the solutions employing series connection of power

electronic devices and parallel connection of converters for high power medium voltage WECS. These solutions in general raise the technical concerns such as reduced reliability due to the increased component count, device voltage balancing and circulating current among converters. An alternative is to employ multi-level converters for WECS, of which the technology is well proven in the medium voltage high power drive application. Multi-level VSCs comprise more devices to help produce AC voltage waveforms with multiple voltage steps. The converter topology and device switching are designed in such a way that each of the devices withstands only a fraction of the total voltage while the outputs added together forms a high voltage level. Compared to the two-level VSCs, they share several common features such as higher quality AC voltage waveforms with lower *dv/dt* and THD, exemption from device series connection and reduced common-mode voltage magnitude. Their price level is competitive and they include fewer components, which is an inherent advantage with respect to reliability.

On the existing market, the only multi-level converter currently being manufactured for large wind turbine systems is the neutral point clamped (NPC) converter. Fig. 2.1-5 demonstrates the NPC converter adopted by ABB for medium voltage PMSG WECS up to 5 MW [32]. Similar inverter structure is also applied by Converteam on its 5MW PMSG [33]. The NPC inverter uses neutral point diodes to switch the neutral point potential to the output terminals. This results in smaller voltage steps at the output and lower current ripple. And those diodes also guarantee the voltage sharing between the two blocking switches without the need of special voltage sharing networks. Each switch withstands only half of the total DC voltage during commutation.
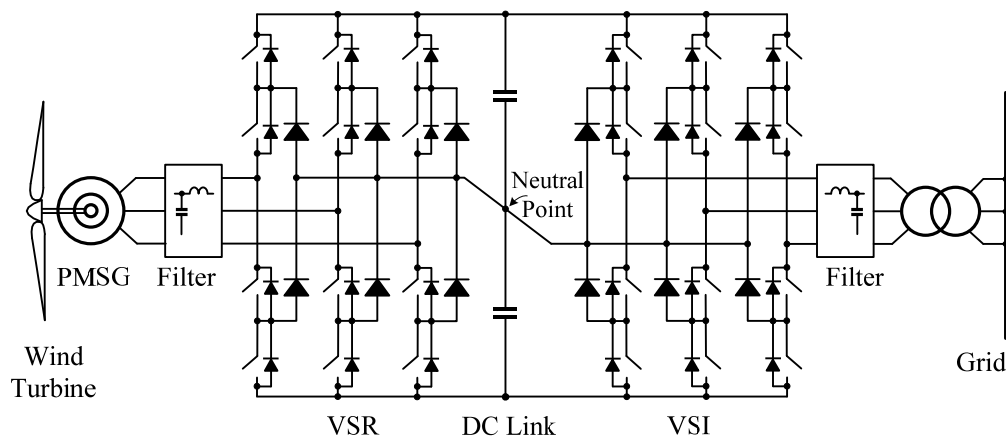

Fig. 2.1-5 Direct drive PMSG with three-level NPC converter

2.2 Current Source Converters

The above listed VSCs are the typical converter topologies being used in the existing WECSs. Rather than focusing on the well-developed VSC topologies, this thesis exams the current source converter topologies for WECS. In the high power medium-voltage range, the current source converter is widely used in industrial drive applications due to simple converter topology, motor-friendly waveforms, and reliable short circuit protection [34]. Although there is no existing WECS product using current source converters, this branch of converters exhibits promising features. A few current source configurations have been proposed in the previous literature and will be discussed in the following subsections.

2.2.1 Back-to-back current source converter

Similar to the back-to-back VSC, the PWM current source rectifier (CSR) and the PWM current source inverter (CSI) can be connected back-to-back for PMSG WECS [35], which is shown in Fig. 2.2-1. Symmetrical gate commutated thyristor (SGCT) with reverse voltage blocking capability is usually applied as the switching device. An inductor is inserted in the DC link to smooth the current. The generator- and grid-side capacitor banks (C_r, C_i) are essential as they assist the current commutations during switching process as well as filter the current harmonics.

In drive applications, this topology can be operated up to 6.6 kV simply by connecting the SGCT devices in series. Compared to multi-level voltage source converter presented in Fig. 2.1-5, the topology has relatively low device count at similar voltage level. The DC link choke helps in limiting the current variation rate, and thus provides natural short circuit protection over grid low voltage or fault conditions. This is preferable for grid integrated WECSs as the grid low voltage ride through capability is now required by most of the grid codes. Furthermore, this topology employs active switching devices in both rectifier and inverter, and therefore gives the most freedoms for the control of active and reactive powers as well as the DC link current, from which the WECS requirements mentioned above can be fully satisfied.

The main concern of the topology is the possible resonances caused by the AC capacitors and grid/generator inductances, which needs to be mitigated by proper design of passive components and control scheme.
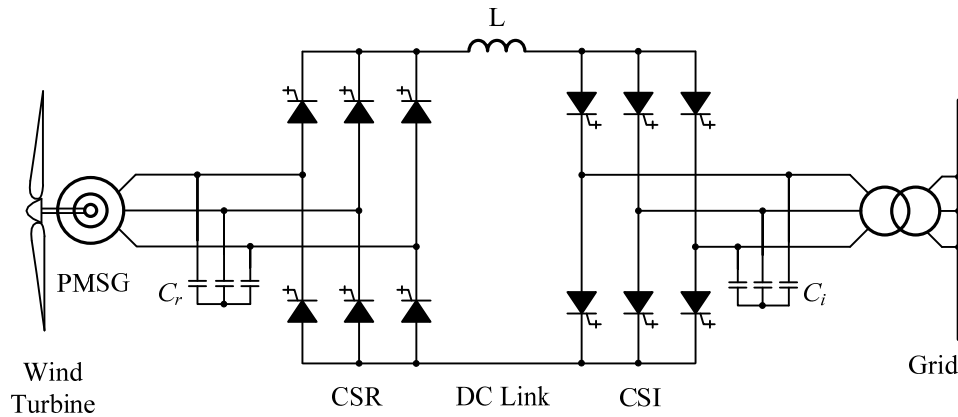
Fig. 2.2-1 Direct drive PMSG WECS with back-to-back current source converters

2.2.2 Thyristor based current source converters

Thyristor is the switching device mainly used for early CSC products. The technology is well-proven, reliable and relatively cheap. Thyristor based converters normally work in phase control mode since the device cannot be actively turned off. Two basic thyristor based CSC topologies proposed in the literature for WECS are: 1) thyristor rectifier and thyristor inverter; and 2) diode rectifier and thyristor inverter.

The thyristor based converter for WECS proposed in [36] is shown in Fig. 2.2-2. The topology resembles the structure of the back-to-back CSC but with line-commutated thyristor. While this topology features simple, inexpensive and robust, the drawbacks are obvious. With limited control freedom, the grid reactive power is not adjusted. External reactive power compensator is necessary for grid integration. Additionally, since the thyristors are switched only once per fundamental cycle, the AC side waveforms are highly distorted. To comply with the grid harmonics requirements, it is necessary to add extra passive filter or active harmonic filter. Similar concerns also apply to the generator side operation.
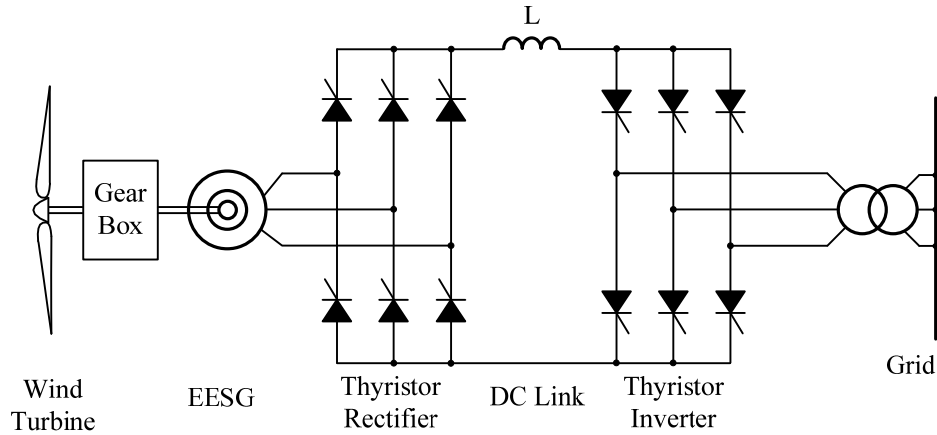
Fig. 2.2-2 Line-commutated thyristor based converter for EESG WECS

The generator side thyristor rectifier can be further replaced by a diode rectifier bridge [36] [37], as shown in Fig. 2.2-3. This topology brings down the converter cost at the price of losing the control freedom from the rectifier, which may narrow down the system operating range. Other disadvantages mentioned above are also found here.
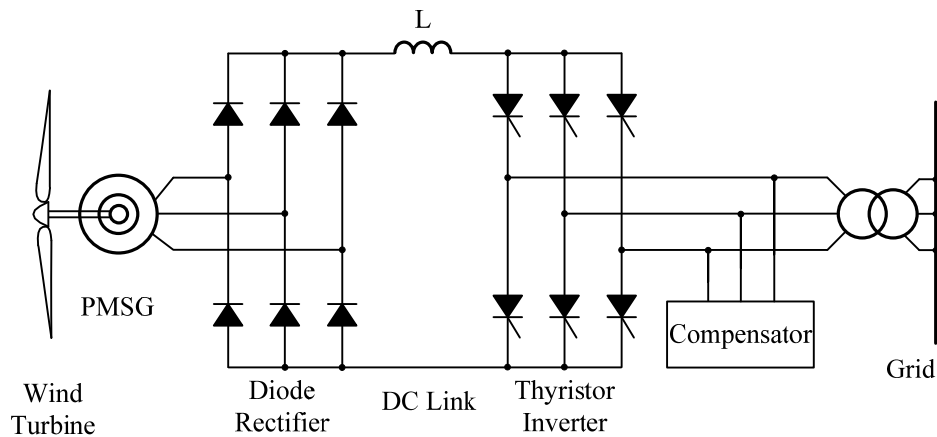
Fig. 2.2-3 Direct drive PMSG WECS using diode rectifier and thyristor inverter

2.2.3 Diode rectifier and PWM CSI

To balance the cost and performance, the topology using diode rectifier and PWM CSI appears to be another promising configuration for high power WECS, which is shown Fig. 2.2-4. PWM CSI serves as the grid interface to optimize the grid side performance, while the low cost diode rectifier is employed to generator power rectification. The following parts in the thesis will

perform detailed theoretical analysis on this topology and propose a novel converter configuration for CSC based WECS.
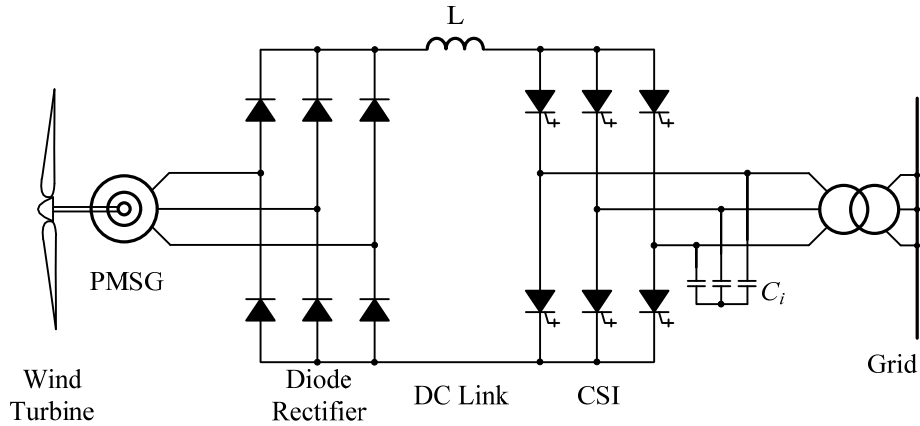
Fig. 2.2-4 Direct drive PMSG WECS using diode rectifier and PWM CSI

2.3 Power Converter Control Techniques

The control technologies applied for wind power conversion is directly related to the safe, premium and economical operation of the WECS. Basically, the power control lies in two aspects: one is the aerodynamic system with the goal to maximize the production based on the available wind power, and the other is the electrical system which aims at delivering the power to the grid smoothly and meeting the requirements of the local utilities. Since aerodynamics is not the main research interest in the thesis, this section focuses on the latter aspect, specifically, the control of the full power converter for variable speed operation of WECS.

As can be referred from Fig. 1.3-4, the full power converter is classified as rectifier (generator side converter) and inverter (grid side converter). There are lots of existing and mature control schemes that are developed for drive applications and can be adapted for wind power generation applications. It should be noted that the following discussions are mainly based on VSCs. The same ideas can be applied to the CSCs with certain modifications.

2.3.1 Generator side converter control

Generator functions as to convert the mechanical power into electrical power. It's desirable

to extract maximum power from the wind turbine under different wind speeds. This is realized by the generator side converter control to keep the generator speed at the optimal values. The main schemes are discussed as follows.

(1) Field oriented control (FOC)

This control scheme simplifies the regulation of AC machine by emulating the way a DC machine is controlled, in which when the flux produced by the field circuit is set as constant, the electromagnetic torque is proportional to armature current. The basic principle is to transform the three phase quantities in the AC machine into *dq* frame aligned to one of the fluxes in the machine. Based on the flux chosen, field orientation can be classified as rotor flux orientation, stator flux orientation and air gap flux orientation. The rotor flux orientation is relatively simple and widely used [34]. Fig. 2.3-1 shows a general diagram of field oriented control using rotor flux orientation [38].
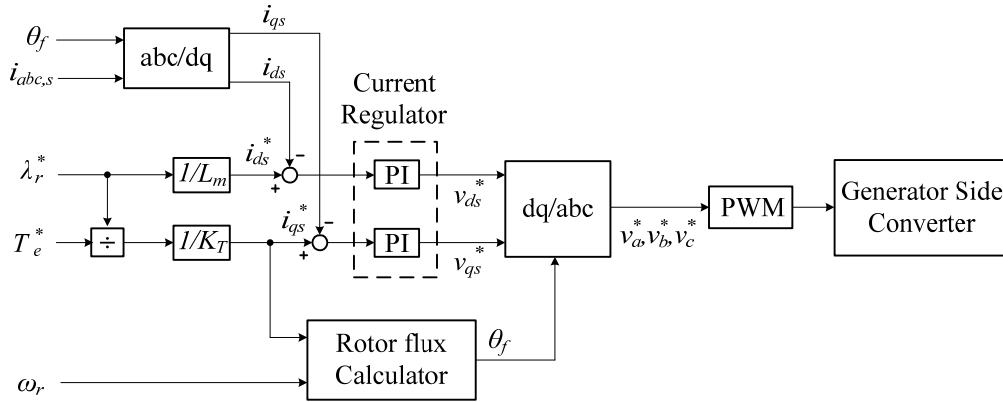
Fig. 2.3-1 General diagram of field oriented control

The three phase stator currents $i_{abc,s}$ are measured and transformed into *dq*-axis variables i_{ds} and i_{qs} using the rotor flux angle θ_f, i_{ds} is used to control the rotor flux and i_{qs} is used to control the electromagnetic torque. λ_r^* and T_e^* are the references of the rotor flux and the electromagnetic torque, respectively. ω_r, L_m and K_T are the rotor angular speed, mutual inductance between rotor and stator field, and machine constant. The outputs of the current regulator v_{ds}^* and v_{qs}^* are transformed into stationary frame AC signals v_a^*, v_b^* and v_c^*, which are utilized to generate the signals for PWM regulation. The FOC makes it possible to control the

torque and flux of the generator independently. To further enhance the dynamic performance , the space vector modulation (SVM) with flexible modulation index and delay angle control is usually applied.

(2) Direct torque control (DTC)

Direct torque control is another widely used strategy to control generator. Originally, DTC is applied to AC machine drives [39], and is naturally extended to AC generator applications. The general diagram of the direct torque control for AC machines is shown in Fig. 2.3-2 [34]. The stator currents and voltages are employed to calculate the actual values of the electromagnetic torque T_e and the stator flux linkage λ_s, which are compared with their corresponding references. Based on the torque and the flux linkage errors, two hysteresis comparators are applied, and the outputs of the hysteresis comparators as well as the flux angle are used directly to determine the switching states of the generator side converter. It can be viewed that the DTC controls directly the magnitude of the stator flux and the electromagnetic torque of the generator. Compared with the FOC, this control scheme features high static and dynamic response. Other characteristics include no coordinate transformation, robustness to the machine parameters, simple structure, and no current control needed [40]. However, there are some disadvantages for DTC, such as the high torque pulsation and fast sampling time requirements. Besides, the torque pulsation is related to the switching frequency. The lower the switching frequency, the bigger the torque pulsation [41].
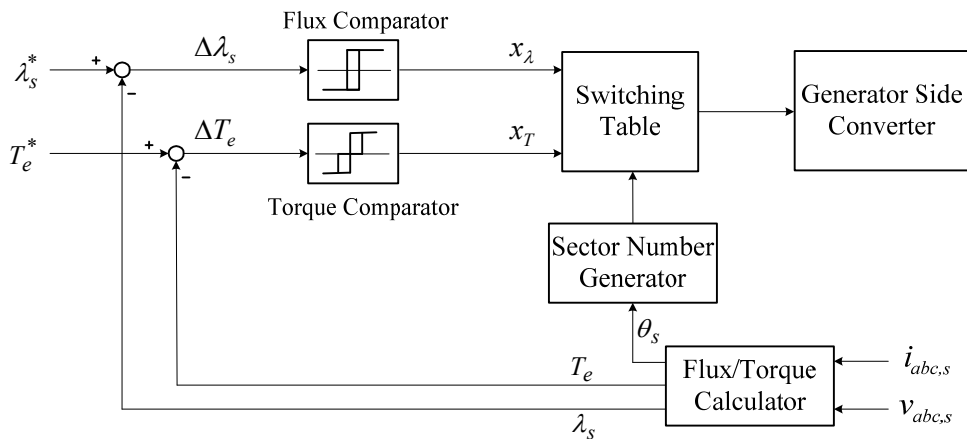

Fig. 2.3-2 General diagram of direct torque control

From the above introduction, both FOC and DTC can be applied for the generator side converter control scheme design with satisfied static and dynamic performance. There are appropriate situations for them to be applied. The FOC is preferable in the applications where wide range speed adjustment is needed, while the DTC is suitable for the applications where fast torque response is priority [42].

2.3.2 Grid side converter control

The grid side converter is mainly responsible for the quality of the output power and the grid code compliance. Different strategies are developed and applied successfully for the grid side power converter. The industrial applications are listed as follows.

(1) Voltage oriented control (VOC)

Voltage oriented control originates from FOC. It provides the fast dynamic response and high static performance through the internal current control loop. Fig. 2.3-3 shows a general diagram of voltage oriented control [43]. The grid side current $i_{abc,s}$ is decoupled into the active and the reactive power components, namely, i_{ds} and i_{qs}, which are compared with their corresponding references. The current errors are used for the PI controller to produce commanded voltage reference to be transformed in $\alpha\beta$-frame, v_α^* and v_β^*, from which the switching signals are generated. A Phase Locked Loop (PLL) is used for the coordinate transformation. It is worth noting that the accuracy of the PLL system for the grid voltage angle estimation directly determines the performance of VOC. Besides, to guarantee the fast response in the transient process, a space vector modulator (SVM) is typically applied.
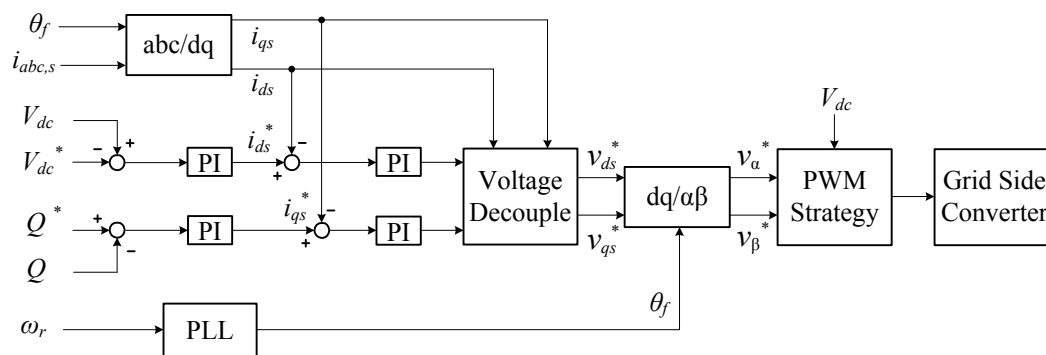

Fig. 2.3-3 General diagram of voltage oriented control

(2) Direct power control (DPC)

Direct power control originates from the aforementioned direct torque control while the control objectives in DTC, namely, the torque and the flux, are replaced by the active and the reactive power. The basic principle of the DPC scheme is the direct control of the active and the reactive power without any internal control loop or PWM modulator. The general diagram of DPC is shown in Fig. 2.3-4 [44]. The switching states are carefully selected via a switching table and the states are chosen based on the instantaneous error between the estimation and the desired active and reactive power, which are limited by a hysteresis band as presented in Fig. 2.3-4. The experimental comparison between VOC and DPC applied for distributed generation has been carried out in [45]. It concludes that the efficiency and average power factor are slightly better when VOC is applied.
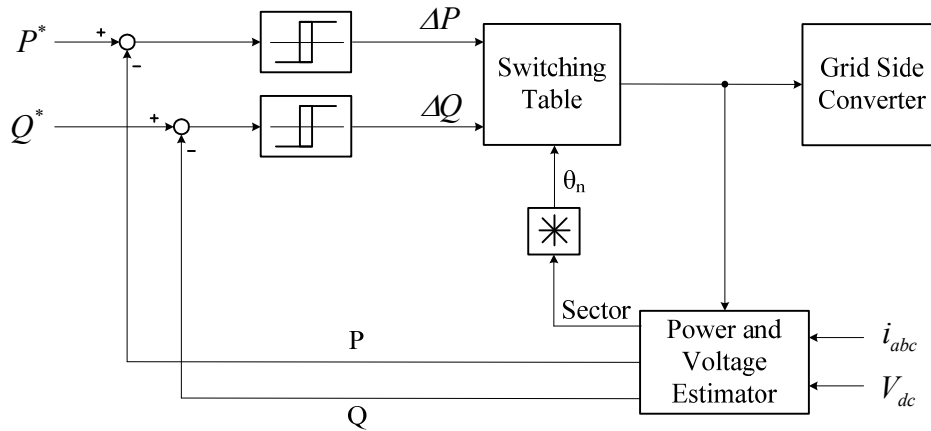
Fig. 2.3-4 General diagram of direct power control

In this chapter, the state-of-the-art wind technologies, including power converter topologies and control schemes are reviewed. A converter topology employing diode rectifier and PWM CSI are considered an interesting topology for wind power applications, and will be studied in the following chapters. Advanced vector control schemes introduced above will be applied to operate the converter to achieve desired system performance.

Chapter 3 Analysis and Control of CSI based WECS with Diode Rectifier and Buck Converter

Based on the above literature review, this chapter proposes a novel full power converter configuration for non-salient-pole PMSG based direct drive WECS. The converter employs PWM CSI together with diode rectifier and buck converter. Detailed steady-state analysis of the proposed configuration is presented to demonstrate the feasibility of the proposed system for achieving desired control objectives and wide operating range. Moreover, advanced control schemes are developed with consideration of appropriate system optimization. Basic functions for wind power system, such as maximum power tracking and grid reactive power compensation, are implemented in the control system. In particular, the control scheme also minimizes the converter system loss through proper DC current regulation without compromising the system performance.

3.1 Proposed System Configuration

The proposed converter configuration for the direct drive PMSG based WECS is shown in Fig. 3.1-1. The converter consists of a six-pulse diode rectifier for interfacing the generator, a PWM CSI for integration into the grid, and a buck converter between the rectifier and the inverter. The PWM current of the CSI, grid side line current and the capacitor bank current are represented by i_{wi}, i_s and i_c, respectively. The voltage and current reference directions are chosen as shown in the figure. The grid is simplified as an infinite voltage source with an equivalent inductance L_s.
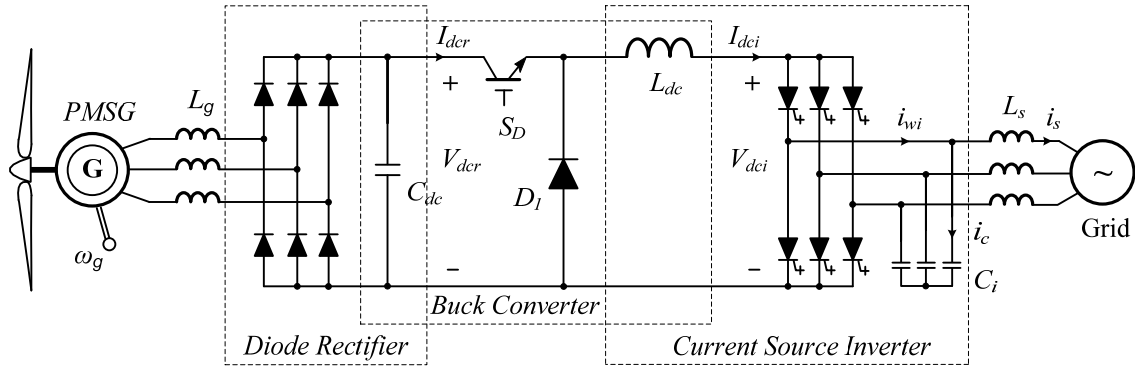
Fig. 3.1-1 Proposed converter configuration for a PMSG-WECS

As discussed earlier in the literature review, the PMSG is a more and more favored choice in high power WECSs. This is mainly due to its higher efficiency, smaller wind turbine blade diameter comparing to the electrically excited synchronous generator, and the advancement of the permanent magnet material as well as the corresponding construction techniques in large scale wind turbine manufacturing. The use of low speed, multi-pole PMSG directly coupled to the wind turbine rotor can further increase the system efficiency, reduce the overall cost and improve the reliability. Another major cost benefit is that a diode rectifier may be used at the generator output terminals since there is no need to provide external excitation for the generator.

The PWM CSI, which has found wide application in high power industrial motor drives, is employed to interface the grid. Its features include simple topology, sinusoidal output waveforms and reliable short circuit protection which makes it particularly suitable for megawatt WECS. The output capacitor C_i helps the current commutation of the PWM CSI for one thing, and smoothes out the current harmonics for another, from which the grid side waveforms are improved. The active switching devices bring the control flexibility for grid active and reactive power regulations.

A buck converter is added in the DC link to interconnect the diode rectifier and PWM CSI. It can be seen from Fig. 3.1-1 that the buck converter shares the same DC link inductor L_{dc} with the PWM CSI, while its filter capacitor C_{dc} assists to smooth out the diode rectifier output. The buck converter is necessary to guarantee full range operation of the system. The DC current from the rectifier output is boosted whenever needed to satisfy the grid side PWM CSI operation.

35

The theoretical analysis of each subsystem functions will be elaborated in the following sections.

3.2 Direct Drive PMSG and Diode Rectifier

The equivalent circuit of the direct drive PMSG in steady state operation is illustrated in this section. With the diode rectifier being connected, the relation between the output DC current of the diode rectifier and the electromotive force as well as the output active power of the PMSG under defined wind speed can be found.

3.2.1 Equivalent circuit of PMSG

The steady state equivalent dq-axis circuits of PMSG in the synchronous frame is shown in Fig. 3.2-1, where R_g is the generator stator winding resistance, v_{dg} and v_{qg} are d- and q-axis stator winding terminal voltages, i_{dg} and i_{qg} are d- and q-axis stator winding currents, L_d, L_q are d-, q-axis synchronous inductances.

(a) d-axis circuit   (b) q-axis circuit
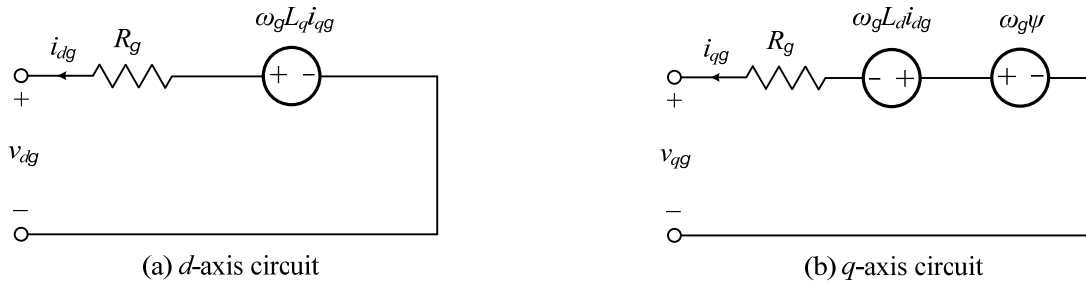
Fig. 3.2-1 Steady state equivalent dq-circuits of PMSG

The PMSG under discussion is the non-salient type, which means $L_d=L_q$, so the dq-circuits can be simplified as the one phase equivalent circuit, which is shown in Fig. 3.2-2 (a); and the phasor diagram is depicted in Fig. 3.2-2 (b). The X_g and R_g are the per phase stator winding synchronous reactance and resistance respectively. I_g and V_p are the stator current and phase voltage. E_p is the induced electromotive force in the stator winding and can be expressed as,

$$E_p = k\omega_g\psi \qquad (3.2\text{-}1)$$

where ω_g is the electrical rotational speed of the generator, and ψ is the rotor flux linkage. E_p leads ψ by 90 degree, k is the constant.

(a) Equivalent circuit   (b) Phasor diagram
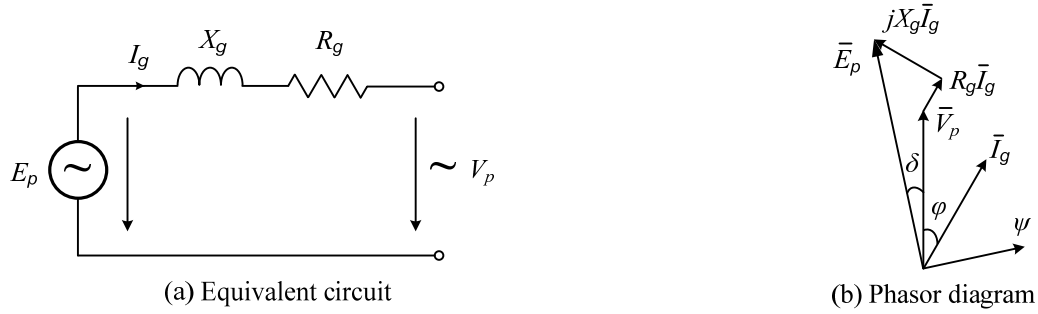
Fig. 3.2-2 Equivalent per phase circuit and the phasor diagram of the PMSG

The corresponding vector equation can be derived as,

$$\overline{E}_p = \overline{V}_p + \overline{I}_g R_g + j\overline{I}_g X_g \qquad (3.2\text{-}2)$$

3.2.2 Steady state operation of PMSG with diode rectifier

The steady state three phase equivalent circuit of the generator and the diode rectifier in the *abc*-frame is shown in Fig. 3.2-3 with the downstream parts of the buck converter being simplified as a DC current source. In the figure, $\overline{E}_g$ is the PMSG line to line induced electromotive force; $\overline{V}_g$ and $\overline{I}_g$ are the input phase voltage and current of the diode rectifier; X_g is the generator synchronous reactance as well as the line reactance, if applicable, the stator winding resistance R_g is relatively small compared to X_g and is thus omitted. V_{dcr} and I_{dcr} are output DC voltage and current of the diode rectifier, respectively.
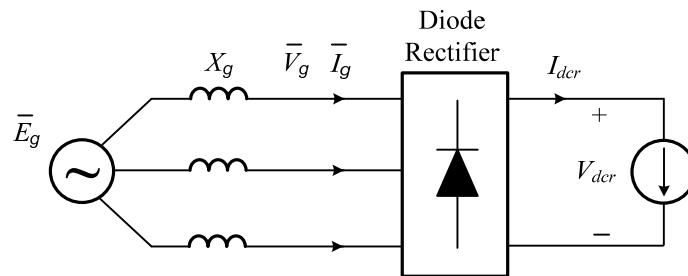

Fig. 3.2-3 Steady state equivalent circuit

Due to the presence of a large X_g, the current commutations in the diode rectifier are not instantaneous and will cause output DC voltage drop. If the commutation angle is less than 60° of the input fundamental frequency, the DC voltage V_{dcr} and the commutation angle δ of the diode rectifier can be calculated as follows [46].

$$V_{dcr} = \frac{3\sqrt{2}}{\pi} E_g - \frac{3}{\pi} X_g I_{dcr} \tag{3.2-3}$$

$$\cos \delta = 1 - \frac{\sqrt{2} X_g I_{dcr}}{E_g} \qquad (0 < \delta < 60°) \tag{3.2-4}$$

Assume the power obtained from the wind is transferred to the DC side with the loss being neglected, there is,

$$P_{dcr} = V_{dcr} I_{dcr} = P_g \tag{3.2-5}$$

Substituting (3.2-3) into (3.2-5) gives,

$$\left(\frac{3\sqrt{2}}{\pi} E_g - \frac{3}{\pi} X_g I_{dcr}\right) I_{dcr} = P_g \tag{3.2-6}$$

The DC current of the diode rectifier I_{dcr} can be calculated by solving (3.2-6), which is represented by (3.2-8) with (3.2-7) being taken into account.

$$X_g = \omega_g L_g \tag{3.2-7}$$

$$I_{dcr} = \frac{3\sqrt{2} E_g \pm \sqrt{18 E_g^2 - 12\pi \omega_g L_g P_g}}{6\omega_g L_g} \tag{3.2-8}$$

It can be derived from (3.2-8) that a constraint of the system parameters should be satisfied to ensure the real solution of I_{dcr}, as illustrated in (3.2-9).

$$E_g \geq \sqrt{\frac{2}{3}\pi \omega_g L_g P_g} \tag{3.2-9}$$

When (3.2-9) is satisfied, there is a real solution to the I_{dcr}, which means the MPPT can be achieved. This is the parameter constraint for the PMSG design which needs to be satisfied.

Based on (1.2-7), (1.2-8), with the constraint described in (3.2-9) satisfied, both solutions for I_{dcr} in (3.2-8) are positive. However, only the smaller one satisfies the pre-conditions described in (3.2-4). This means that for some certain PMSG parameters and specific wind turbine speed, there is a definite DC current at the output of diode rectifier. Suppose the DC current reaches 1 pu under rated wind speed, which is assumed as 1 pu too, we define the ψ and the L_g under this condition as original values, represented by x. Fig. 3.2-4 shows a family of relations in per unit system between I_{dcr} and the wind speed v_w with different ψ and L_g for the proposed configuration. The red solid lines represent the situation that L_g is the original value, the green dashed lines represent the situation that L_g is oversized to 1.2 times original value, and the black dashed lines represent the situation that L_g is decreased to 80% of the original value. The influence of the various flux linkage on I_{dcr} is also illustrated in the diagram. It is obvious that a larger inductance leads to an increase of the diode rectifier output DC current while an increasing magnet flux linkage leads to a decreased diode rectifier output DC current.
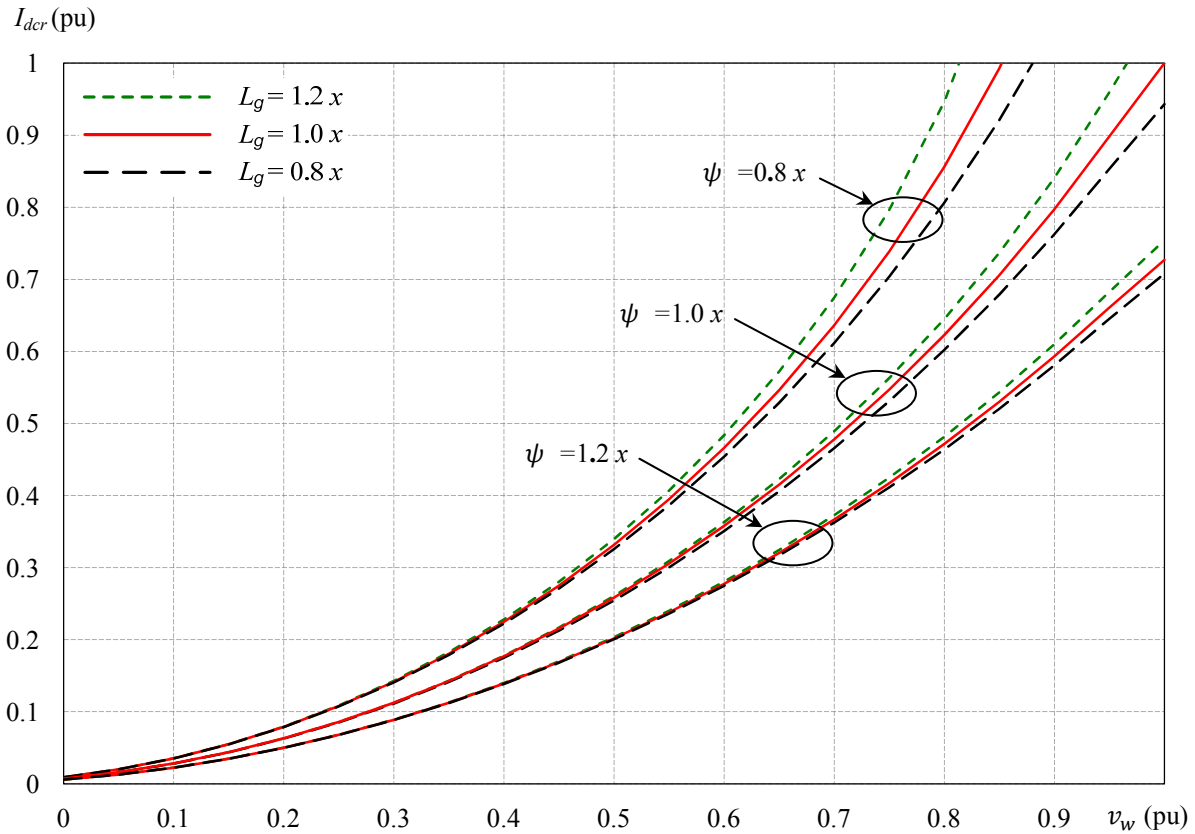

Fig. 3.2-4 DC link current produced by diode rectifier based on system parameters

3.3 Grid-connected PWM Current Source Inverter

3.3.1 PWM current source inverter

A simplified circuit diagram of the PWM CSI is shown in Fig. 3.3-1. The converter is composed of six switching devices, which is usually SGCT. The input DC current for the inverter is defined as I_{dci}, and the inverter produces defined PWM current i_{wi}. The line inductance on the grid side, the grid voltage, grid current, voltage across the capacitor bank are represented by L_s, v_s, i_s, and v_c, respectively.
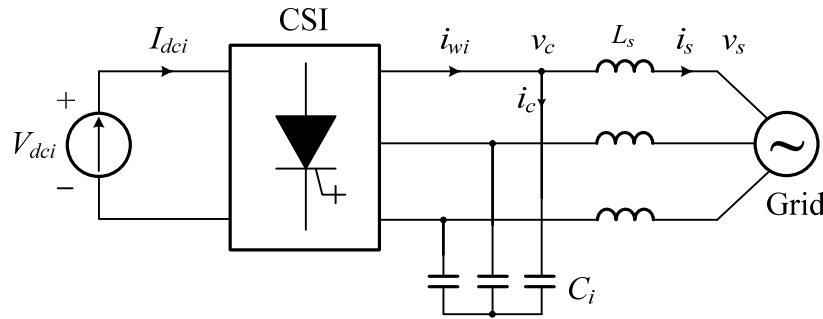

Fig. 3.3-1 Simplified system diagram of PWM CSI

As can be seen in Fig. 3.3-1, there is a large AC capacitor bank connected in parallel with the PWM CSI, which draws a large amount of reactive current. This current can be either provided by the grid or by the converter. If the required power factor (UPF, lagging or leading) is to be achieved at the grid connection point, proper capacitor current compensation needs to be provided by the PWM CSI.

This implies that the DC current for CSI needs to satisfy both active and reactive power being transferred to the grid. Since I_{dci} is provided by I_{dcr}, it is obvious from Fig. 3.2-3 and Fig. 3.3-1 that I_{dcr} should be greater than I_{dci} to ensure proper power flow from the wind turbine to the grid.

The DC current I_{dci} and PWM current i_{wi} are related with each other through modulation index m_i which is given in (3.3-1).

$$I_{dci} = \frac{i_{wi}}{m_i}$$
(3.3-1)

3.3.2 DC current requirement and comparison

The phasor diagram of grid side voltage and current is shown in Fig. 3.3-2 based on Fig. 3.3-1. Since L_s is relatively small, the voltage across capacitor bank v_c can be assumed to be the same as grid voltage v_s to simplify the analysis. From the phasor diagram the inverter PWM current i_{wi} as well as the DC current I_{dci} for the CSI can be derived.

| (a) Unity PF | (b) Lagging PF | (c) Leading PF |
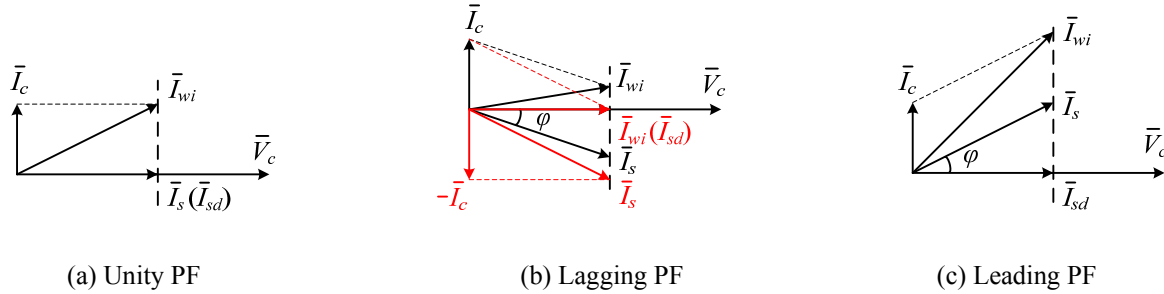
Fig. 3.3-2 Phasor diagram of grid side voltage and current

The vertical dashed line represents the trajectory of i_s corresponding to a given active power delivered to the grid, the active component of i_s is depicted as i_{sd}.

Assume the active power delivered to the grid is given, the value of i_{wi} changes with the grid power factor. For UPF operation shown in Fig. 3.3-2 (a), the PWM current i_{wi} not only provides the real current needed for maintaining the system active power flow, but also fully compensates the capacitor currents. The lowest value of i_{wi} happens when the grid current solely supplies the reactive current for the capacitor, and thus i_{wi} contains only the necessary active component. In this case, the grid power factor is lagging as shown in Fig. 3.3-2 (b). On the contrary, leading grid PF adds to the reactive current component of i_{wi} and thus results in the highest converter current among all of the three cases.

The DC current I_{dci} and PWM current i_{wi} are related with each other through modulation index m_i which is given in (3.3-1). The minimum value of I_{dci} can be derived when m_i equals its maximum value, 1, leading to:

$$I_{dci} = i_{wi} \tag{3.3-2}$$

41

Based on the direction of the current reference shown in Fig. 3.3-1, the currents for UPF operation can be derived with the assumption that the system losses are neglected, also, v_c is assumed to be the same as v_s. Suppose the grid frequency is f_s, there are,

$$i_s = P_g/(3v_s) \tag{3.3-3}$$

$$i_c = 2\pi f_s C_i v_c \tag{3.3-4}$$

$$i_{wi} = \sqrt{i_s^2 + i_c^2} \tag{3.3-5}$$

From (3.3-4) and (3.3-5), it can be seen that the value of i_{wi} is dependent on the capacitance of the capacitor bank when the active power is given. The capacitance generally varies from 0.3 to 0.6 pu for medium voltage drives. The capacitance values of 0.3 to 0.6 pu are introduced in the following analysis.

Fig. 3.3-3 shows the relation in per unit system between I_{dci} and the wind speed with different C_i in comparison with the diode rectifier output current I_{dcr}, in which the solid red lines represent I_{dcr} and the dashed green lines represent I_{dci}. The value for generator side inductance L_g is not oversized, nor is it decreased. Since DC current for the CSI operation originates from the diode rectifier, only when the diode rectifier output DC current is greater than the DC current required by the PWM CSI can the whole system work properly. It is obvious that the normal operation area in Fig. 3.3-3 is rather limited, which means the DC current needs to be boosted to satisfy the full range operation. The DC-DC buck converter is thus added to satisfy the control purpose.
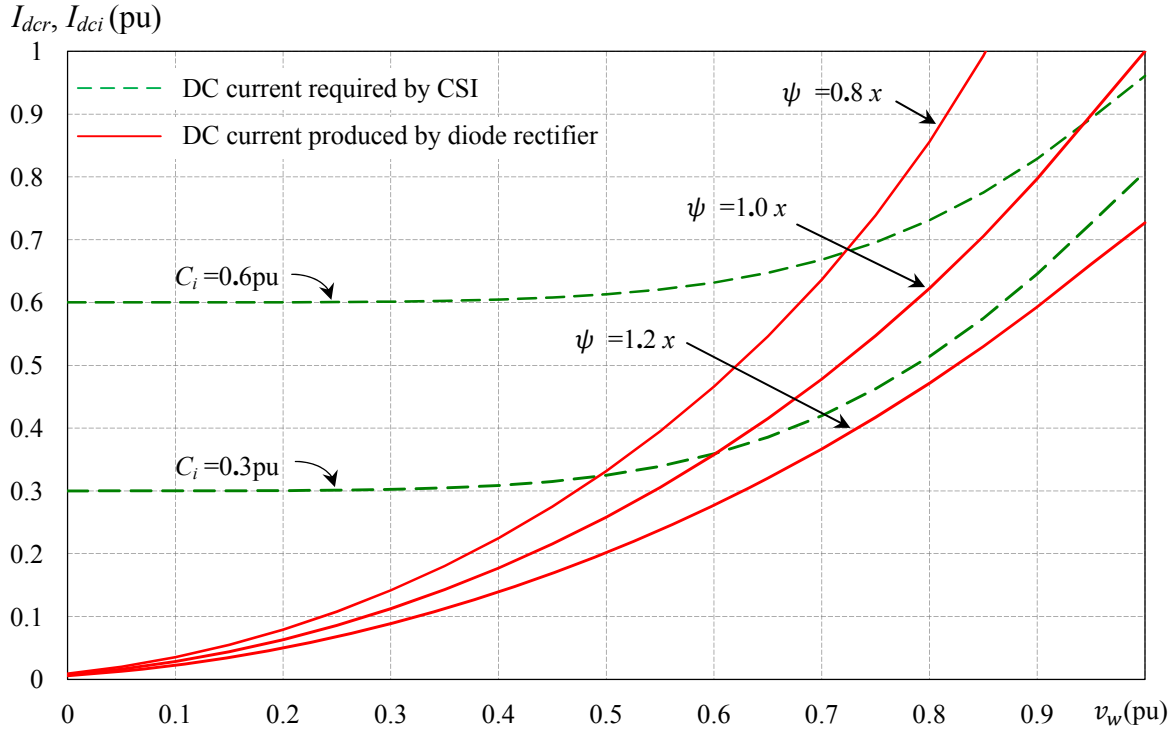
Fig. 3.3-3 DC currents comparison with the variation of wind turbine speed (UPF)

Similar analysis can be conducted for the lagging power factor operation. From the relation between the current phasors in Fig. 3.3-2 (b), there are,

$$i_{sd} = P_g/(3v_s) \tag{3.3-6}$$

$$i_c = 2\pi f_s C_i v_c \tag{3.3-7}$$

$$i_{wi} = \sqrt{(\frac{i_{sd}}{PF})^2 + i_c^2 - 2 \cdot \frac{i_{sd}}{PF} \cdot i_c \cdot \cos(90° - \cos^{-1}(PF))} \tag{3.3-8}$$

Fig. 3.3-4 shows the relation in per unit system between I_{dci} and the wind speed with different C_i in comparison with the diode rectifier output current I_{dcr}, in which power factor is chosen as 0.95. The other symbols are the same as those in Fig. 3.3-3. It can be noticed from Fig. 3.3-4 that although the DC current required for the PWM CSI is decreased slightly, which means the capacitor bank current is partly compensated by the grid, resulting in the expansion of the operation range; the limitation caused by the capacitor current is still obvious. The operation range is still limited.
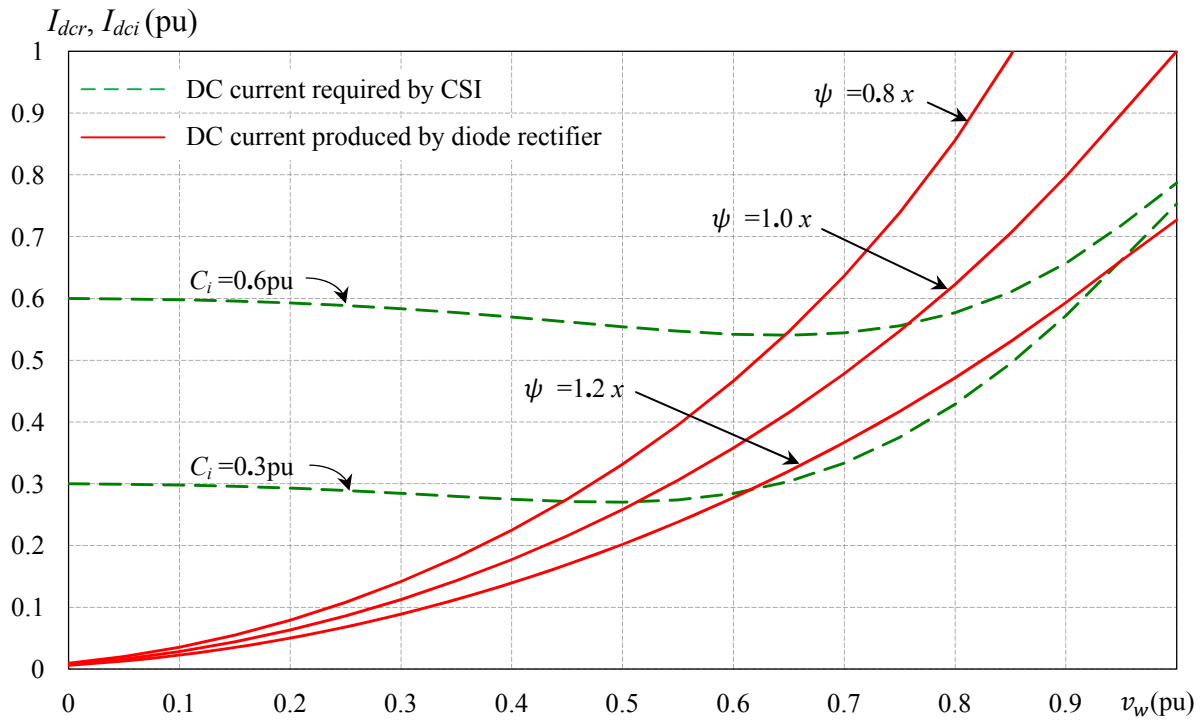
Fig. 3.3-4 DC currents comparison with the variation of wind turbine speed (PF=0.95, Lagging)

It can be seen directly from Fig. 3.3-2 (c) that i_{wi} under leading power factor operation is greater than those under unity or lagging power factor operation, which means the required DC current for the PWM CSI is higher according to (3.3-1), leading to an even narrower operation range. The related curves are thus omitted.

3.3.3 Grid reactive power analysis

With the increasing of wind power penetration, there is a trend that wind turbine units should be able to provide some reactive power support to the grid, just like the conventional generators. Due to the presence of the parallel connected capacitor bank, the reactive power control is somewhat complicated. This section focuses on the possible maximum reactive power that can be delivered to the grid taking account of the following factors.

(a) Rated capacity of the PWM CSI;

(b) The capacitance on the grid side;

(c) Power factor requirement from the grid.

The grid is assumed to operate under normal condition, under which the voltage is 1pu. The voltage across the capacitor bank is assumed the same as the grid nominal voltage, with the voltage drop on the line reactance being neglected. Grid voltage frequency is always at its rated value, 1 pu. The power losses in the system are neglected for simplicity. The following equations are provided in per unit values.

Since the reactive power delivery is required, the maximum power rating for the CSI needs to be oversized. Assume the whole system works under MPPT, the output active power of the CSI is 1 pu under rated wind speed, and the capacity of the PWM CSI is oversized arbitrarily to be 1.2 pu. The grid side active power can be expressed according to the relation described in (1.2-7) and (1.2-8), from which the maximum reactive power to the grid can be calculated by,

$$P_s = P_g = P_T = \omega_T^3 \tag{3.3-9}$$

$$Q_i = \pm\sqrt{S^2 - P_s^2} \tag{3.3-10}$$

$$Q_c = v_c^2 \omega_s C = v_s^2 \omega_s C = C \tag{3.3-11}$$

$$Q_s = Q_i - Q_c \tag{3.3-12}$$

where P_s and P_g are the grid and the generator active powers respectively, P_T and ω_T are the mechanical power and the rotational speed of the turbine, Q_i, Q_c and Q_s are the reactive power produced by the PWM CSI, the capacitor bank and delivered to the grid, respectively. S is the grid side apparent power, ω_s is the angular frequency of the grid voltage, and C is the capacitance of the capacitor bank. It is clear that the grid reactive power is dependent on the value of the capacitance.

Fig. 3.3-5 demonstrates how the maximum deliverable reactive power varies with the changing of the wind turbine speed based on different capacitance. The upper area above the zero X-axis is the leading power factor operation seen from the grid, which corresponds to the capacitive reactive power output; while the lower area is the lagging power factor operation, which corresponds to the inductive reactive power output.
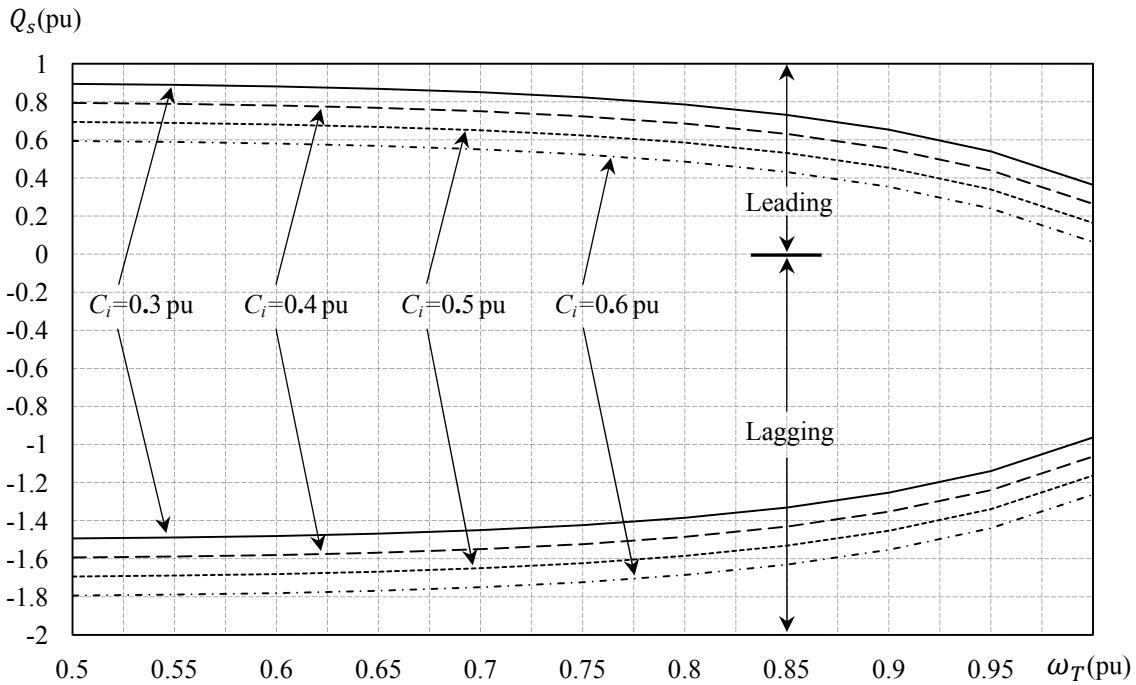
Fig. 3.3-5 Effect of capacitance on maximum deliverable reactive power

Obviously, the reactive power delivered to the grid is limited by the power rating of the CSI, the active power produced by the wind turbine and the capacitance of the grid side capacitor.

Assume the CSI operates with full power, apparent power S is fixed. The active power output to the grid increases with the wind speed. For a given capacitance of the CSI, it can be inferred from (3.3-10) that the absolute value of reactive power Q_i decreases with the rising wind speed. With the increment of the capacitance, the curves representing the maximum capacitive reactive power go down towards the zero axis, meaning that the capacity of delivering capacitive reactive power becomes smaller; meanwhile, the curves representing the maximum inductive reactive power moves far away from the zero axis, indicating the capacity of delivering inductive reactive power becomes larger.

Fig. 3.3-6 values the reactive power capacity from another aspect – grid power factor, which is usually defined in the grid code. With the advancement of the WECS, there is a growing anticipation that wind farms or large wind turbines can operate under normal condition the same or similar way as the conventional power plant.
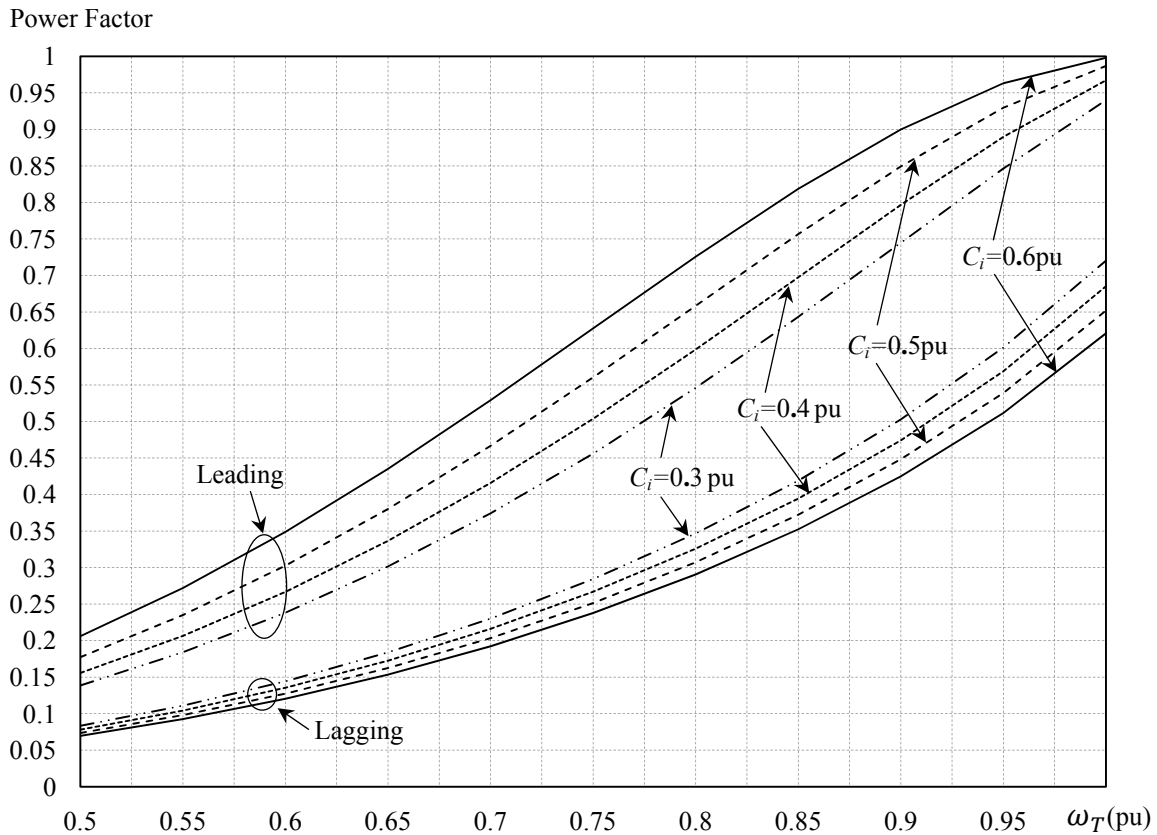
Fig. 3.3-6 Effect of capacitance variation on achievable power factor range

The curves in Fig. 3.3-6 indicate the minimum leading or lagging power factors that can be obtained at various capacitance values. The upper groups of curves represent the variation of the minimum leading power factor when the active power changes with the wind speed, while the lower groups of curves represent that of the minimum lagging power factor. It is noticed that when the wind speed increases towards the rated value, indicating the increase of the output active power, the limit for both lagging and leading power factor tends to increase given the fixed capacitance. However, the impacts of the capacitance variation on the leading or the lagging power factor are different. The increasing capacitance narrows the range of the leading power factor, but extends the range of lagging power factor. Even the capacity of the PWM CSI is oversized to be 1.2 pu, the leading power factor cannot afford as low as 0.95 when the capacitance is 0.4 pu, 0.5 pu and 0.6 pu, which means the power factor requirement (0.95 leading) cannot be satisfied. For the lagging power factor operation, it is sufficient to meet the power factor requirement (0.95 lagging) within a relatively large area with all capacitance.

The curves in Fig. 3.3-7 illustrate the requirement for the PWM CSI capacity when the defined power factor is to be satisfied. Assume the defined power factor is 0.95 (Lagging or leading), which is based on the British codes.
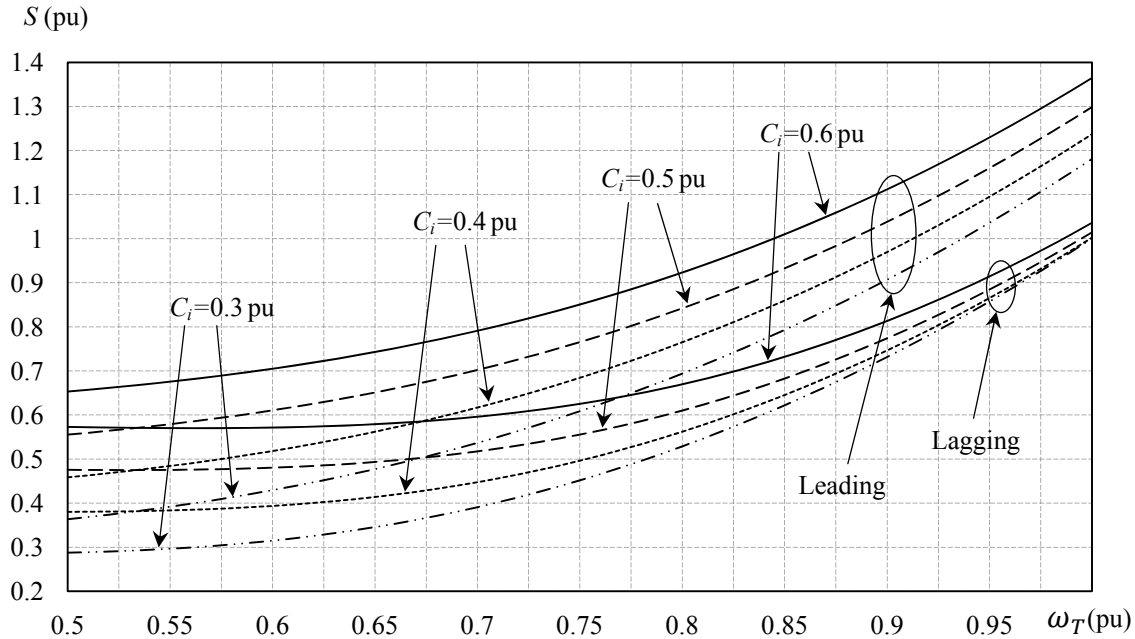

Fig. 3.3-7 Effect of capacitance variation on apparent power (PF=0.95 leading or lagging)

Fig. 3.3-7 illustrate that, with the increasing of the capacitance, the capacity of the PWM CSI needs to be enlarged no matter the power factor is lagging or leading. The ramps for the capacity increasing under leading power factor are sharper than those under lagging power factor. Besides, if the leading power factor is to be satisfied, the CSI requests more converter capacity than that for satisfying the lagging power factor. For example, under the rated situation, in which the output active power of the CSI is 1 pu, when the capacitance is 0.6 pu, the capacity of the CSI should be about 1.36 pu to fulfill the leading power factor (0.95), while 1.03 pu CSI capacity is sufficient to attain lagging power factor (0.95). Even with the capacitance of 0.3 pu, the capacity of the CSI should be enlarged at about 1.2 pu if the leading power factor (0.95) is required.

Based on above analysis, it can be inferred that the power rating of the CSI is the key factor which limits both the power delivery and the power factor requirements. By appropriately choosing the capacitance of the capacitor bank, the limitation can be somewhat alleviated, however, the over-sizing of the CSI power rating is the final solution.

3.4 Buck Converter

Based on the above analysis, the DC current required from the PMSG and diode rectifier doesn't satisfy the DC current requirements from the grid side PWM CSI operation in the full range. An intermediate DC-DC current boost stage is thus necessary to help balance the current requirements from both sides.

The circuit diagram of the voltage buck converter is shown in Fig. 3.4-1. The inductor L_{dc}, switching device S_D and diode D_1 are essential components while the filter capacitor C_{dc} is optional. The capacitor can be placed at the input or output of the buck converter to help smooth the DC voltages. The buck converter steps down the input voltage, which implies the current boost character since the input DC power equals the output DC power.

The PMSG and diode rectifier serve as the input to the buck converter. The rectifier DC current I_{dcr} is then boosted to desired level for the proper operation of the PWM CSI.
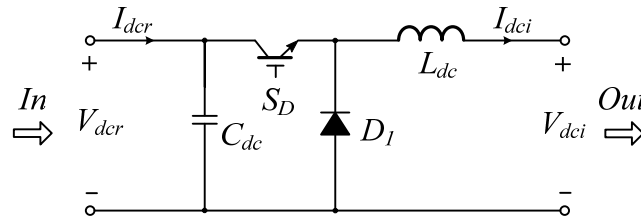

Fig. 3.4-1 Buck converter Circuit diagram

The relations between the output and the input voltages/currents of the buck converter are,

$$V_{dci} = DV_{dcr} \tag{3.4-1}$$

$$I_{dci} = I_{dcr}/D \tag{3.4-2}$$

where D is the duty cycle and varies between 0 and 1. Based on (3.2-8) and (3.4-2), it can be inferred that for the defined operational speed of the wind turbine, the DC current for the PWM CSI is determined.

3.5 General Control Scheme

The control system for the proposed configuration is developed in this section. The main control objectives of the system are to achieve maximum power point tracking from the wind turbine generator; to output the desired active and reactive powers to the grid; and in the meantime, to minimize the overall system loss.

3.5.1 Overview of the control system

The block diagram of the control scheme for the system is shown in Fig. 3.5-1. The system control objectives are achieved through proper control of the active switching devices in the buck converter and the PWM CSI. The buck converter provides one control freedom through duty cycle adjustment of the device S_D, from which the maximum power point tracking can be realized, while the PWM CSI offers both modulation index (m_i) and delay angle (α) adjustment by employing the space vector modulation (SVM) scheme, from which the reactive power and the DC current control can be achieved.

On the grid side, the control scheme is developed based on the grid voltage oriented synchronous frame. The DC current minimization is realized through active calculation of the reference value based on the system active and reactive power flows. On the generator side, the extracted power is optimized through the speed adjustment of the wind turbine, which is reflected in duty cycle regulation of the buck converter. The three phase grid voltage, current and capacitor voltage are measured. As introduced in Chapter 2, a phase locked loop (PLL) is needed to track the grid voltage vector and generate the grid voltage angle θ_s for voltage oriented control (VOC). Those components are transformed into corresponding dq-axis variables in the grid voltage reference frame via the grid voltage angle.
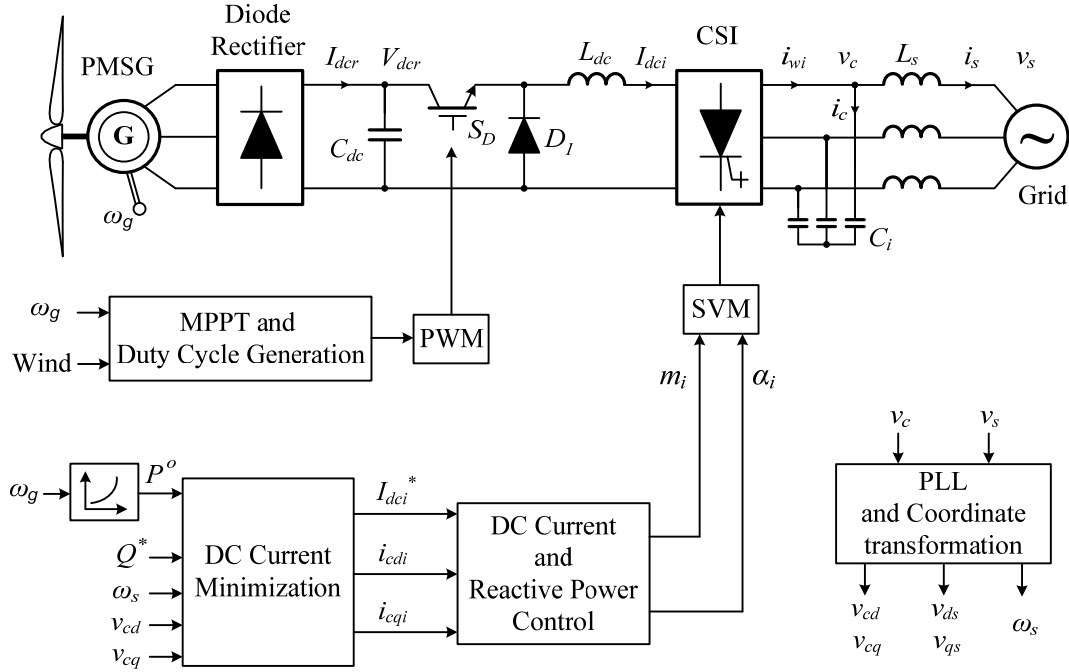
Fig. 3.5-1 Block diagram of the control scheme for the proposed system

3.5.2 Maximum power point tracking

Based on the analysis in section 3.4, the buck converter is controlled to satisfy full range operation of maximum power point tracking. The MPPT is obtained through the generator speed regulation to the optimum values. As illustrated in (3.2-8), the diode rectifier output current can be expressed as a function of the wind turbine speed and generator output power. The control of generator speed demands the variation of generator torque, which directly reflected in the change of generator power and thus the DC current at the rectifier output. This rectifier output DC current again is associated with the PWM CSI DC current by the factor of duty cycle D, given in (3.4-2). The DC current of the CSI is regulated by the CSI at a faster rate than that of the generator speed control, and therefore can be assumed constant for the generator speed control loop design. To sum up, the generator speed loop can be simplified as in Fig. 3.5-2, where the speed regulator output directly tunes the duty cycle of the buck converter. In steady state, the regulator automatically adjusts the rectifier output DC current to the level corresponding to the MPPT point, as calculated in Section 3.2.2.
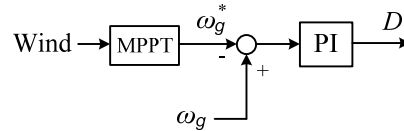
Fig. 3.5-2 Control of buck converter

3.5.3 DC-link current minimization

The proposed system employs a full power PWM CSI, in which switching devices are turned on and off in the process of energy conversion. The total loss in the converter consists of both switching and conduction losses. The currents flowing through the DC link inductance and the switching devices are all defined by the DC link current. The conduction loss is mainly produced by its equivalent series resistance. This power loss is the product of the series resistance and the DC current square, which implies that any small decrease of the DC current may lead to a great reduction of the conduction loss. Moreover, the switching loss is mainly caused by the overlap of the current and voltage across the devices, which is also associated with the DC link current level. It is therefore necessary to minimize the DC link current especially in such a high power application.

When the PMSG is fit in the position, the parameters such as the winding resistance, inductance, and magnetic field leakage are almost constants. As the PMSG is connected with the diode rectifier having no control freedom, the losses in the PMSG are relatively fixed. However, the DC link current for the PWM CSI can be regulated by the control of the CSI. The DC current I_{dci} can be set as a constant or a variable; for the former, it has to be set as the maximum value, under which the aforementioned DC current requirement is satisfied in the full operating range; for the latter, based on the active and the reactive power delivered to the grid, together with the reactive power of the capacitor, the PWM current of the CSI can be calculated. By keeping the modulation index as large as possible at the same time, the DC current for the PWM CSI is then kept at its minimum value according to (3.3-1).

The control of PWM CSI is based on the grid voltage oriented synchronous frame. The block of the grid voltage PLL and coordinate transformation is shown in Fig. 3.5-3. Through the PLL,

the grid voltage angle θ_s is determined, and the angular frequency ω_s is calculated by differentiating θ_s. The measured three-phase grid voltage v_s and capacitor voltage v_c in the stationary frame are transformed into dq-components via the grid voltage angle θ_s.
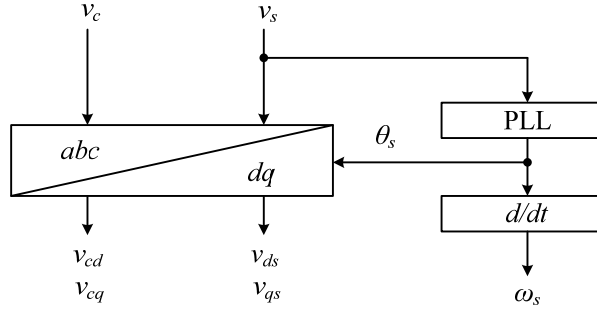

Fig. 3.5-3 Grid voltage PLL and coordinate transformation

Through the coordinate transformation, the grid voltage vector is aligned with the d-axis of the grid side synchronous frame. The q-axis grid voltage v_{qs} is then equal to zero. The active and the reactive powers to the grid can be calculated by,

$$P = 1.5(v_{ds}i_{ds} + v_{qs}i_{qs}) = 1.5v_{ds}i_{ds} \tag{3.5-1}$$

$$Q = 1.5(v_{qs}i_{ds} - v_{ds}i_{qs}) = -1.5v_{ds}i_{qs} \tag{3.5-2}$$

The related d-, q-axis grid currents, i_{ds} and i_{qs}, are then derived by,

$$i_{ds} = P/(1.5v_{ds}) \tag{3.5-3}$$

$$i_{qs} = -Q/(1.5v_{ds}) \tag{3.5-4}$$

The d-, q-axis capacitor bank currents, i_{cdi} and i_{cqi}, are calculated based on (3.5-5) and (3.5-6), in which v_{cd} and v_{cq} are the dq-components of v_c.

$$i_{cdi} = -\omega_s v_{cq} C_i \tag{3.5-5}$$

$$i_{cqi} = \omega_s v_{cd} C_i \tag{3.5-6}$$

The proposed control scheme for DC current minimization based on above consideration is detailed in Fig. 3.5-4. The objective active power P^o, which is correspondent to the value under

MPPT, and the reactive power reference Q^*, which is based on the requirement from the grid, are applied to calculate the objective d-axis (i_d^o) and q-axis (i_q^o) components of the grid current; with the capacitor bank compensation taken into account, the d-axis (i_{dwi}^o) and q-axis (i_{qwi}^o) components of the PWM current can be derived. The objective magnitude of the PWM current (i_{wi}^o) is calculated by the Cartesian to Polar transformation, which is the minimum AC current corresponding to the power delivery under this specific situation. Divide this magnitude of PWM current by the maximum modulation index, which is 1 for SVM, the minimum DC current reference I_{dci}^* can be derived.
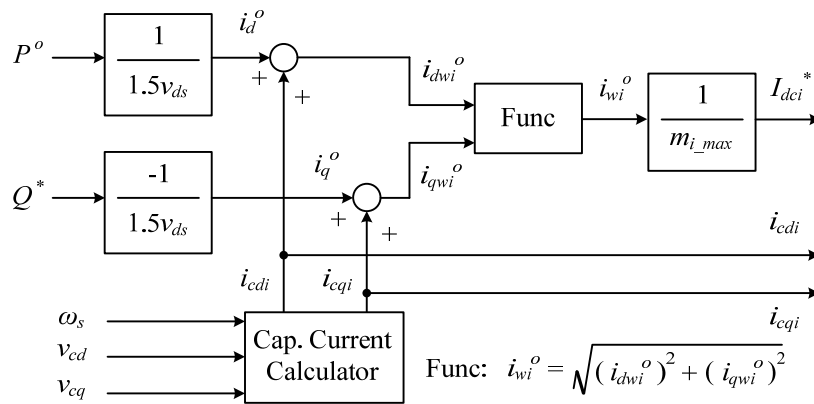
Fig. 3.5-4 DC current minimization

3.5.4 Grid reactive power control

The control scheme of the PWM CSI is drawn in Fig. 3.5-5 in detail.
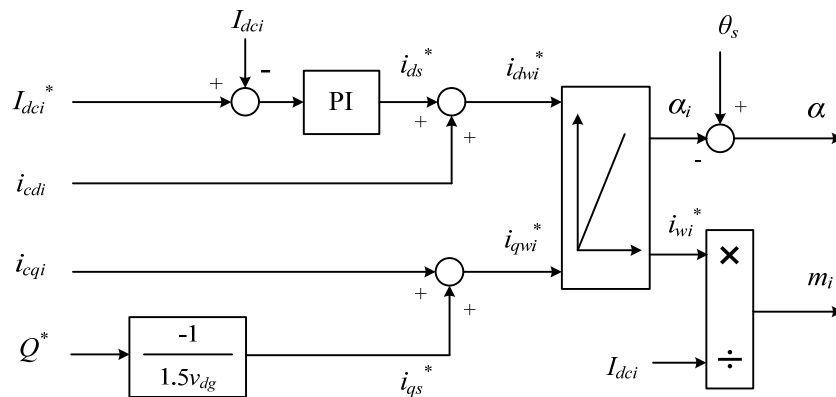
Fig. 3.5-5 Control scheme of the PWM CSI

In Fig. 3.5-5, the reactive power and the DC current for the CSI are tightly controlled based on the adjustment of the modulation index (m_i) and delay angle (α).The DC current reference for inverter I_{dci}^* is compared with the actual I_{dci}, the error is applied as the input of the PI regulator, from which the active (*d*-axis) grid current reference i_{ds}^* is derived, the reactive (*q*-axis) grid current reference i_{qs}^* is calculated according to (3.5-4). The active and the reactive PWM current, i_{dwi}^* and i_{qwi}^*, can be calculate with capacitor bank current compensation being taken into account, as described in (3.5-7) and (3.5-8).

$$i_{dwi}^* = i_{ds}^* + i_{cdi} \tag{3.5-7}$$

$$i_{qwi}^* = i_{qs}^* + i_{cqi} \tag{3.5-8}$$

The magnitude of the PWM current reference i_{wi}^* and the inverter firing angle α_i are calculated by (3.5-9) which can be applied for SVM scheme.

$$\begin{cases} i_{wi}^* = \sqrt{(i_{dwi}^*)^2 + (i_{qwi}^*)^2} \\ \alpha_i = \tan^{-1}(i_{qwi}^*/i_{dwi}^*) \end{cases} \tag{3.5-9}$$

3.6 Conclusion

In this chapter, a novel converter configuration is proposed and corresponding control system is developed for a PMSG based direct drive WECS. Previous literature review indicates the trends toward PMSG WECS using full power converter to improve variable-speed operation and satisfy the grid code requirements. In addition to other previously introduced advantages, the PMSG brings another major cost benefit that a low-cost and robust diode rectifier bridge may be used at the generator output terminals without the external excitation circuit or magnetizing current control from the stator. PWM CSI is considered to interface the grid for providing flexible control over grid active/reactive power flow and desired voltage and current waveforms. Steady-state calculations are performed for the configuration and a buck converter is found necessary in the DC link to help balance the current requirements from both generator and grid sides for the full range operation of the system.

An overall control scheme is developed for the proposed system. The control scheme allows the buck converter to perform maximum power point tracking while the reactive power control (leading, lagging or unity power factor) and the DC current control are realized by the PWM CSI. Meanwhile, the DC current reference is adjusted accordingly under various operating conditions so that the system operating current level is kept minimum to lower the overall system loss.

Chapter 4　Simulation　Verification　of　the　Proposed System

This chapter presents the verification of the proposed system and control scheme described in Chapter 3 by computer simulation. The simulation model is developed using Matlab® R2009b and is introduced in the first section. Both the electrical parts and the control components are illustrated in detail. The second section provides the related waveforms obtained from the simulation results verify the feasibility of the proposed system control scheme.

4.1 Simulation Model Construction

The simulation model is built in Matlab® R2009b Simulink. To reflect the characteristics of the system and to simplify the simulation, there are following assumptions:

(a) The pitch angle of the turbine blade is defined as zero degree and kept constant;

(b) The switching devices are considered ideal;

(c) The grid is simplified as a three-phase stiff voltage source;

(d) The wind speed is simplified as step input function

4.1.1 Block diagram of the simulation model

The top level block diagram of the simulation model is shown in Fig. 4.1-1, in which different blocks from the Simulink Library are chosen and connected according to the circuit diagram depicted in Fig. 3.1-1. The grid side resistance is relatively small compared with the line inductance and the transformer inductance, and is thus neglected; at the generator side, the line inductance is integrated with the PMSG winding inductance which is not explicitly shown. The capacitor bank is the standard star connection. The grid is modeled by three phase voltage source which is also a star connection.
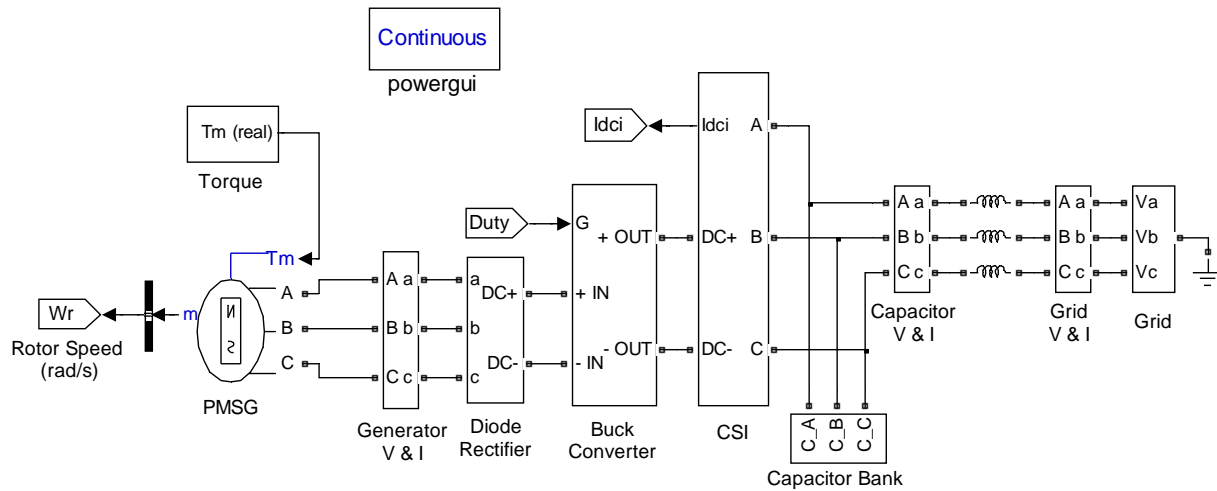
Fig. 4.1-1 Top level block diagram of the simulation model

The detailed connection of the diode rectifier, buck converter and the PWM CSI is shown in Fig. 4.1-2. Ideal switches are applied as the switching devices for buck converter and CSI. A diode (Diode8) is used in the DC link to mimic the unidirectional power flow. It can be viewed from Fig. 4.1-2 that diode rectifier shares the filter capacitor with the buck converter, and the buck converter shares the same inductor with the CSI, which gives a compact structure of this system.
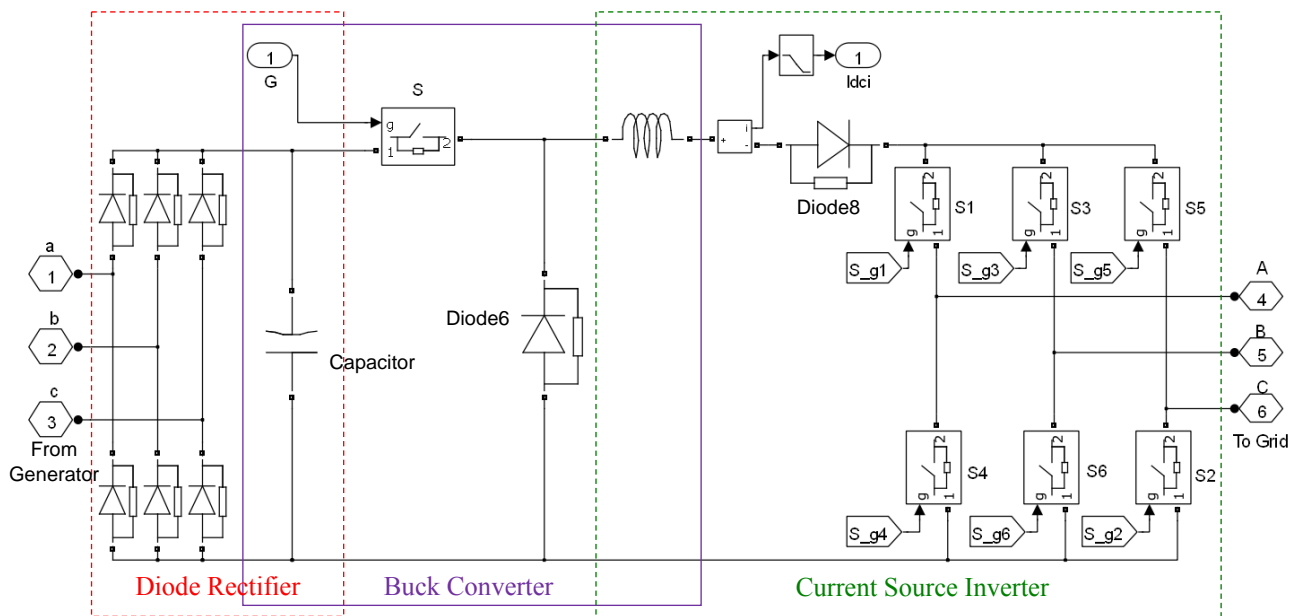
Fig. 4.1-2 Detailed model of the AC-DC-AC power converter in simulation

4.1.2 Wind turbine aeromechanical model

The wind turbine aeromechanical model is detailed in Fig. 4.1-3. The key part is the wind turbine mathematical model coming from the Matlab Simulink Library. The rated power of the wind turbine system is set as 2 MW and the rated wind speed is 12 m/s. The pitch angle is assumed zero degree for this simulation.

The wind turbine model collects the information of wind speed, generator speed and turbine pitch angle, and then calculates the mechanical torque being applied to the generator. Inside the model, the extracted wind power in per unit value can be calculated according to (1.2-2) to (1.2-5). The real power can be calculated by multiplying the per unit value with the base value. Dividing the real power by the turbine speed, the real mechanical torque can be derived and applied to the PMSG model. It should be noted that the mechanical torque is negative to indicate the generator mode operation of the PMSG.
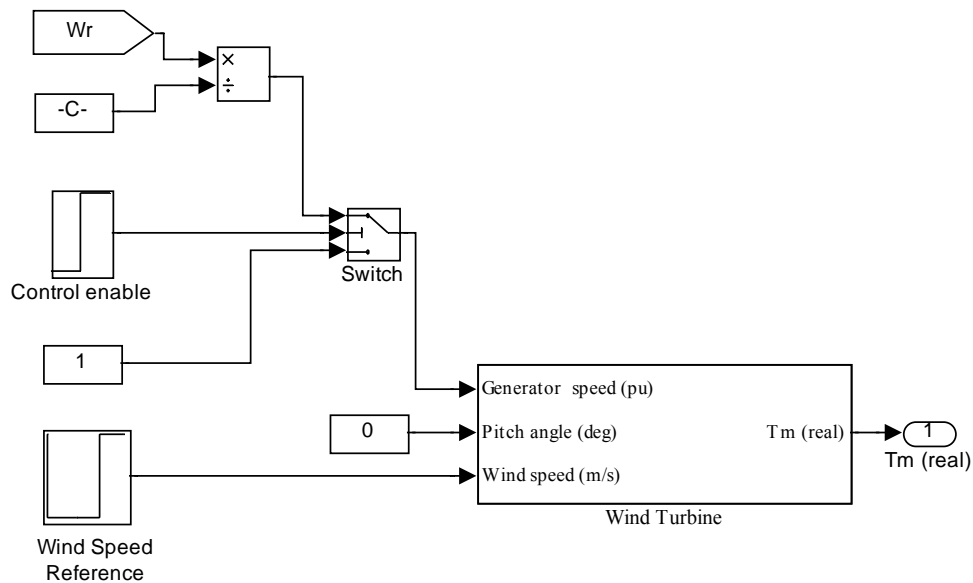
Fig. 4.1-3 Wind turbine aerodynamical model

4.1.3 Grid-side current source converter controller modeling

(1) Voltage *dq* components and the phase angle

The control scheme for the PWM CSI is based on voltage oriented vector control, and the performance is directly related to the estimation of the voltage phase angle. Fig. 4.1-4 illustrates

the derivation of the *dq* components and the grid voltage angle for the coordinate transformation. The grid voltage is measured and normalized before being sent to the PLL block, which gives the grid voltage phasor angle. This angle is applied to transform the grid voltage and the voltage across the capacitor bank from *abc* frame to *dq* frame by following equations.

$$\begin{bmatrix} v_d \\ v_q \end{bmatrix} = \frac{2}{3} \begin{bmatrix} \sin \omega t & \sin(\omega t - 2\pi/3) & \sin(\omega t + 2\pi/3) \\ \cos \omega t & \cos(\omega t - 2\pi/3) & \cos(\omega t + 2\pi/3) \end{bmatrix} \cdot \begin{bmatrix} v_a \\ v_b \\ v_c \end{bmatrix} \qquad (4.1\text{-}1)$$

$$\begin{bmatrix} i_d \\ i_q \end{bmatrix} = \frac{2}{3} \begin{bmatrix} \sin \omega t & \sin(\omega t - 2\pi/3) & \sin(\omega t + 2\pi/3) \\ \cos \omega t & \cos(\omega t - 2\pi/3) & \cos(\omega t + 2\pi/3) \end{bmatrix} \cdot \begin{bmatrix} i_a \\ i_b \\ i_c \end{bmatrix} \qquad (4.1\text{-}2)$$
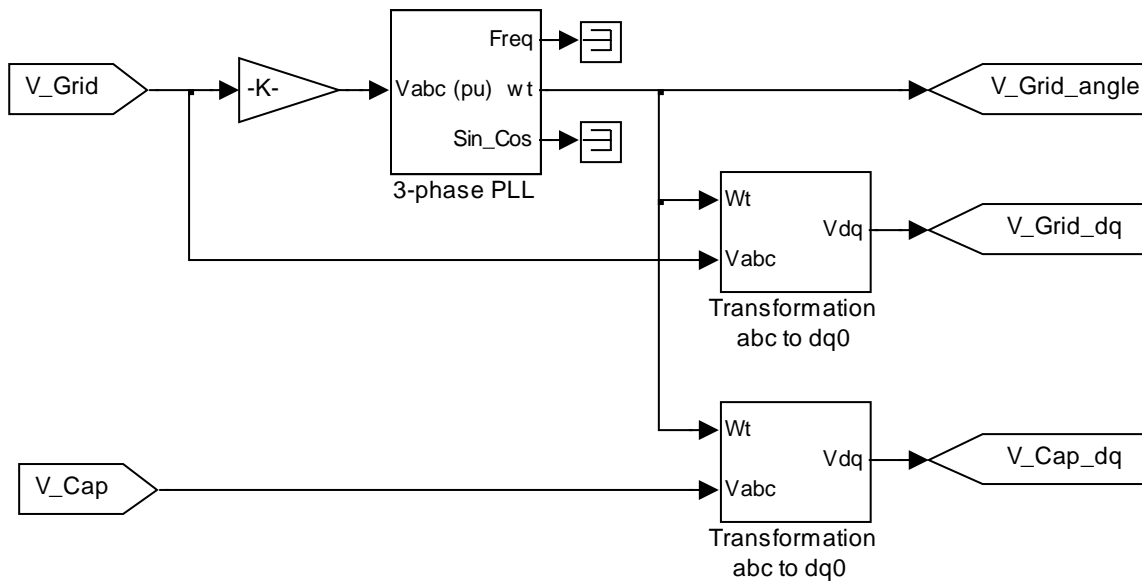
Fig. 4.1-4 *dq* transformation of the grid side three-phase quantities

(2) DC current reference for the PWM CSI regulation

The DC current is regulated by the CSI according to the calculation of the possible active and reactive power delivering; which is based on the power drawn from the wind and the power from the capacitor bank. Fig. 4.1-5 shows the simulation block for the calculation of the *dq* axis capacitor currents. The equations applied in these two Function blocks in Fig. 4.1-5 are based on (3.5-5) and (3.5-6). The frequency of the grid voltage is fixed at 60 Hz.
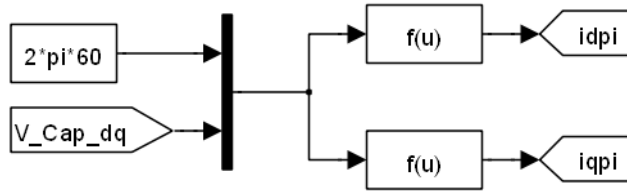
Fig. 4.1-5 *dq* components of the capacitor current
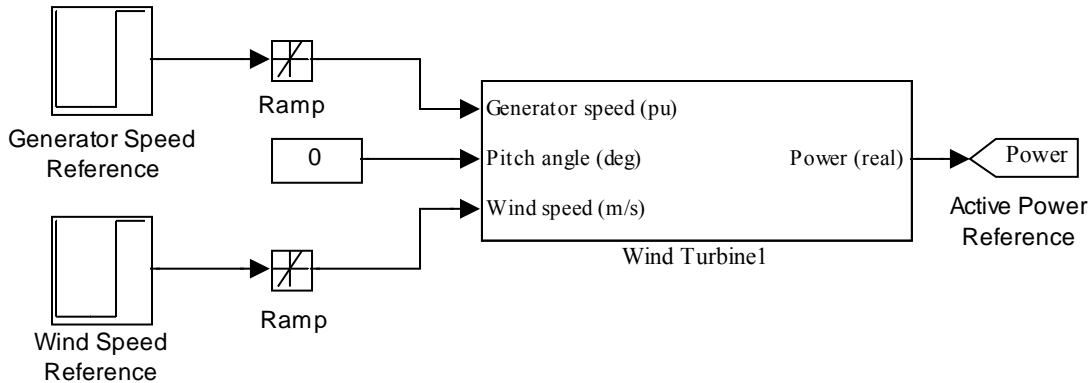
Fig. 4.1-6 Active power reference derivation

Active power reference is requested for DC current reference calculation and its derivation is provided in Fig. 4.1-6. The wind turbine block is the same as that in Fig. 4.1-3, but the purpose here is to estimate the optimum power output at the existing wind speed. Therefore, the generator reference speed correspondent to the MPPT under this wind speed is used, and the output is now changed to optimum active power instead of the mechanical torque.

The final calculation of the DC current reference is completed by the blocks shown in Fig. 4.1-7. Based on (3.5-3) and (3.5-4), the *dq*-axis grid side currents together with the *dq*-axis capacitor currents provides the references for converter currents, from which the DC current reference can be calculated by the block of Cartesian to Polar transformation.

It should be pointed out that the reactive power reference in Fig. 4.1-7 is set based on different values, these values can be changed as long as the operational requirement from the grid codes and the predefined capacity ratings of the CSI are both satisfied.
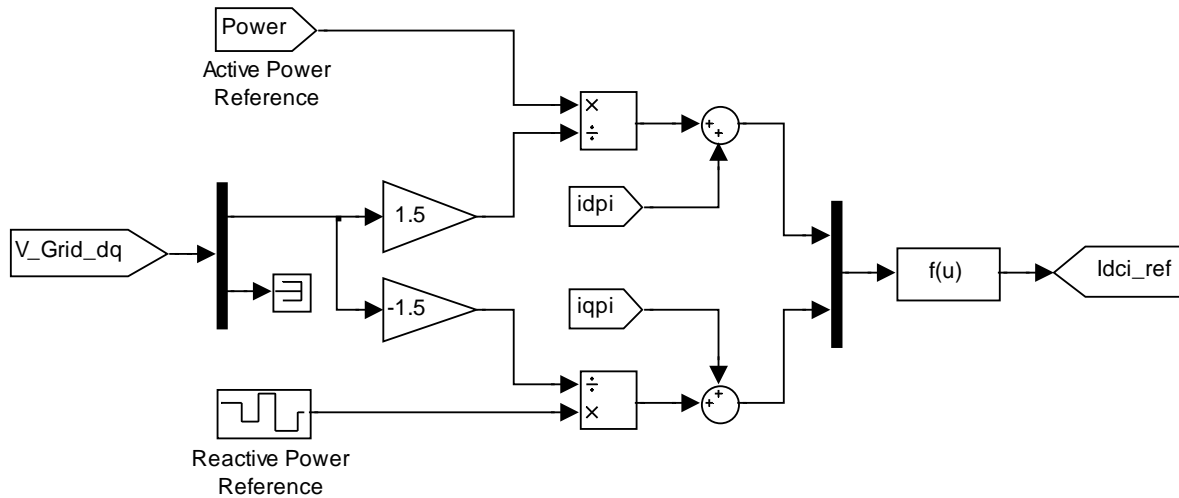
Fig. 4.1-7 DC current reference for the CSI

(3) Control of the PWM CSI

The construction of the PWM CSI controller is provided in Fig. 4.1-8. The switching scheme used for the PWM CSI is SVM, of which both modulation index and the delay angle can be adjusted to attain control objectives. The grid active and reactive current references are derived from dc-link current regulator and reactive power reference. With consideration of the capacitor currents, the converter current references are then obtained and utilized to determine the modulation index and delay angle for gating signal generation.
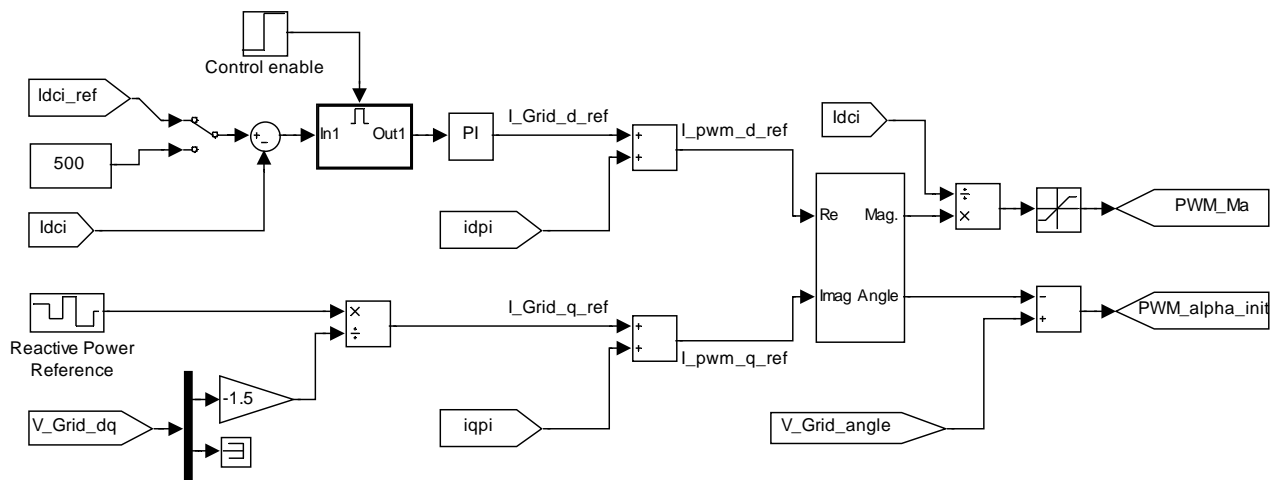
Fig. 4.1-8 Controller for the PWM CSI

(4) Gating signal generation for PWM CSI
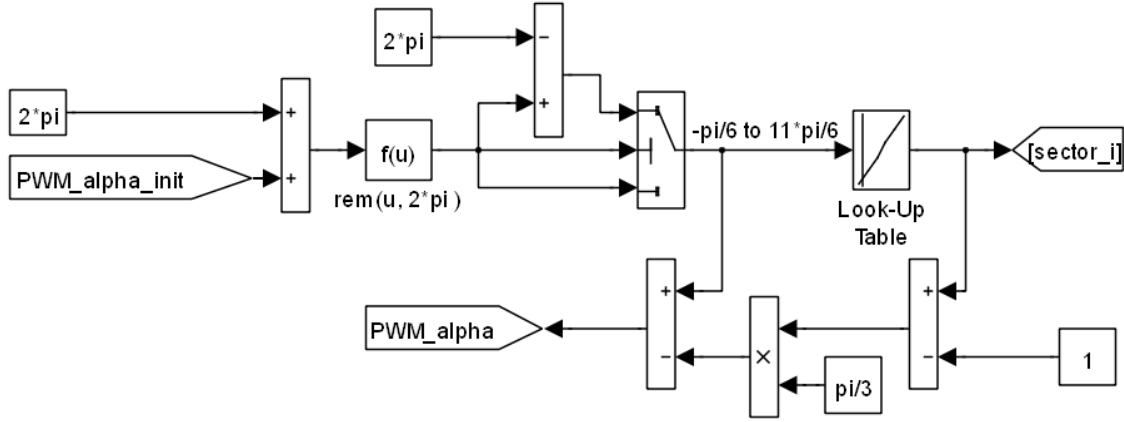
Fig. 4.1-9 Derivation of sector number and the relative angle within the section for CSI SVM

The angle derived in Fig. 4.1-8 is the angle of the reference vector with regard to the phase A of the grid and was round about in Fig. 4.1-9 between $-\pi/6$ to $(11 \cdot \pi)/6$. A look-up table is configured to determine the correspondent sector of the reference current vector. This relative angle of the vector within the sector (ranges between $-\pi/6$ and $\pi/6$) is then calculated by following algorithm [34].

$$\theta = \theta' - (k-1)\pi/3 \qquad (4.1\text{-}3)$$

In which θ is the angle between $-\pi/6$ and $\pi/6$ used for the SVM gating signals and θ' is the remainder (angle) between $-\pi/6$ to $(11 \cdot \pi)/6$ and k is the sector number ($k = 1, 2, 3, 4, 5, 6$).

Fig. 4.1-10 shows the block diagram used to generate SVM gating signals. The triangular carrier wave has a frequency of 1080 Hz, which indicates the sampling frequency of the CSI. T_0, T_1 and T_2 are dwell times for the zero vector and two active vectors, which are calculated by following expressions [34].

$$\begin{cases} T_1 = m_a \cdot sin\left(\frac{\pi}{6} - \theta\right) \cdot T_s \\[2mm] T_2 = m_a \cdot sin\left(\frac{\pi}{6} + \theta\right) \cdot T_s \\[2mm] T_0 = T_s - T_1 - T_2 \end{cases} \qquad (4.1\text{-}4\ )$$

63

where m_a and T_s are the modulation index and sampling time respectively. The sampling time is denoted by $1/F_c$ and F_c equals 1080 Hz. A 3-D look-up table is configured to select the appropriate switching states for each switching device.
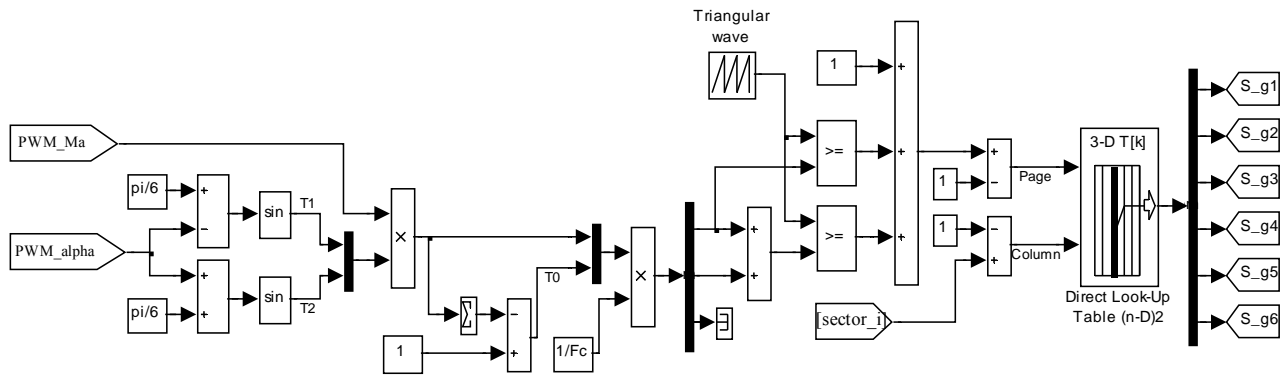

Fig. 4.1-10 SVM gating signal generator for PWM CSI

4.1.4 Buck converter controller modelling

The duty cycle control and device gating signal for the buck converter are produced by circuit diagram in Fig. 4.1-11. An enable block is applied to activate the controller when the wind turbine reaches the cut-in speed. The output of the speed PI regulator issues the duty cycle for the buck converter. A triangular carrier wave with the frequency of 1 kHz is applied to generate the correspondent gating signals. The resultant device switching frequency is 1 kHz.
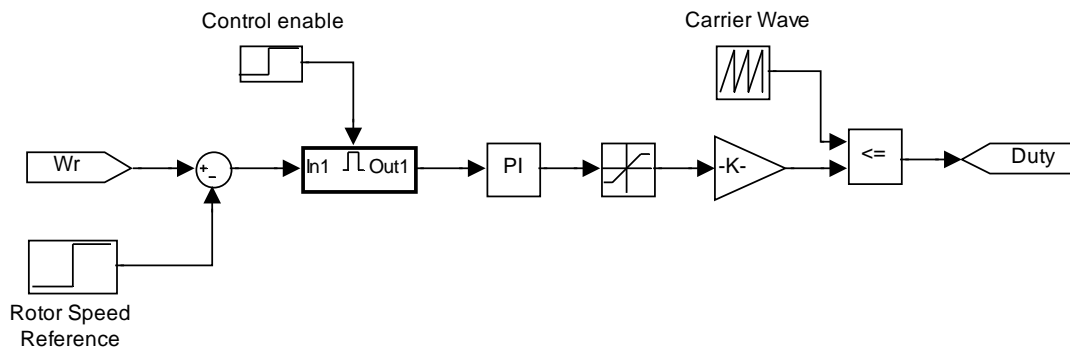

Fig. 4.1-11 Circuit diagram of the duty cycle control

4.2 Simulation Results

Based on the model constructed in the above section, the simulation results are presented here to prove that the proposed WECS functions properly according to the design requirements. A 2 MW/3000 V non-salient permanent magnet synchronous generator is used in the simulation. The system parameters are listed in Table 4.2-1.

Table 4.2-1 Parameters for the proposed WECS

Generator parameters (Based on generator-side per unit system)		
Rated shaft input power	2 MW	
Rated stator winding phase voltage	1732 V (rms)	1 pu
Rated rotor speed	22 rpm	1 pu
Rated rotor flux linkage	32.6 Wb	1 pu
Stator winding resistance	0.0168 Ω	0.005 pu
Line resistance	0.01 Ω	0.003 pu
Number of pole pairs	30	
d-axis synchronous inductance	19.4 mH	0.398 pu
q-axis synchronous inductance	19.4 mH	0.398 pu
DC link parameters (Based on generator-side per unit system)		
DC capacitor	2100 μF	0.488 pu
DC inductor	48.8 mH	1 pu
Grid side parameters (Based on grid side per unit system)		
Rated grid phase voltage	1732 V (rms)	1 pu
Grid frequency	60 Hz	1 pu
Power factor	0.95	Lagging/Leading
Line inductance	1.08 mH	0.12 pu
Commutation capacitor capacitance	472 μF	0.6 pu

4.2.1 Gating signal generations

(1) PLL performance

Fig. 4.2-1 verifies the tracking of the grid voltage angle realized by the PLL block. The

triangular wave is the grid voltage angle normalized to 2π, and the sine wave is the grid phase a voltage normalized to the base voltage.
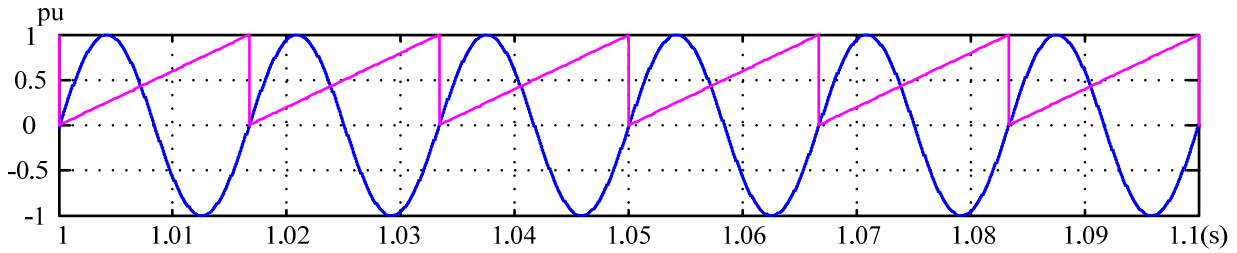

Fig. 4.2-1 Grid phase a voltage waveform and PLL phase angle

(2) Gating signals for buck converter control

The gating signal for the buck converter is derived from the comparison of the triangular wave and the output of the wind turbine speed control block, which is shown in Fig. 4.2-2.
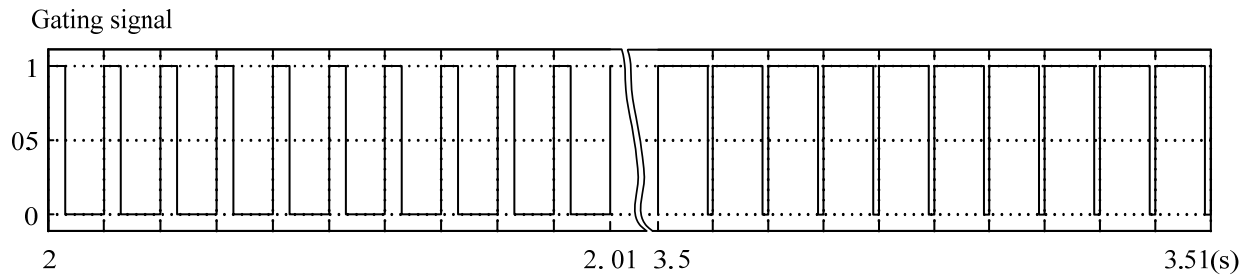

Fig. 4.2-2 Gating signal for the switching device in the buck converter

The left part gives the gating signal when the active power is 0.125 pu, while the right part shows the gating signal when the active power is 1 pu. The reactive power reference is set to zero in both cases. It can be seen that the duty cycle is higher under full power than that under partial power. This is reasonable if referred to Fig. 3.3-3. At rated wind speed rated power, the current requirements for both generator and grid sides are close to each other and thus need lower current boost factor in the buck converter. At low wind speeds when the available active power is substantially reduced, the DC current of the PWM CSI is dominated by the capacitor reactive power compensation requirement and is much higher than that of the generator side operating requirement. The duty cycle is therefore lowered to balance the difference.

(3) Gating signals for PWM CSI control

Fig. 4.2-3 shows the gating signals for the PWM CSI. The blue lines represent the sector numbers (from 1 to 6) for the SVM, and the rose lines denote the gating signals for each switching devices. To facilitate the reading, the gating signals are amplified in magnitude.
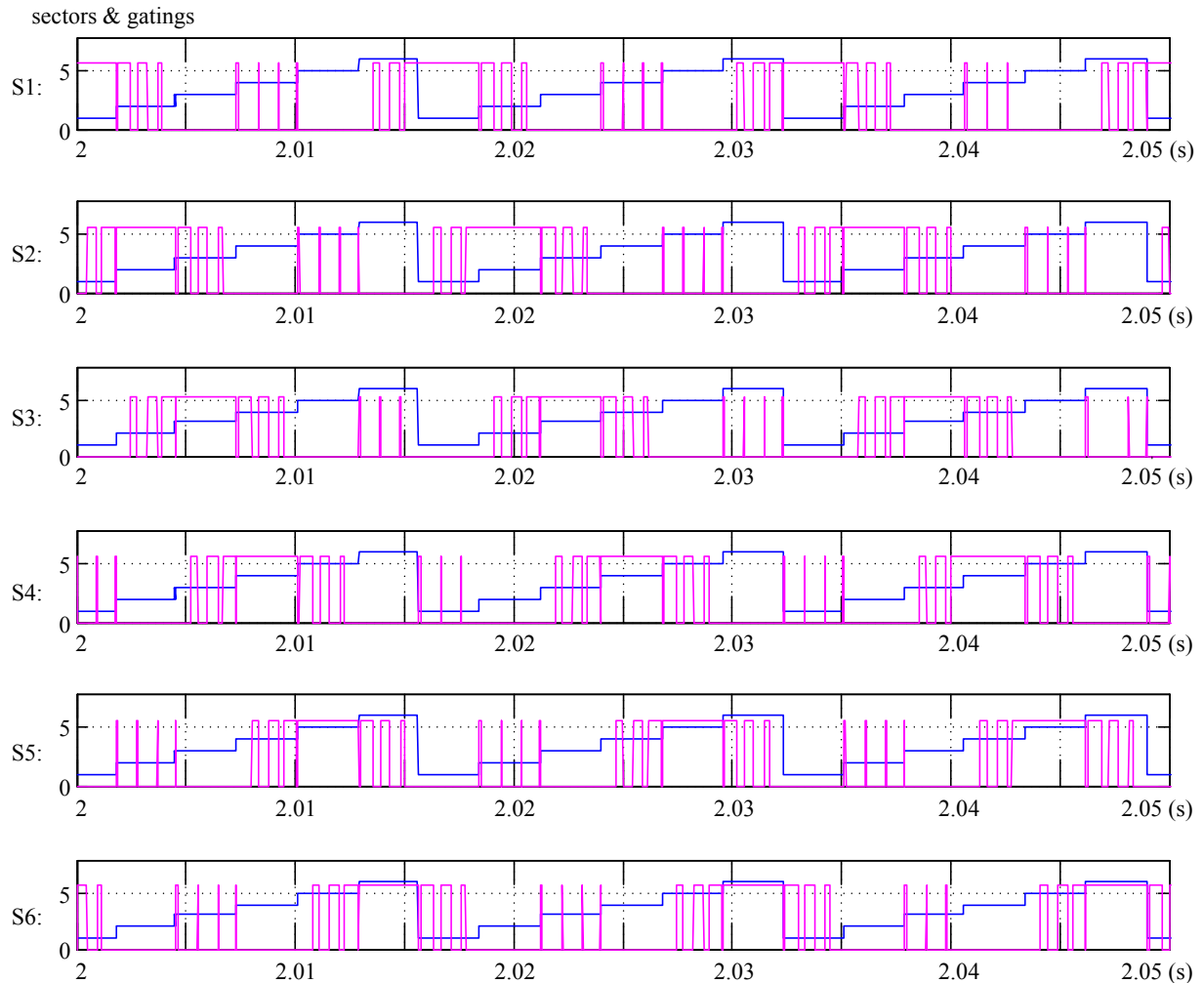

Fig. 4.2-3 Gating signals for the switching devices in PWM CSI

4.2.2 Maximum power point tracking

In this subsection, the feasibility of MPPT of the proposed system and control scheme will be demonstrated under unity power factor operations, as shown in Figs. 4.2-4 and 4.2-5.

The wind speed experiences a step change from 6m/s to 12m/s at 3s in the simulation. The simulation results of the output power (active and reactive) as well as the references of the wind

turbine speed, the DC current, modulation index, duty cycle and their correspondent actual values are listed in Fig. 4.2-4.

The active power shown in Fig. 4.2-4 (a) changes from 0.25 MW (0.125pu) to 2 MW (1 pu) while the reactive power remains zero during the whole simulation, which verifies the UPF operation. The rotational speed of the PMSG is changed accordingly as shown in Fig. 4.2-4 (b). The actual rotor speed follows the reference very well in steady state. It is obvious in Fig. 4.2-4 (c) that the DC current for the CSI decreases significantly under low power operations, which shows the necessity of the DC current minimization for the sake of system efficiency. The modulation index of the PWM CSI in Fig. 4.2-4 (d) is maintained close to 1 during the whole simulation without saturation, which guarantees the regulation of DC current minimization. In Fig. 4.2-4 (e)，the duty cycle increases when wind speed rises to the rated value and there is still some margin for the duty cycle even when the rated power is delivered. This can be utilized for additional grid reactive power support when needed.

P & Q $(\times 10^6)$ (W/Var)

(a) Active and reactive power

ω_{g_ref} & ω_g (rad/s)
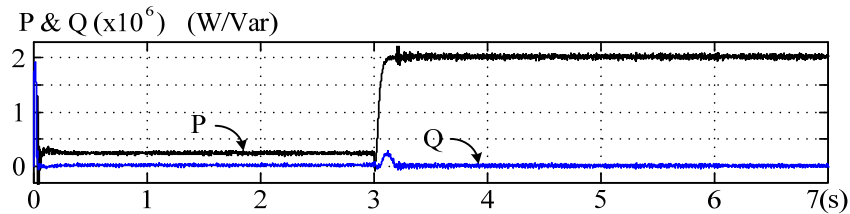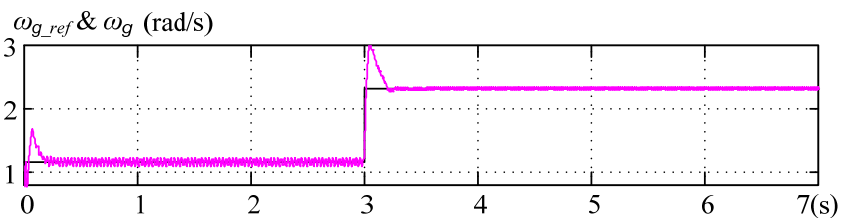
(b) PMSG rotor speed reference and its actual value

I_{dci_ref} & I_{dci} (A)
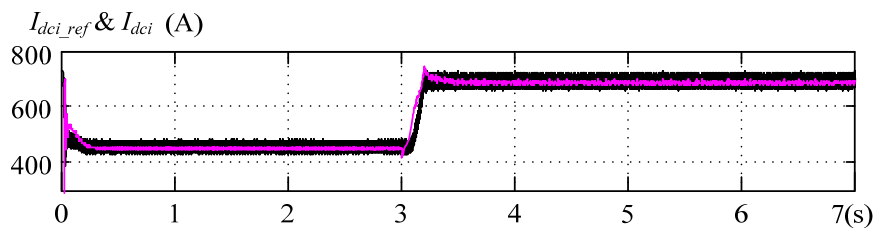
(c) DC current reference for PWM CSI and its actual value
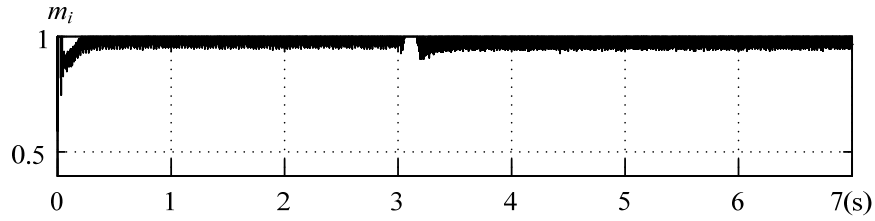
(d) Modulation index of the PWM CSI
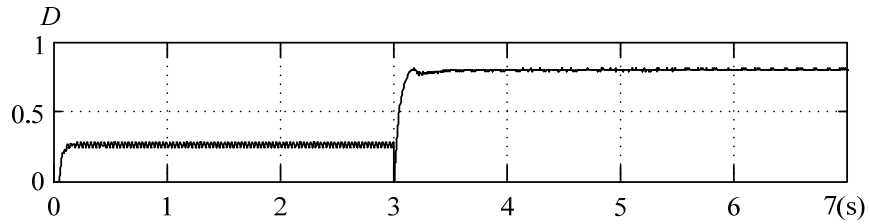
(e) Duty cycle of the buck converter

Fig. 4.2-4 Simulation results of the control variables (UPF operation)

Fig. 4.2-5 shows the waveforms of the grid side voltage and current. It can be seen that the grid side voltage and current waveforms are in phase under different active power levels. This verifies the unity power factor operation from another aspect.
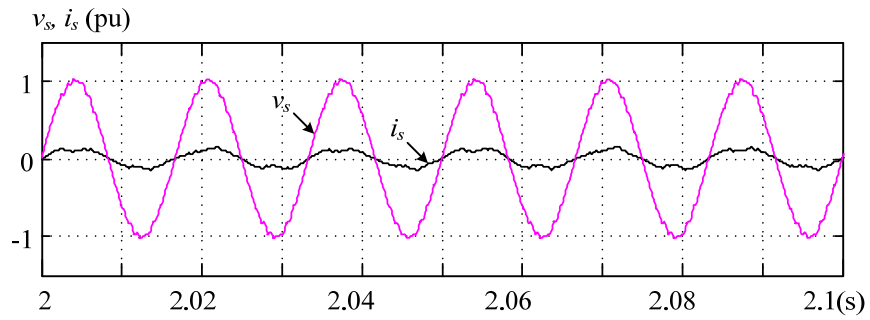
(a) Grid side voltage and current at 6m/s
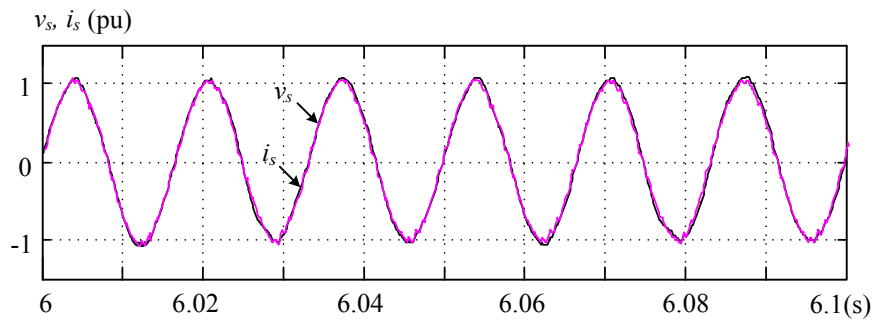
(b) Grid side voltage and current at 12m/s

Fig. 4.2-5 Waveforms of the grid side voltage and current (UPF operation)

4.2.3 Variable power factor control

While the wind energy penetration continues to increase and the technologies of the WECS become mature, the anticipation of the wind turbine/farm to provide reactive power support for the grid arises from both the grid operator and the wind power provider. The proposed system and the control scheme are also suitable for flexible reactive power control other than unity power factor control. In the following simulation, the boundary of power factor is chosen as 0.95 (lagging or leading) according to the British Code. The wind speed change is the same as that under UPF operation (6m/s to 12m/s, at 3s).

Table 4.2-2 provides the detailed profile of the wind speed, the power factor and the reactive power references used in simulation. The reactive power is assumed to be positive when the PWM CSI exports inductive reactive power to the grid.

Table 4.2-2 Wind speed, power factor and reactive power reference profile

| Time (s)	0-1	1-2	2-3	3-4	4-6	6-7
V_w (m/s)	6				12 (rated)	
Power factor	0.95		1		0.95	
	Leading	Lagging			Leading	Lagging
Q (kVar)	-82.17	82.17	0		-657.37	657.37

Fig. 4.2-6 gives the simulation results of the output power (active and reactive) as well as the references of the wind turbine speed, the DC current, modulation index, duty cycle and their correspondent actual values when the power factor is set as 0.95 (lagging/leading).
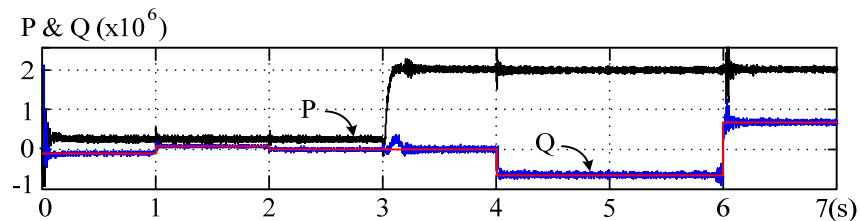

(a) Active and reactive power
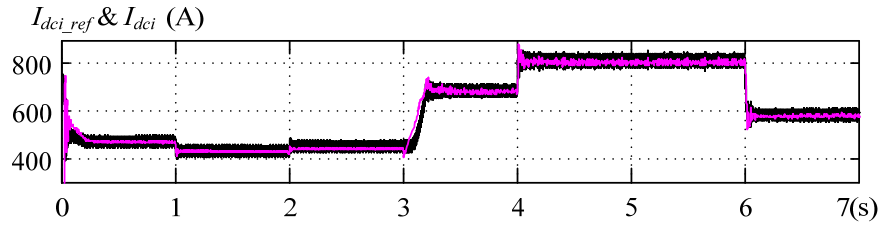
(b) DC current reference for PWM CSI and its actual value
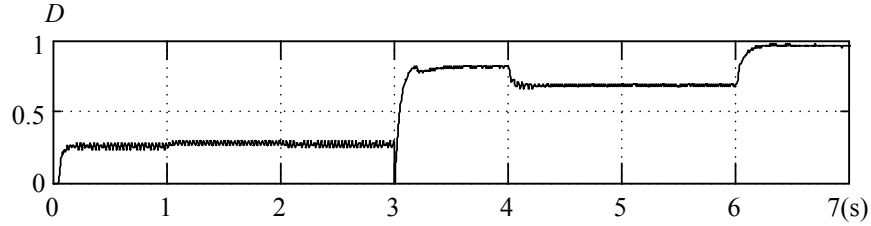
(c) Duty cycle of the buck converter
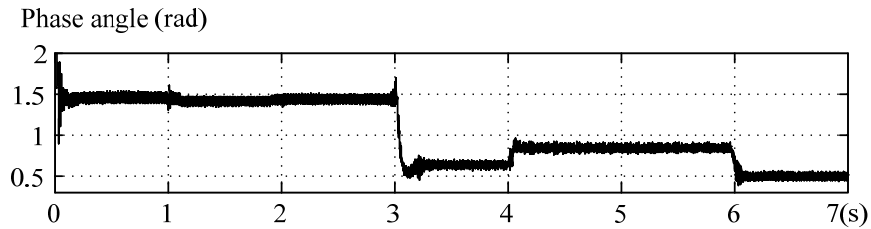

(d) PWM CSI phase angle
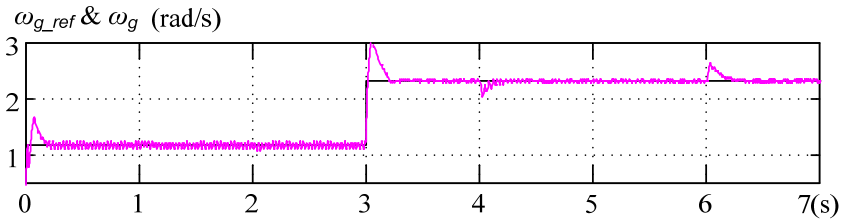
(e) PMSG rotor speed reference and its actual value
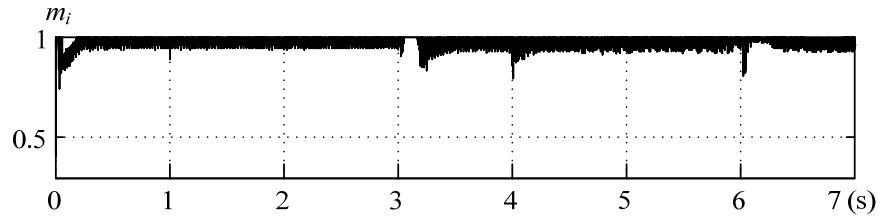
(f) Modulation index of the PWM CSI

Fig. 4.2-6 Simulation results of the control variables (PF=0.95 lagging/leading)

It can be viewed from Fig. 4.2-6 (a) that the active power resembles the variation under UPF operation, and the actual reactive power follows the reference well in steady state. The DC

current reference for the CSI varies with the power factor references, shown in Fig. 4.2-6 (b). Since the generator side current is fixed under the same wind speed, the duty cycle of the buck converter is adjusted accordingly to match the DC current variation. as verified in Fig. 4.2-6 (c). Compared to Fig. 4.2-4 (e), the duty cycle is fully utilized at rated wind speed and 0.95 lagging power factor requirement. The PWM CSI phase angle in Fig. 4.2-6 (d) varies accordingly to accommodate the changes in active/reactive powers. The actual rotational speed of PMSG tracks the reference in steady state, given in Fig. 4.2-6 (e). The modulation index in Fig. 4.2-6 (f) is again maintained closed to 1 under all conditions, resulting in minimum DC current.

The waveforms of the grid side voltage and current are shown in Fig. 4.2-7, which verifies the reactive power control from another aspect. The power factor is able to be adjusted to 0.95 leading or lagging.
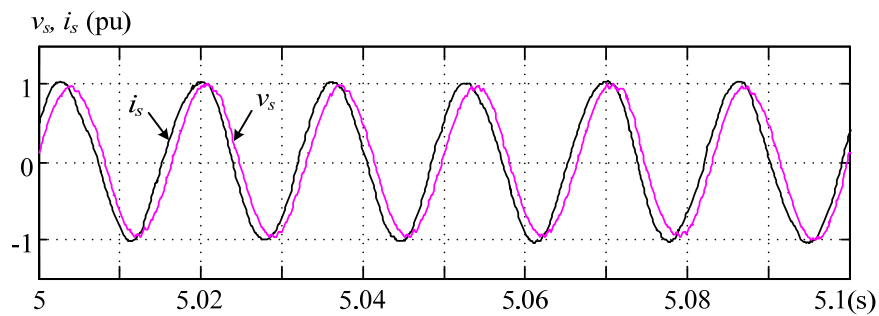
(a) Grid side voltage and current when PF=0.95 leading
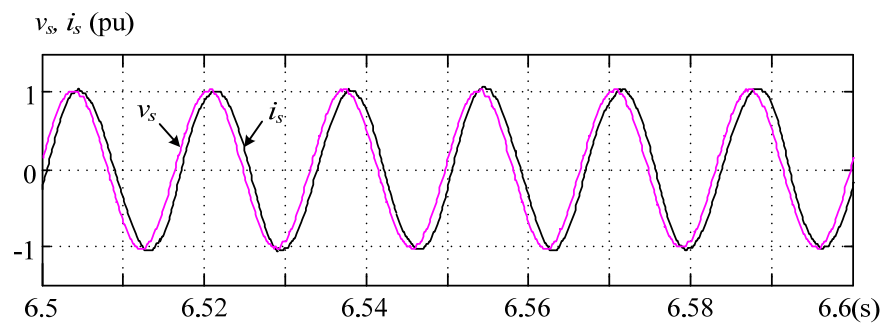
(b) Grid side voltage and current when PF=0.95 lagging

Fig. 4.2-7 Grid voltage and current with various power factor (V_w=12m/s)

4.2.4 DC current minimization

Minimum DC current control is verified and demonstrated in this subsection. The UPF operation is applied to facilitate the observation. In the following discussion, the proposed DC current reference is noted as I_{dci}^*, which is the minimum DC current reference calculated by the controller. A test is performed to further decrease the DC current reference to $0.95I_{dci}^*$ to display the effect. Table 4.2-3 shows the profile of wind speed and the DC current references.

Table 4.2-3 Wind speed, DC current reference profile

Time (s)	0 - 1.5	1.5 - 3	3 - 4.5	4.5 - 6
DC current reference	$0.95I_{dci}^*$	I_{dci}^*	$0.95I_{dci}^*$	I_{dci}^*
V_w	10 m/s		12 m/s	

The simulations results are listed in Fig. 4.2-8 to Fig. 4.2-10. It can be observed from Fig. 4.2-8 (a) and (b) that active power is tightly control according to the variation of the wind speed, which is achieved by regulating duty cycle of the buck converter, as shown in Fig. 4.2-9 (a). The actual DC current follows the corresponding reference well in Fig. 4.2-9 (b), resulting from the control of the PWM CSI phase angle in Fig. 4.2-9 (c).

However, the reactive powers are out of control in the time period of 0 to 1.5s and 3 to 4.5s, during which the DC current references are forced to $0.95I_{dci}^*$, as shown in Fig. 4.2-8 (a). As a result, the PWM CSI cannot provide enough current for reactive power compensation, and the modulation index is saturated during these periods, as can be seen from Fig. 4.2-9 (d).
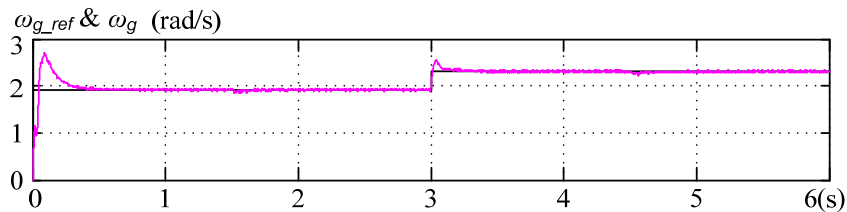
(a) PMSG rotor speed reference and its actual value
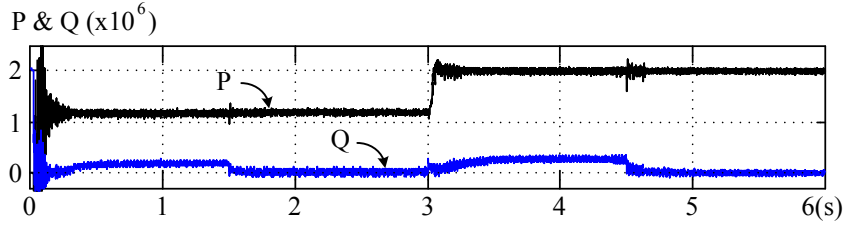
(b) Active power and reactive power

Fig. 4.2-8 Power delivery under the verification of the minimum DC current (UPF)
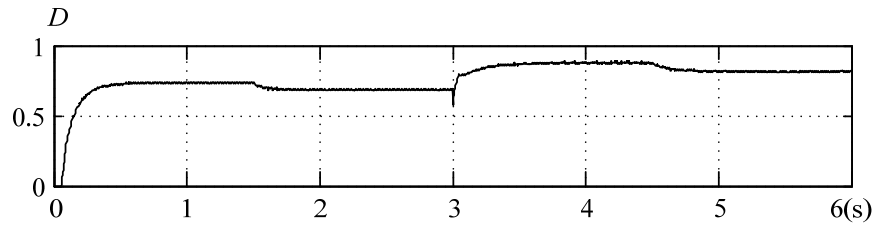
(a) Duty cycle of the buck converter
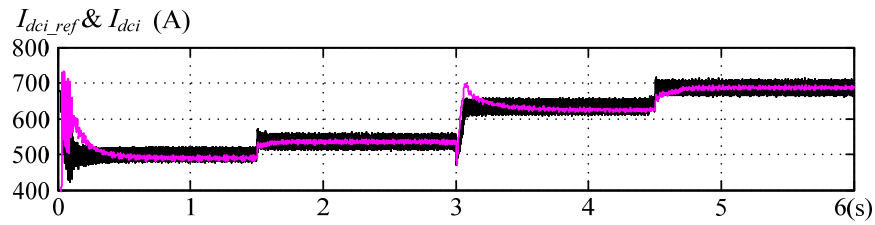
(b) DC current reference for PWM CSI and its actual value
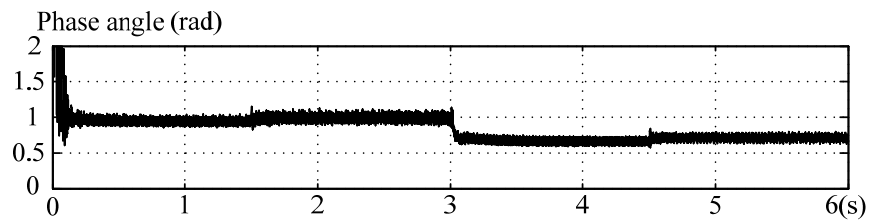
(c)PWM CSI phase angle
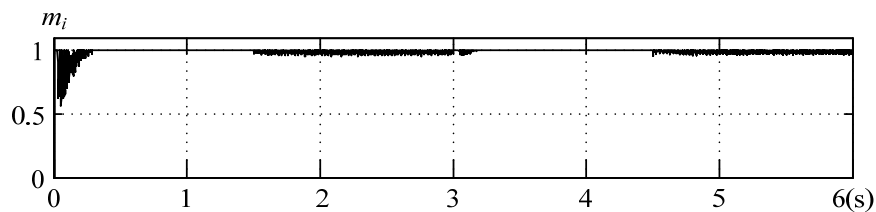
(d) Modulation index of the PWM CSI

Fig. 4.2-9 Control objectives under the verification of the minimum DC current (UPF)

74

Grid voltage and current waveforms are provided in Fig. 4.2-10. A phase displacement between the grid voltage and the current can be observed in Fig. 4.2-10 (a) and (c), which indicate that UPF operation is not achieved.
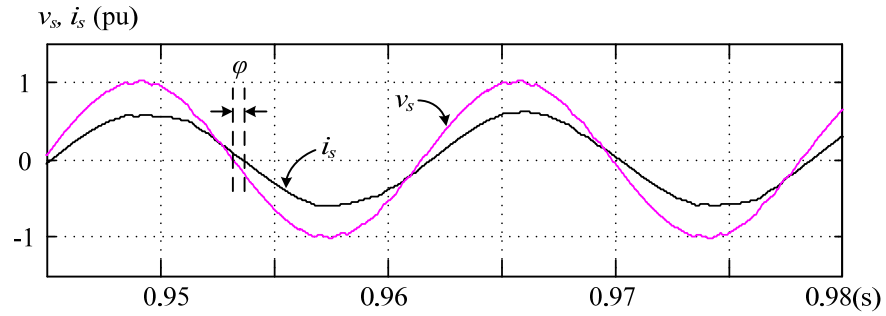
(a) Grid side voltage and current under $0.95 I_{dci}^*$ ($V_w=10$m/s)
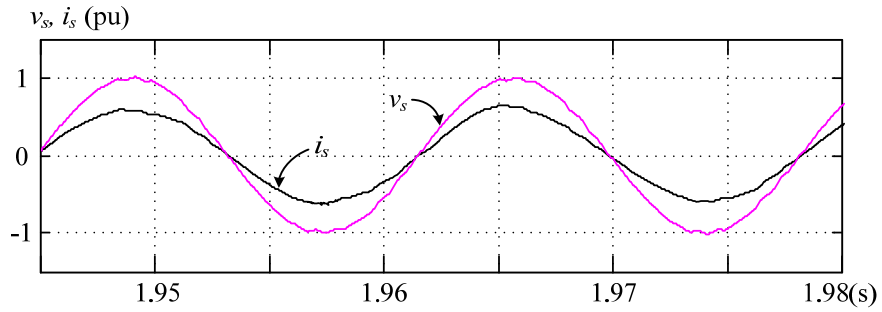
(b) Grid side voltage and current under minimum I_{dci}^* ($V_w=10$m/s)
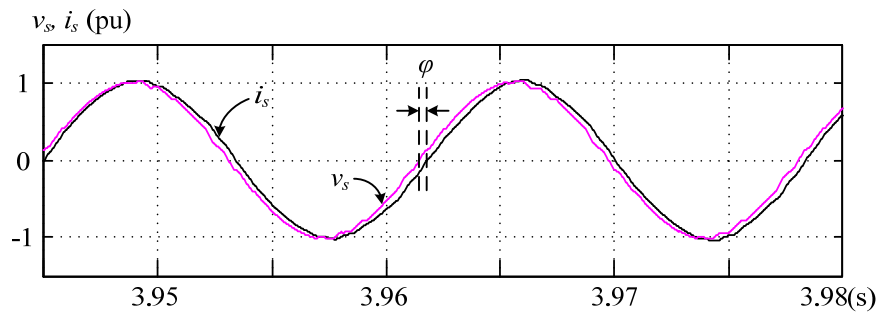
(c) Grid side voltage and current under $0.95 I_{dci}^*$ ($V_w=12$m/s)

v_s, i_s (pu)
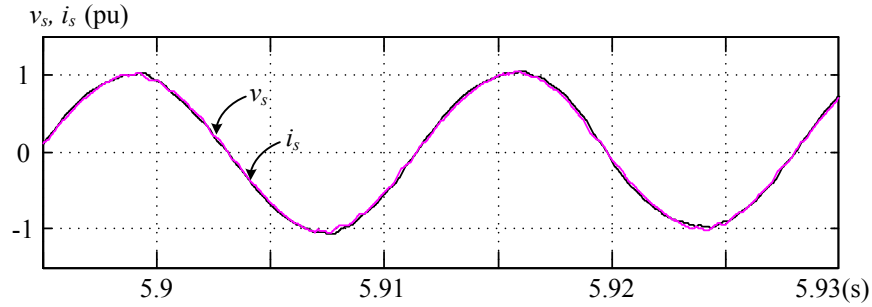
(d) Grid side voltage and current under minimum I_{dci}^* (V_w=12m/s)

Fig. 4.2-10 Grid voltage and current under the verification of minimum DC current (UPF)

Comparing the DC current level at the above operating conditions in Fig. 4.2-4 to Fig. 4.2-10 , the value can be as low as 420A at 6m/s wind speed and 0.95 lagging PF, or as high as 800A at rated wind speed with 0.95 leading PF. The latter generates almost four times conduction loss than that of the former assuming the same equivalent line resistance. Instead of keeping the DC current at the maximum value for all operating conditions, the strategy of minimum DC current control significantly lowers the converter loss.

In summary, the proposed control strategy ensures that the DC current is adjusted at its minimum level for overall loss reduction without sacrificing the performance of grid side power factor control.

4.3 Conclusion

Supported by the theoretical analysis in Chapter 3, this chapter verifies the proposed system and the control scheme in simulation. The construction of the simulation model is elaborated and demonstrated, followed by the simulation waveforms under different wind speed and power factor requirement. It is verified that the whole system remains stable and proper operation under all these conditions. Both maximum power extracting and flexible reactive power support to the grid can be achieved. The DC link current is minimized to reduce system loss through tracking the power delivered to the grid and maximizing the modulation index of the PWM CSI

Chapter 5　Conclusions

This chapter concludes and highlights the main contributions and outcome of the research presented in this thesis.

5.1　Summary

Wind energy conversion system is experiencing dramatic development and market growth that stimulate technology advancements in industry. Grid codes are defined to address the concerns of wind energy penetration to the grid. The unit capacity of wind turbines grows towards multi-megawatt level for maximum energy capture. Simplicity, reliability and efficiency are always important design factors for WECS development. In terms of power electronic converters, most commercial WECSs use voltage source converters. However, when it comes to high power application current source converter based configurations stand out to be promising solutions, as it features compact topology, simple control scheme and grid friendly waveforms.

The proposed system configuration is direct drive permanent magnet synchronous machine using a converter consisting of a diode, a buck converter and a PWM CSI. The switching devices for medium voltage high power applications are relatively expensive. Considering the fact that the active power flow is unidirectional from the wind turbine-generator to the grid, the passive diode rectifier can be applied to provide simple, reliable and low cost solution for generator power rectification. On the grid side, due to the existence of the capacitor bank for PWM CSI commutation, extra reactive power compensation is needed for grid code compliance, resulting in higher demand of DC current in PWM CSI than that provided by the generator and diode rectifier. Thus a buck converter is necessary to boost the DC current. The active power (MPPT), reactive power and DC current are therefore fully controlled by the joint effort of the PWM CSI and buck converter. In addition, the circuit current in the converter, mainly defined by the DC link current is regulated to its minimum value to maximize the converter efficiency.

5.2 Contributions

The main contributions of the thesis are detailed as follows:

1. **A novel configuration of PWM CSI assisted with buck converter and the diode rectifier is proposed for high power WECS.** A detailed review of WECS configurations and wind power converter technology is provided, based on which a novel current source converter based WECS configuration is proposed. The proposed system employs the well-proven PWM CSI technology in high power drive industry. When migrated from drive to power generation application, diode rectifier is identified to be an option for fulfilling AC-DC conversion due to the unique feature of the wind power generation system. The proposed configuration offers another suitable alternative for high power WECS.

2. **Theoretical analysis on the proposed configuration has been conducted to evaluate the feasibility of the system and select power components.** The steady-state analysis of a PMSG connected to a three-phase diode rectifier has been studied. Calculations of the average DC link current/voltage for maximum power point tracking of the WECS are formulized. The effects of the generator parameters on the system operating variables are also demonstrated. Moreover, the PWM CSI steady-state operating values for variable grid power factor requirements are derived and used to evaluate the impact of CSI capacitor value to grid power factor performance. In the end, the theoretical analysis on the generator and grid sides are then combined together to assess the system operating range and justify the necessity of the buck converter.

3. **An overall control scheme is developed for grid reactive power support, maximum energy extraction and minimum system loss.** Grid connection code compliance becomes one of the main requirements for modern large WECS. Active and reactive power adjustments according to the grid operating conditions are defined in most of the grid codes. The control scheme developed in this thesis can flexibly regulate the grid output powers based on the given reference. Additionally, MPPT is achievable at various wind speeds while the DC link current is optimized in the full operating range to effectively reduce power loss.

4. **Simulations are carried out to verify the feasibility of the proposed configuration and control scheme.** The proposed system is simulated in Matlab 2009b. The simulation results demonstrate the proper operation of the system under various conditions, which proves the practicability of the proposed system for high power WECS.

5.3 Future Work

In this thesis, the novel power converter configuration and corresponding control scheme are proposed, analyzed, and verified in simulation for normal operating conditions. The next step will be experimental verification in low voltage prototype. Besides, fully grid integration demands not only the active/reactive power adjustability, but also controlled WECS behavior under grid fault conditions, such as grid low voltage ride through. Further investigation of the proposed system under abnormal grid conditions is another possible future work.

Reference

[1] W. W. E. Association. *World Wind Energy Report 2010*. Available: http://www.wwindea.org/home/images/stories/pdfs/worldwindenergyreport2010_s.pdf

[2] D. S. Tony Burton, Nick Jenkins and Ervin Bossanyi, *WIND ENERGY HAND BOOK*: John Wiley & Sons Ltd., December 2001.

[3] G. W. E. Council. *GLOBAL WIND 2009 REPORT*. Available: http://www.gwec.net/fileadmin/documents/Publications/Global_Wind_2007_report/GWEC _Global_Wind_2009_Report_LOWRES_15th.%20Apr..pdf

[4] R. F. Frank, "Wind Power in Canada," *Canadian Copper & Brass Development Association Publications,* March 2008.

[5] G. W. E. Council. *GLOBAL WIND 2008 REPORT*. Available: http://www.gwec.net/fileadmin/documents/Publications/Global%20Wind%202008%20Rep ort.pdf

[6] C. W. E. Association, "WIND VISION 2025 POWERING CANADA's FUTURE," *CanWEA's 24th Annual Conference and Trade Show,* October 2008.

[7] O. p. authority. *Renewable energy Feed-in tariff program*. Available: http://fit.powerauthority.on.ca/Page.asp?PageID=1115&SiteNodeID=1052

[8] M. d. R. n. e. d. l. Faune. *Wind energy projects in Québec*. Available: http://www.mrnf.gouv.qc.ca/english/energy/wind/wind-projects.jsp

[9] Hydro-Québec. *Call for tenders for 2,000 MW of wind power*. Available: http://www.hydroquebec.com/distribution/fr/marchequebecois/pdf/tableau_repartitionregio nale_2000mw.pdf

[10] M. Stiebler, *Wind Energy Systems for Electric Power Generation*. © Springer-Verlag Berlin Heidelberg, 2008.

[11] S. Heier, *Grid Integration of Wind Energy Conversion Systems*. © John Wiley & Sons Ltd, 1998.

[12] M. Sathyajith, *Wind Energy: Fundamentals, Resource Analysis and Economics*. © Springer-Verlag Berlin Heidelberg, 2006.

[13] H. Davitian, "Wind Power and Electric Utilities: A Review of the Problems and Prospects," *Wind Engineering,* vol. 2, no. 4, 1978.

[14] A. D. H. Florin Iov, Clemens Jauch, Poul Sørensen and Frede Blaabjerg, "Advanced Tools for Modeling, Design and Optimization of Wind Turbine Systems," *Journal of Power Electronics,* vol. 5, no. 2, pp. 83-98, 2005.

[15] M. R. Khadraoui and M. Elleuch, "Comparison between OptiSlip and Fixed Speed wind energy conversion systems," in *Systems, Signals and Devices, 2008. IEEE SSD 2008. 5th International Multi-Conference on*, 2008, pp. 1-6.

[16] S. Muller, M. Deicke, and R. W. De Doncker, "Doubly fed induction generator systems for wind turbines," *Industry Applications Magazine, IEEE,* vol. 8, pp. 26-33, 2002.

[17] J. A. Baroudi, V. Dinavahi, and A. M. Knight, "A review of power converter topologies for wind generators," *Renewable Energy,* vol. 32, no. 14, pp. 2369-2385, 2007.

[18] M. Popesci, M. V. Cistelecan, L. Melcescu, and M. Covrig, "Low Speed Directly Driven Permanent Magnet Synchronous Generators for Wind Energy Applications," in *Clean Electrical Power, 2007. ICCEP '07. International Conference on*, 2007, pp. 784-788.

[19] S. Krohn, "Danish Wind Turbines: An Industrial Success Story," Feburary 2002.

[20] P. E. Morthorst, "Wind power development - Status and perspectives," Risoe National Laboratory, RoskildeAugust 1998.

[21] "Wind Power - A Reality Check," SFA Pacific Inc. Quarterly Report, First Quarter, 2008.

[22] "wind turbines in Denmark," Danish Energy Agency2010.

[23] (REpower press release, June 15, 2010). *REpower Offshore turbines at Thornton Bank and alpha ventus achieve first class operational results*. Available: http://www.repower.de/index.php?id=151&backPID=25&tt_news=2923&L=1

[24] (Februry 15, 2010). *Sway to develop a 10 MW offshore wind turbine with funding from Enova*. Available: http://www.renewbl.com/2010/02/15/sway-to-develop-a-10-mw-offshore-wind-turbine-with-funding-from-enova.html

[25] N. Haluzan. (November, 2010). *Offshore wind energy info* Available: http://www.renewables-info.com/renewable_energy_info/offshore_wind_energy_info.html

[26] H.-J. Wagner and J. Mathur, *Introduction to Wind Energy Systems: Basics,Technology and Operation*. © Springer-Verlag Berlin Heidelberg, 2009.

[27] R. Mittal, K.S.Sandhu, and D.K.Jain, "An Overview of Some Important Issues Related to Wind Energy Conversion System," *International Journal of Environmental Science and Development,* vol. 1, no.4, October 2010.

[28] I. Schiemenz and M. Stiebler, "Control of a permanent magnet synchronous generator used in a variable speed wind energy system," in *Electric Machines and Drives Conference, 2001. IEMDC 2001. IEEE International*, 2001, pp. 872-877.

[29] R. Teodorescu and F. Blaabjerg, "Flexible control of small wind turbines with grid failure detection operating in stand-alone and grid-connected mode," *Power Electronics, IEEE Transactions on,* vol. 19, pp. 1323-1332, 2004.

[30] V. 70/77 and P. presentation, "Vensys Gearless Technology - High Energy Production plus Built-in Reliability," November 13, 2006.

[31] X. Xiong and H. Liang, "Research on multiple boost converter based on MW-level wind energy conversion system," in *Electrical Machines and Systems, 2005. ICEMS 2005. Proceedings of the Eighth International Conference on*, 2005, pp. 1046-1049 Vol. 2.

[32] A. Faulstich, J. K. Steinke, and F. Wittwer, "Medium Voltage Converter for Permanent Magnet Wind Power Generators up to 5 MW," presented at the Power Electronics and Applications, European Conference, 2005.

[33] Converteam. (2011). *Wind Technology - Converters*. Available: http://www.converteam.com/majic/pageServer/0h04000141/en/Wind-Converters.html

[34] B. Wu, *High-Power Converters and AC Drives*. © IEEE Press & John Wiley, March 2006.

[35] J. Dai, D. Xu, and B. Wu, "A Novel Control System for Current Source Converter Based Variable Speed PM Wind Power Generators," in *Power Electronics Specialists Conference, 2007. PESC 2007. IEEE*, 2007, pp. 1852-1857.

[36] S. A. Papathanassiou, G. A. Vokas, and M. P. Papadopoulos, "Use of power electronic converters in wind turbines and photovoltaic generators," in *Industrial Electronics, 1995. ISIE '95., Proceedings of the IEEE International Symposium on*, 1995, pp. 254-259 vol.1.

[37] Z. Chen and E. Spooner, "Current source thyristor inverter and its active compensation system," *Generation, Transmission and Distribution, IEE Proceedings-,* vol. 150, pp. 447-454, 2003.

[38] C. Busca, A. Stan, T. Stanciu, and D. I. Stroe, "Control of Permanent Magnet Synchronous Generator for large wind turbines," in *Industrial Electronics (ISIE), 2010 IEEE International Symposium on*, 2010, pp. 3871-3876.

[39] D. Rekioua and T. Rekioua, "A new approach to direct torque control strategy with minimization torque pulsations in permanent magnets synchronous machines," in *Power Tech, 2005 IEEE Russia*, 2005, pp. 1-6.

[40] C. French and P. Acarnley, "Direct torque control of permanent magnet drives," *Industry Applications, IEEE Transactions on,* vol. 32, pp. 1080-1088, 1996.

[41] D. Casadei, G. Grandi, G. Serra, and A. Tani, "Effects of flux and torque hysteresis band amplitude in direct torque control of induction machines," in *Industrial Electronics, Control and Instrumentation, 1994. IECON '94., 20th International Conference on*, 1994, pp. 299-304 vol.1.

[42] D. Casadei, F. Profumo, G. Serra, and A. Tani, "FOC and DTC: two viable schemes for induction motors torque control," *Power Electronics, IEEE Transactions on,* vol. 17, pp. 779-787, 2002.

[43] M. Malinowski, M. P. Kazmierkowski, and A. Trzynadlowski, "Review and comparative study of control techniques for three-phase PWM rectifiers," *Mathematics and Computers in Simulation,* vol. 63, pp. 349-361, 2003.

[44] L. A. Serpa, S. Ponnaluri, P. M. Barbosa, and J. W. Kolar, "A Modified Direct Power Control Strategy Allowing the Connection of Three-Phase Inverters to the Grid Through LCL Filters," *Industry Applications, IEEE Transactions on,* vol. 43, pp. 1388-1400, 2007.

[45] G. Giglia, M. Pucci, C. Serporta, and G. Vitale, "Experimental comparison of three-phase distributed generation systems based on VOC and DPC control techniques," in *Power Electronics and Applications, 2007 European Conference on*, 2007, pp. 1-12.

[46] N. Mohan, T. M. Undeland, and W. P. Robbins, *Power Electronics: Converters, Applications, and Design*: Wiley, 2nd Edition, January 9, 1995.